



The Department of Health Sciences

Università degli Studi del Piemonte Orientale "Amedeo Avogadro"
University Of Eastern Piedmont "Amedeo Avogadro"

HIGH-THROUGHPUT PROFILING OF ANTIBODY REPERTOIRE IN OVARIAN CANCER ASCITIC FLUID

Dottorato In Biotecnologie Per L'Uomo
PhD Program In Biotechnology For Human Health

Cycle XXVI

PhD student: Frank Antony

Tutor: Prof. Daniele Sblattero

Coordinator: Prof. Claudio Santoro

Academic year 2011- 2014

HIGH-THROUGHPUT PROFILING OF ANTIBODY REPERTOIRE IN OVARIAN CANCER ASCITIC FLUID

A thesis submitted to
The Department of Health Sciences
Università degli Studi del Piemonte Orientale “Amedeo Avogadro”
University Of Eastern Piedmont “Amedeo Avogadro”

By
Frank Antony

In partial fulfillment of the requirements
for the degree of
Doctor of Philosophy

February 2014

Acknowledgements

This Ph.D. thesis contains the result of research undertaken at the Department of Health Sciences in Università degli Studi del Piemonte Orientale “Amedeo Avogadro”. This research was realized within the framework of the program: Innovative Biomedical Technologies (IBT), funded by the Fondazione Cariplo . Certainly, I would have never reached the point of finishing my dissertation without the help and support of other personnel.

I would first like to thank Prof. Daniele Sblattero and Prof. Claudio Santoro for providing me with the opportunity to carry out my research within the Università degli Studi del Piemonte Orientale “Amedeo Avogadro” and making the whole deal possible. Moreover, for their help and invaluable advice, encouragement and unfailing patience throughout the course of this study.

I wish to express my heartfelt thanks and gratitude to Dr. Diego Cotella and Dr. Cecilia Deantonio for their guidance is truly appreciated and their constant support towards the completion of this thesis.

Special thanks goes to all my colleagues at the department: Silvia Saragozza, Eleonora Rizzato, Maria Felicia, Szilvia Bako, Laura Patrucco, Sara Zonca, Valentina Sadini, Marta Armilli, Omar Sabry, Andrea Chiesa for many useful discussions, comments, suggestions and their timely assistance in the laboratory.

I want to extend my thanks to Dr. Delia Mezzanzanica, Department of Experimental Oncology, as well as Dr. Canevari Silvana, Department of Functional Genomics at Istituto Nazionale dei Tumori, Milan. Dr. Rosalba Minisini, Department of Clinical and Experimental Medicine, University of Eastern Piedmont and the Department of Molecular Biotechnology and Health Sciences, University of Turin.

In addition, I want to thank Dr. Paolo Macor, Department of Life Sciences, Università degli Studi di Trieste for his help in this study. Prof. Francesco Novelli and Dr. Giorgia Mandili, Department of Molecular Biotechnology and Life Sciences, University of Torino who were gracious to share their research with us.

Dedication

To my beloved family.

HIGH-THROUGHPUT PROFILING OF ANTIBODY REPERTOIRE IN OVARIAN CANCER ASCITIC FLUID

PhD Student: Frank Antony¹

PhD Program In Biotechnology For Human Health,

Cycle: XXVI

Year: 2011-2014

Tutor: Prof. Daniele Sblattero¹

Coordinator: Prof. Claudio Santoro¹

Institution: ¹Department of Health Sciences, University of Eastern Piedmont, Via Solaroli 17, Novara 28100, Italy

Abstract

Background-aims: Circulating antibodies directed against self-antigens are a hallmark of several chronic diseases including autoimmune diseases and cancer. There is a growing need for the discovery of new autoantigens useful as biomarkers for the diagnosis, the prognosis and to guide therapeutic strategies. Here we present a high-throughput and unbiased approach to profile the immune responses in ovarian cancer as a model disease by identifying those tumor associated antigens (TAA) recognized by autoantibodies.

Experimental design: Our technological platform combines a selection of a Phage display cDNA library followed by protein microarray and ELISA analyses of readouts and finally the correlation with clinical data. As an initial step, we characterized ascitic fluids from patients for their antibody response respectively to soluble, insoluble intracellular proteins and cell surface expressed antigens present in an ovarian cancer cell line (OVCAR3). Secondly, the most reactive ascites were used in biopanning experiments, where an ORF cDNA phage library was screened in order to isolate ORFs recognized by antibodies present in those ascitic fluids. Further, hundreds of selected ORFs were produced as GST-fusion proteins and used to construct proteins microarray. These were tested with a set of ascitic antibodies from cancer patients. Candidate antigens were validated by ELISA screening on ascitic fluids from 153 patients that includes ovarian cancer patients, other cancer and non-cancerous controls.

Result and discussion: We describe here an unbiased high-throughput (HT) approach to profile the ovarian cancer antibody repertoire. With this approach, we have identified and validated a set of different ovarian cancer specific IgG interacting tumor-associated antigens, which have significantly proven to correlate with patient survival. Moreover, we demonstrated the presence of autoantibodies in ascites targeting cell surface antigens expressed by tumor cells and its role in tumor regulation by activating the complement system.

Table of Contents

Chapter 1

1. Introduction	
1.1 Ovarian cancer: An Overview.....	1
1.2 Epidemiology of Ovarian Cancer.....	2
1.3 Risk Factors in Ovarian Cancer.....	3
1.4 Etiology of Ovarian Cancer.....	4
1.5 Inherited genetic syndrome.....	5
1.6 Classification of ovarian cancer.....	6
1.7 Signs and Symptoms of Ovarian Cancer.....	8
1.8 Screening Tests.....	9
1.9 Diagnosis.....	10
1.10 Staging of Ovarian Cancer.....	10
1.11 Treatment.....	11
1.12 Biomarkers for Ovarian Cancer.....	13
2. Ascitic Fluid.....	16
2.1 Complement System in Ascitic Fluid.....	18
3. Proteomic Technology for the study of diseases.....	19
4. Expression Library.....	21
5. Display systems.....	22
5.1 Phage Display.....	23
5.2 Phage display selection.....	26
5.3 Application of phage display.....	27
5.3.1 Identification of protein-protein interactions: in vitro.....	27
5.3.2 Phage display selection on live cells.....	28
5.3.3 In vivo phage library selection.....	29
5.3.4 Antibody phage display.....	30
5.4 Recent innovations in phage display technology.....	30
5.5 Selection of Open Reading Frames.....	30
5.6 Phage display for cancer biomarker.....	32
6. Protein Microarray.....	33
6.1 Protein microarray production.....	35
6.1.1 Printing methods.....	35
6.1.2 Protein immobilisation considerations, formats and surfaces.....	35
6.1.3 Detection methods.....	36
6.2 Applications of Microarray.....	37
6.3 Application of protein array in discovery of autoantigens in cancer.....	37
7. Rationale of the project.....	40
8. Objective Of the research.....	42
9. Project Summery.....	43

Chapter 2

10. Results.....	44
10.1 Introduction to results.....	44
10.2 cDNA Library construction and characterization.....	46
10.3 Sample preparation.....	47
10.4 Characterization of ascitic fluid based on autoantibody response.....	49
10.4.1 Western Blot of Ovarian cancer cell lysate.....	49
10.4.2 Ovarian Cancer Whole Cell ELISA.....	50

10.4.3 Ovarian Cancer Cell Lysate ELISA.....	51
10.4.4 Immunofluorescence Assay on OVCAR3 Cells (IFA).....	52
10.5 Selection of ORF Phage Display Library.....	53
10.6 High-throughput protein production of the selected clones.....	56
10.7 Immunoscreening of the selected antigen by protein microarray.....	61
10.8 Identification novel putative tumour-associated antigens (TAA) by sequencing.....	62
10.9 Large Scale Production of Novel Putative Antigens.....	64
10.10 Validation of Putative Antigenic Protein by Indirect ELISA.....	65
10.11 Analysis for the prognostic potential of the novel antigens and their clinical correlation.....	68
10.12 Verification of Cell Surface Targets by Cell Surface ELISA on Live OVCAR-3 Cell Line.....	69
10.13 Role of Cell Surface Antigen Interacting Antibodies in Tumor Regulation by Complement Dependent Cytotoxicity (CDC).....	71
 <i><u>Chapter 3</u></i>	
11. Discussion.....	73
11.1 Background.....	73
11.2 Immunoproteomic approach in the identification of TAAs.....	74
11.3 Antigens Identified As Most Immunoreactive.....	78
11.4 Validation of novel putative antigens.....	81
11.5 Tumor regulation mediated by cell surface tumor antigen targeting antibodies.....	84
 <i><u>Chapter 4</u></i>	
12. Conclusion.....	86
 <i><u>Chapter 5</u></i>	
13. Materials and Methods.....	87
13.1 Section 1: Abbreviations.....	87
13.2 Section 2: Solutions and buffers.....	87
13.3 Section 3: Standard protocols.....	89
13.4 Section 4: Methods.....	92
13.4.1 Patient samples and cell line.....	92
13.4.2 Characterization of ascitic fluid based on autoantibody response.....	92
13.4.3 Selection of cDNA Phage Display library.....	94
13.4.4 High-throughput recombinant protein production of the selected clones in autoinducing medium.....	96
13.4.5 Immunoscreening of the selected antigen by protein microarray.....	96
13.4.6 Identification novel putative tumour-associated antigens (TAA) by sequencing.....	96
13.4.7 Large Scale Production of Novel Putative Antigens.....	97
13.4.8 Validation of Putative Antigenic Protein by Indirect ELISA.....	98
13.4.9 Analysis for the prognostic potential of the novel antigens and their clinical correlation.....	98
13.4.10 Verification of Cell Surface Targets by Cell Surface ELISA on Live OVCAR-3 Cell Line.....	98
13.4.11 Role of Cell Surface Antigen Interacting Antibodies in Tumor Regulation by Complement Dependent Cytotoxicity (CDC).....	99
14. References.....	100

List of Figures

Figure 1: Normal and cancerous ovaries.....	1
Figure 2: Ovarian cancer prevalence, Incidence, Mortality worldwide in 2012.....	2
Figure 3: View of ovary at tissue level.....	6
Figure 4: Pathophysiology of malignant ascite.....	17
Figure 5: M13 filamentous bacteriophage displaying fusion protein.....	25
Figure 6: The three types of phage display.....	26
Figure 7: Phage display selection cycle.....	27
Figure 8: Schematic representation of ORF filtering.....	31
Figure 9: Types of protein microarrays and their possible applications.....	34
Figure 10: Workflow of the project.....	45
Figure 11: Affinity purification of immunoglobulins.....	48
Figure 12: Western blot of OVCAR3 cell lysate.....	49
Figure 13: Ovarian Cancer Whole Cell ELISA.....	50
Figure 14: Ovarian Cancer Cell Lysate ELISA.....	51
Figure 15: Immunofluorescence assay on OVCAR3 Cells.....	53
Figure 16: Schematic representation of the four steps followed for the selection of phages selection.....	54
Figure 17: Random clones checked for the input and the output of the selections.....	56
Figure 18: pGEX 4T- 1 mut BssHII NheI Vector Map.....	57
Figure 19: Subcloning of the selected cDNA fragments from phagemid vector into modified pGEX vector.....	57
Figure 20: PCR confirms the presence of insert.....	58
Figure 21: Mini-fermenter.....	59
Figure 22: Workflow of the high-throughput protein production and purification protocol.....	60
Figure 23: Coomassie staining of GST-fusion proteins produced by high-throughput approach.....	61
Figure 24: Immuno-screening by protein microarray.....	62
Figure 25: PCR of immunoreactive clones amplified with pGEX primers.....	63
Figure 26: Expression and Purification of Antigens.....	65
Figure 27: Validation of antigenic protein by ELISA.....	66
Figure 28: Antigenic markers with potential prognostic value.....	69
Figure 29: The ratio of surface targets which are accessible for humoral and cytotoxic immunity.....	69
Figure 30: Ovarian cancer Cell Surface ELISA.....	70
Figure 31: Complement dependent Cytotoxicity Assay.....	72

List of Tables

Table 1: classification ovarian cancer.....	7
Table 2: Diagnostic and prognostic biomarker for ovarian cancer.....	14
Table 3: Potential ovarian cancer biomarker currently not used in clinics.....	14
Table 4: Panel of Biomarker.....	16
Table 5: Biomarker for ovarian cancer identified by phage display.....	33
Table 6: Different types of protein microarray surfaces.....	36
Table 7: Autoantigens in ovarian cancer identified by Protein Microarray.....	39
Table 8: Gene abundance.....	46
Table 9: Summary of ascetic fluids used.....	47
Table 10: Purified ascites used for phage display selection.....	55
Table 11: Input and Output of phage populations for each selection round with different ascitic fluid.....	55
Table 12: Identified novel putative tumor associated antigens selected for validation.....	64
Table 13: Sensitivity and specificity of detection.....	68
Table 14: Oligonucleotide sequences.....	88

Chapter 1

1. Introduction

1.1 Ovarian cancer

Ovarian cancers are among the most lethal gynaecological malignancies worldwide. These cancers arise from ovaries which are a pair of almond-shaped female reproductive glands located on each side of the uterus and are responsible for generating ova (eggs) and the female sex hormones, estrogen and progesterone. The disease is characterized by few early symptoms, typical presentation at an advanced stage, and poor survival statistics. Depending on the kind of originating cells, cancer of the ovary can be sub-divided into three main types: epithelial ovarian cancer occurs in 80% of the ovarian cancer patients, gonadal stromal cancer in 5-10% and germ cell cancer in 10-15% of the patients (Fig. 1). This disease, produced by rapid growth and division of cells in the ovary ranges from benign to aggressive malignant and includes an intermediate class referred to as borderline carcinomas. In this chapter, an updated overview of ovarian cancer including diagnosis, screening and treatment strategy as well as the known potential biomarker for ovarian cancer are described. In addition, the role of high-throughput profiling techniques for the analysis of protein interactions and their importance in finding markers and targets for ovarian cancer therapy are discussed.

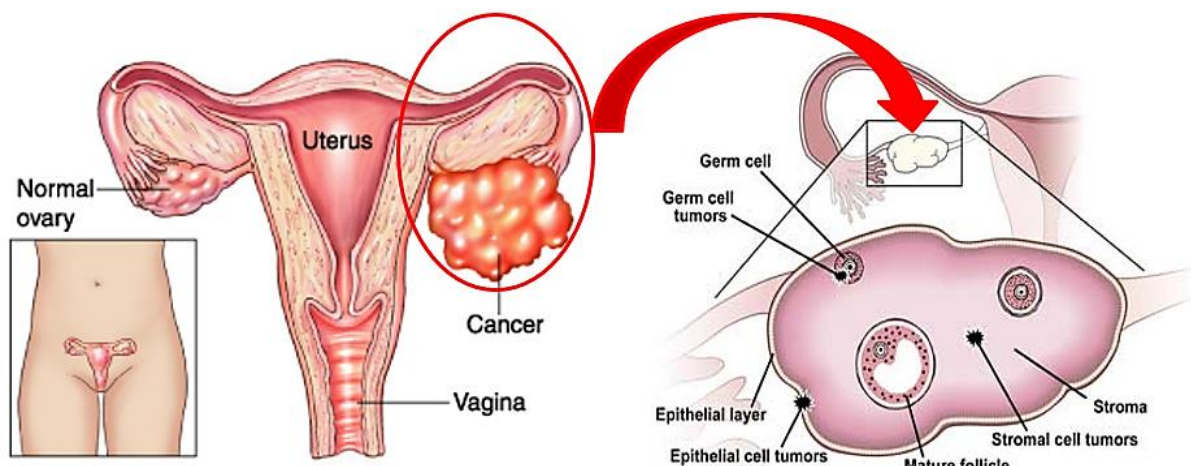
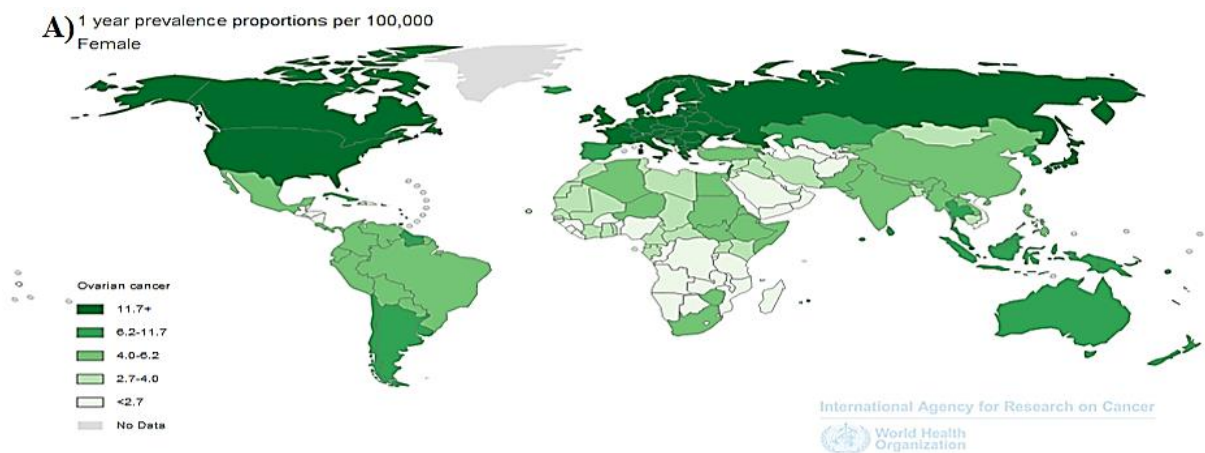


Figure 1: Normal and cancerous ovaries. Types of ovarian cancer originated from different kind of cells of ovaries. [1]

1.2 Epidemiology of Ovarian Cancer

Ovarian cancer is the seventh most common cancer among women with approximately 5900 new cases are diagnosis annually in Italy alone and over 238000 cases worldwide (Fig.2). Ovarian cancer is the leading cause of death from gynecological cancers in the Western world and is the eighth cause of death from cancer in women worldwide, accounting for more than 151000 deaths (as estimated by GLOBCAN 2012) [1]. Malignant tumors of the ovaries occur at all ages with variation in histological subtype by age. Germ cell tumors predominate in women younger than 20 years of age, whereas borderline tumors typically occur in women in their 30s and 40s. Epithelial ovarian cancers, the most prevalent type of ovarian cancer usually occur after the age of 50 years [2]. Ovary cancer rates are highest in women aged 55-64 years and the median age of patients diagnosed with ovarian cancer is 63 years. A woman's risk of getting ovarian cancer during her lifetime is approximately 1.43% (1 in 72). Her lifetime chance of dying from ovarian cancer is about 1 in 100, with a median age of 71 years at the time of death. Most women diagnosed with ovarian cancer are ethnically white and postmenopausal (approx. 55 or older). The relative five-year survival rate women diagnosed with ovarian cancer, regardless of disease progression is 44.2 percent. Survival rates vary depending on the stage of diagnosis. A 5-year survival rate of 92% can be attained, if the cancer can be diagnosed at its early stage when it is localized to ovaries. However, only 14.5% of ovarian cancer are diagnosed while the disease is confined to ovaries. The 5 year survival get drastically reduced to 27.3% as the cancer advances and spread to the distant organs (Cancer statistical data published by SEER Program of the National Cancer Institute) [3].



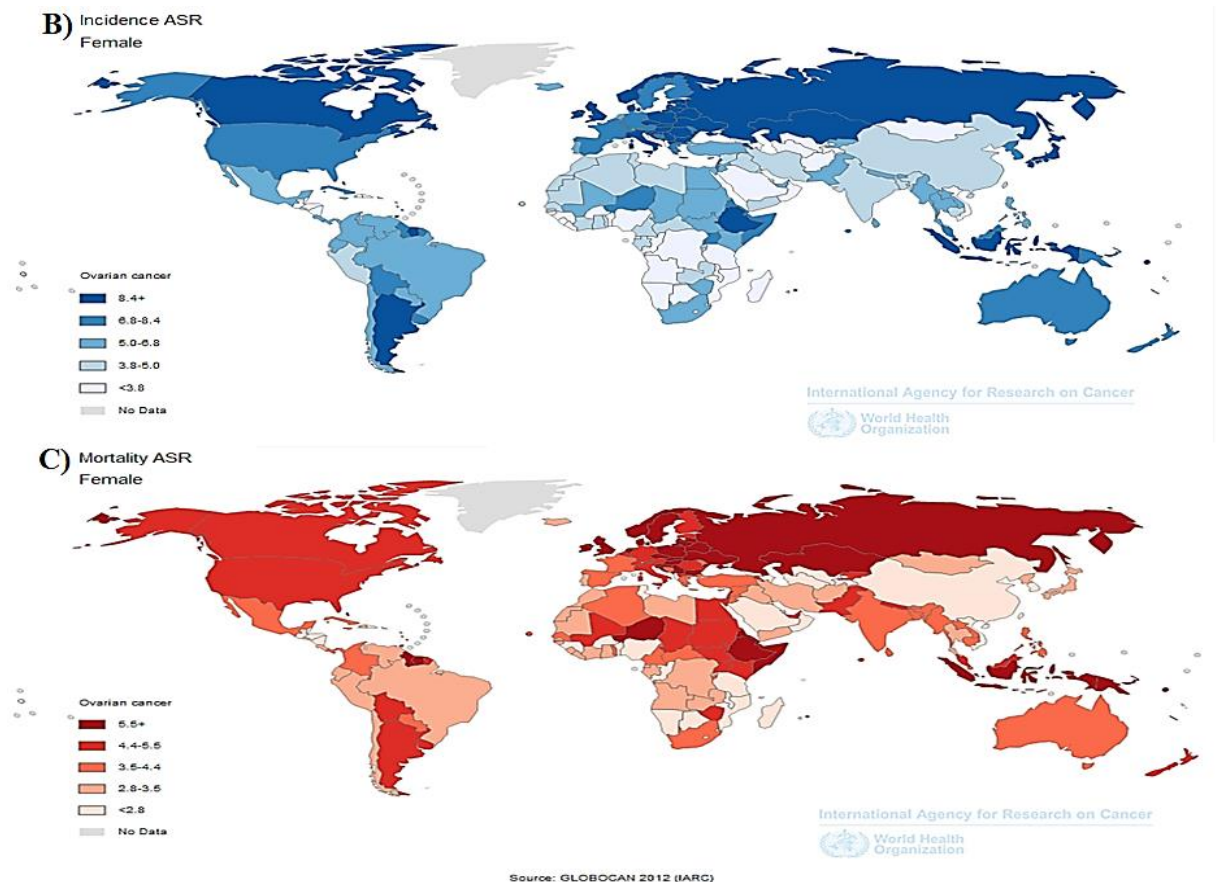


Figure 2: Ovarian cancer Prevalence, Incidence, Mortality worldwide in 2012 [2]: A) worldwide 1-year prevalence proportions per 100000 females. It shows the number of persons across the world that have been diagnosed with ovarian cancer, and who are still alive at the end of a given year, the survivors. B) Incidence. C) Mortality caused by ovarian cancer across the world. An age-standardized rate (ASR) of incidence or mortality is the measure of the rate that a population would have if it had a standard age structure.

1.3 Risk Factors in Ovarian Cancer

The factors involved in the development of ovarian cancer are still largely unknown, but several risk factors, familial or not, have been described. A risk factor is something that may increase the chance of developing a disease. Studies have found the following risk factors for ovarian cancer:

- i) **Age:** The risk of developing ovarian cancer gets higher with age and increases dramatically in women over the age of 45 (median age at diagnosis of 63) [3].
- ii) **Ethnic origin:** Most women diagnosed with ovarian cancer are ethnically white [3].
- iii) **Obesity:** Obese women with a body mass index of at least 30 have a higher risk of developing ovarian cancer [4]
- iv) **Reproductive history:** Nulliparity is associated with an increased risk of ovarian cancer, whereas the risk goes down with each full-term pregnancy and breastfeeding may reduce the risk even further [5,6].

- v) **Birth control:** Use of oral contraceptives decreases the chances of having ovarian cancer[5,6].
- vi) **Gynecologic surgery:** Women that underwent tubectomy or hysterectomy seems to reduce the risk of getting ovarian cancer considerably.
- vii) **Fertility drugs:** Fertility drugs seem to increase the risk of the type of ovarian tumors known as "low malignant potential".
- viii) **Estrogen therapy and hormone therapy:** Some recent studies suggest women using estrogens after menopause have an increased risk of developing ovarian cancer.
- ix) **Family history of cancer:** Up to 10% of ovarian cancers are familial cancer. A family history of ovarian, breast or colorectal cancer is an important risk factor.
- x) **Personal history of breast cancer:** The risk of ovarian cancer after breast cancer is highest in those women with a family history of breast cancer. A strong family history of breast cancer may be related to the presence of an inherited mutation in one of two genes, known as BRCA1 and BRCA2. These mutations can also cause ovarian cancer [4].

1.4 Etiology of Ovarian Cancer

Although the causes of ovarian cancer are not well understood, there have been several hypotheses proposed regarding the cause of ovarian cancer. The "Incessant ovulation" theory postulated by Fathalla in 1971 suggested that a continuous cycle of damage and repair of the surface epithelium during ovulation increased the risk of developing mutation and their exposure to estrogen-rich follicular fluid may stimulate epithelium to malignant transformation. A number of findings have backed this hypothesis. Women with multiple pregnancies, increased time of lactation, and oral contraceptive use are associated with a reduced risk of ovarian cancer clearly correlates with decreased lifetime ovulatory events [6, 7].

Later in 1975, Stadel proposed the "gonadotrophin" hypothesis for ovarian carcinogenesis. This hypothesis suggest in elevated levels of pituitary gonadotrophins promotes increased generation of estrogen or estrogen precursors, which are capable of stimulating the ovarian surface epithelial cells to undergo rapid cell division and produce malignancies [7-9].

Toxic oxidants formed from inflammation or inflammatory reaction can cause direct damage to DNA, proteins, and lipids and may, therefore, play a direct role in carcinogenesis. Hence, inflammation may also provide biologic rationale for the increased ovarian cancer risk associated with talc and asbestos exposure, endometriosis, pelvic inflammatory disease, and mumps infection [7]. In 1997, Green et al. examined effect of tubal ligation and hysterectomy, which resulted in lower the risk of ovarian cancer. Thus, explained a theory that cancer-causing contaminants gain

access to peritoneal cavity through the vagina and pass through the uterus and fallopian tubes to reach the ovaries [7,10].

Molecular alterations have been identified in a significant fraction of ovarian cancers. These DNA mutations that turn on oncogenes or turn off tumor suppressor genes can cause cancer upto a certain extent.

1.5 Inherited genetic syndromes

Studies suggest that 10% of all ovarian cancer cases have hereditary causes. Several inherited genetic syndromes known to have association with a greater risk of developing ovarian cancer are been described.

- Hereditary breast–ovarian cancer syndromes (HBOC)

BRCA1 (chromosomes 17q) and BRCA2 (chromosomes 13q) are human genes that produce tumor suppressor proteins. These proteins are localized in the nucleus and are involved in DNA repair. Specific inherited mutations in BRCA1 and BRCA2 increase the risk of female breast and ovarian cancers. Women with a germ line BRCA1 mutation have a lifetime risk of 16% to 44%. While, mutation of the BRCA2 gene also increases the risk of ovarian cancer, but to a lesser degree with a lifetime risk is approximately 11-17%. Ovarian cancer associated with germ-line BRCA1 and BRCA2 mutations may tend to develop at younger ages than sporadic form of this disease [5,11].

- Hereditary nonpolyposis colon cancer

Hereditary non-polyposis colorectal cancer (HNPCC) syndrome (also known as Lynch syndrome II) is another familial disorder that carries with it an increased risk of ovarian cancer. This syndrome is caused by germline mutations in one of the five mismatch repair genes: MSH2 (chromosome 2q), MLH1 (chromosome 3p), PMS1 (chromosome 2q) PMS2 (chromosome 7p) and MSH6 (chromosome 2p) [4, 12]. The lifetime risk of ovarian cancer in women with HNPCC is about 12% with a mean diagnostic age of 42.5 years [13].

- Li-Fraumeni syndrome

Ovarian cancer is also a component of the rare Li-Fraumeni syndrome (LFS), which resulted from germline mutation and loss of TP53 function. It is one of the most frequent genetic abnormalities in ovarian cancer and is observed in 60–80% of both sporadic and familial cases [14]. TP53 (chromosome 17p), encodes for a 53kd nuclear phosphoprotein that binds DNA and function as

tumor suppressor [15], negatively regulates cell growth and proliferation with damaged DNA leading to programmed cell death. A mutation in TP53 is directly correlated with a short-term survival benefit in ovarian cancer patients [16].

- Cowden's syndrome

50-75% women of average age of 40 years with Cowden's syndrome (also known as multiple hamartoma syndrome) develop breast or ovarian cancer or thyroid cancer. This inherited genetic disease caused again by mutations in the PTEN tumor suppressor gene (chromosome 10q23). This gene encodes a tyrosine phosphatase protein which effectively regulates cell proliferation [14, 17].

- Peutz–Jeghers syndrome

The Peutz–Jeghers syndrome (PJS) is an autosomal dominant polyposis disorder with very high relative and absolute risk for gastrointestinal and nongastrointestinal cancers, in which germline mutations in the STK11 tumor suppressor gene on chromosome 19p13.3 has been identified. The lifetime risk of ovarian cancer in women with PJS is estimated to be 21% [18].

1.6 Classification of ovarian cancer

Ovarian cancer can be categorized mainly into three based on the origin of cells (Fig.3): A) Tumor developed from germ cells known as Germ cell tumor, B) Sex cord-stromal tumors from stromal cells or the connective tissue within the ovaries and which produces female reproductive hormones and C) Epithelial ovarian cancers or epithelial tumor of epithelial cells which cover the ovary.

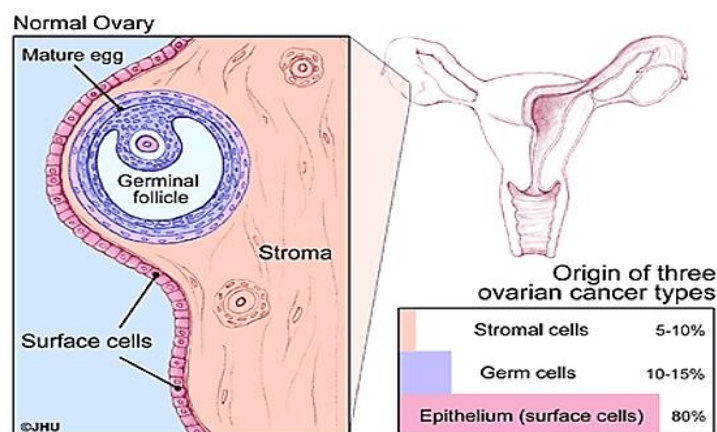


Figure 3: View of ovary at tissue level, includes Germ cells, Stromal cells and Surface epithelial cells or the surface cells [3]

Approximately 60% of ovarian cancer in young women nearly 20 years of age have originated from germ cell tumors. Most germ cell tumors are benign but some malignant cases have been reported. Common subtypes of germ cell tumors are teratomas, dysgerminomas, endodermal sinus tumors, and primary choriocarcinomas. Almost 5-10% of all ovarian cancer cases are effected by germ cell tumors [4, 9]. Sex cord-stromal tumors account for approximately 10- 15% of all ovarian cancer cases. More than half of stromal tumors are found in postmenopausal women older than 50 and seen to occur in young girls to a lesser extent. Postmenopausal vaginal bleeding or precocious puberty due to production of female reproductive hormone (estrogen) by these tumors is one of the most common symptom. In rare cases, stromal tumor makes male hormone resulting in menstrual irregularities, hirsutism, and virilism. Common types of malignant stromal cell tumors include low-grade cancers such as granulosa cell tumors (most common type), theca cell tumors, sertoli-leydig cell tumors and hilar cell tumors (benign tumor) [4, 9].

Epithelial ovarian cancers are the most common type of ovarian malignancies, causing more than 80% of all ovarian cancer cases. This type of cancer arises from ovarian surface epithelium and they can be either benign or malignant. Benign tumors are typically incapable to metastasize beyond the ovaries. There are several types of benign epithelial tumors including serous adenomas, mucinous adenomas, and Brenner tumors. Malignant tumors of the ovarian surface epithelium are known as carcinomas. These type cancers can spread to other parts

1. Common epithelial tumors

- A. Serous tumors
- B. Mucinous tumors
- C. Endometrioid tumors
- D. Clear cell carcinomas
- E. Brenner tumors
- F. Mixed epithelial tumors
- G. Undifferentiated carcinomas
- H. Unclassified tumors

2. Specialized stromal cell cancers

- A. Granulosa cell tumors
- B. Theca cell tumors
- C. Sertoli-Leydig cell tumors
- D. Hilar cell tumors

3. Germ cell tumors

- A. Teratomas
- B. Mature teratomas
- C. Immature teratomas
- D. Struma ovarii
- E. Carcinoids
- F. Dysgerminomas
- G. Embryonal cell carcinomas
- H. Endodermal sinus tumors
- I. Primary choriocarcinomas
- J. Gonadoblastomas

4. Soft tissue tumors not specific to the ovary

5. Unclassified tumors

6. Secondary (metastatic) tumors

7. Tumor-like conditions

Table 1: classification ovarian cancer [1]

of the body and can be fatal. Several tissue morphological features can be used to classify epithelial ovarian carcinomas into different types. i) Serous tumor, most common form and makes up to 40% of epithelial ovarian cancer cases. ii) Endometrioid tumors, the second most common type of EOC and comprising about 10-20% of EOC cases. iii) Clear-cell tumors accounts for 5-10%. While, iv) mucinous tumors make up approximately 1% of all of malignancies related to epithelium of ovary. v) Brenner tumors, mostly benign and less than 5% are proliferating or borderline constitutes 1.4-2.5% of all ovarian cancer cases [9].

If the morphology does not resemble any of the previous subtypes, these poorly differentiated tumor is called vi) undifferentiated tumors. Undifferentiated epithelial ovarian carcinomas tend to grow and spread more quickly than the other types. They are characterized as having low malignant potential that do not clearly appear to be cancerous. Approximately 15% of all EOC are undifferentiated tumors. vii) Mixed epithelial tumors are composed of 2 or more of the 5 major cell types of common epithelial tumors [9]. The list of ovarian cancer types are shown in Table 1 Epithelial ovarian cancer may also be sub-classified by grading.

- GX: Grade cannot be assessed.
- G1: Well differentiated.
- G2: Moderately differentiated.
- G3: Poorly differentiated [2].

1.7 Signs and Symptoms of Ovarian Cancer

Early cancers of the ovaries often cause no symptoms. However, as the cancer progress, symptoms may include:

- Bloating, a feeling of fullness, gas
- Frequent or urgent urination
- Nausea, indigestion, constipation, diarrhea
- Menstrual disorders, pain during intercourse
- Fatigue, backaches.

It is highly recommended to consult a doctor if any of these symptoms last more than 2-3 weeks. A recent study conducted by Eltabbakh et. al suggest 78% of ovarian cancer patients persisted with presenting symptoms. The most commonly reported symptoms includes abdominal or pelvic pain (35%), bloatedness (32%) and vaginal bleeding (20%) [19].

1.8 Screening Tests

Screening tests are intended to detect early stage cancer in patients even before the onset of any symptoms. Identifying ovarian cancer in its early stages is very important because treatment is most effective while the disease is confined to the ovaries. Although there is no efficient screening test with a high sensitivity and specificity, the following available tests are recommended especially for those women with a family history of ovarian cancer.

- **Pelvic Exam:** done to check the condition of ovaries and nearby organs for lumps or other changes in their shape or size [20].

- **Transvaginal Ultrasonography (TVUS):** this imaging technique is another strategy to screen ovarian cancer. TVUS is enabled to detect changes in size and architectural features such as cystic features, solid features, septations, papillations, nodules, or free peritoneal fluid. This test is performed once with the development of any symptoms and with an abnormal pelvic exam. Transvaginal ultrasonography have been reported to possess the ability to differentiate benign from a malignant tumor by combining informations such as the size and the morphologic characteristics of ovarian masses [21].

- **CA-125 blood test:** this test is approved by the Food and Drug Administration for screening women who are suspected for having ovarian cancer or abnormal pelvic exam. CA125 test measures the level of a protein tumor marker called CA-125 in patient's blood. CA-125 - cancer antigen-125 (MUC16) is a glycoprotein which is overexpressed by ovarian cancer cells. A CA-125 test result of titer greater than 35 U/ml is generally accepted as being elevated. Although the CA-125 blood test is more widely used to screen women for ovarian cancer, it can often be positive for reasons other than ovarian cancer (eg, endometriosis, fibroids, menstruation, ovarian cysts, pregnancy), thus reducing the specificity of the test. It is also not reliable early detection test for ovarian cancer. In about 20 percent of advanced stage ovarian cancer cases and 50 percent of early stage cases, the CA-125 is not elevated even though ovarian cancer is present. Generally, a better result can be obtained when CA-125 blood test used in combination with a transvaginal ultrasound. Currently, CA125 blood test is used to monitor the recurrence of ovarian cancer after treatment [20-25].

There are no recommended screening tests for germ cell tumors or stromal tumors. Some germ cell cancers release certain protein markers such as human chorionic gonadotropin (HCG) and alpha-fetoprotein (AFP) into the blood. After these tumors have been treated by surgery and chemotherapy, blood tests for these markers can be used to see if treatment is working and to determine if the cancer is coming back [4].

1.9 Diagnosis

Based on the results of the blood tests and ultrasound, a chest radiograph should be taken to screen for a pleural effusion while a computed axial tomography (CT) scan of the abdomen and pelvis should be performed to determine the extent of the disease. Depending on the factors such as age, symptoms, accumulation of ascites, elevated tumor markers, ultrasonographic data, CT findings, a suspected ovarian cancer patient undergoes surgery such as a pelvic laparoscopy or exploratory laparotomy. This involves a detailed examination of the contents, including all the peritoneal surfaces, ovaries, neighboring lymph nodes, other abdominal organs, omentum, surface of the diaphragm and all the suspicious sites. In addition, biopsy should be carried out for the histopathological examination of the tissue or fluid to look for cancer cells. This initial surgery provides a definite diagnosis as well as the staging of tumor according to the size, extent, and location of the cancer [2, 20, 25].

1.10 Staging of Ovarian Cancer.

Staging describes where the tumor is located, or how far it has metastasized. Staging in ovarian cancer and other gynecologic cancers has been standardized by the International Federation of Gynecology and Obstetrics (FIGO). This system is currently been used by most gynecologic oncologists and which rely on the results of surgery for the actual stages. Stages are expressed in Roman numerals from stage I (the least advanced stage) to stage IV (the most advanced stage) [2].

Stage I: Tumor confined to ovaries

- **Stage IA** cancer has developed in one ovary, intact capsule, no tumor present on the surface of the ovary, no malignant cells in ascites or washings
- **Stage IB** cancer has developed in both ovaries, intact capsule, no tumor on ovarian surface, no malignant cells in ascites or washings

- **Stage IC** one or both ovaries involved, ruptured capsule, tumor is on the outer surface of at least one of the ovaries, contains malignant cells in ascites or washings. However, the tumor has not metastasized to other organs

Stage II: Pelvic extension

- **Stage IIA** the cancer has spread to the uterus and/or the fallopian tubes, no malignant cells in ascites or washings
- **Stage IIB** the cancer has spread to other nearby pelvic organs such as the bladder, the sigmoid colon, or the rectum, no malignant cells in ascites or washings
- **Stage IIC** the cancer has spread to pelvic organs with all the features of stage IIA or IIB and contains malignant cells in the ascites or washings.

Stage III: Peritoneal metastasis -Cancer spread beyond the pelvis to the lining of the abdomen and/or to lymph nodes

- **Stage IIIA** cancer limited to the pelvis, microscopic implants on abdominal surfaces, no metastasis to the lymph nodes.
- **Stage IIIB** abdominal implants but smaller than 2 cm in diameter and no metastasis to the lymph nodes.
- **Stage IIIC** ovarian cancer has spread to lymph nodes, abdominal implants larger than 2cm.

Stage IV: Distant metastasis beyond the peritoneal cavity- Cancer spread to the inside of the liver, the lungs, or other organs located outside the peritoneal cavity.

Accurate staging is very important in determining a woman's long-term outcome (prognosis) and choosing the appropriate treatment regimen after surgery, since different prognoses at different stages are treated differently.

1.11 Treatment

Depending on the patient's age, stage and grade of the disease, the histopathologic type, and overall health, there are three main treatment options available for ovarian cancer. Primarily, surgical removal of the cancerous growth is the most common method of diagnosis and therapy for ovarian cancer, which is employed by a specially trained gynecologic oncologist. Chemotherapy uses anticancer drugs to kill cancer cells, and the third modality is radiation therapy, which is rarely used to treat ovarian cancer.

Early diagnosed women with stage I ovarian cancer are mostly treated to cure by surgery and reported to have a five year survival rate of 90% [23, 24, 26]. Once ovarian cancer is confirmed,

surgery is performed which involves a total hysterectomy (removal of the uterus), bilateral salpingo-oophorectomy (removal of the fallopian tubes and ovaries on both sides), omentectomy (removal of the fatty tissue that covers the bowels), lymphadenectomy (removal of one or more lymph nodes). If the cancer has spread, an optimal debulking surgery is done to remove as much cancer as possible, leave behind no tumors larger than 1 cm. Most experts agree that optimum debulking ensued an improved survival rate in patients and helps to improve the patient's response to chemotherapy [26].

Often, the treatments given in different combinations are more effective for treating advanced form of this disease. Surgical tumor debulking, followed by adjuvant chemotherapy is the standard treatment for advanced ovarian cancer. The typical course of platinum-based chemotherapy for epithelial ovarian cancer involves 3 to 6 cycles seems to be most effective with a 5-year survival rate of 10-30% of women diagnosed with ovarian cancer at stage III or IV [27,28]. A combination of 2 or more drugs usually a platinum-based along with a taxane based compounds are used for chemotherapy. Debulking surgery followed by paclitaxel- carboplatin has become the 'gold standard' firstline treatment for ovarian cancer [28].

Debulked epithelial ovarian cancer have shown a 20–30% improvement in both progression-free and overall survival when cisplatin was administrated intraperitoneal as primary chemotherapy when compared to intravenous delivery. Whereas, neoadjuvant chemotherapy followed by interval surgical cytoreduction produced a comparable result as primary debulking followed by chemotherapy in stages IIIC and IV disease [26,27].

First-line chemotherapy, patients are clinically followed up for a period of 2-6 months where level of CA-125 have shown no survival benefits. Although 80% of the patients initially respond to platinum-taxane chemotherapy, most of these patients will develop recurrent disease. Progression-free interval or the platinum-free interval (PFI) is the time from cessation of primary platinum based chemotherapy is now been widely used as the clinical surrogate for predicting response to subsequent chemotherapy and prognosis. Based on PFI, patients age is generally categorized into 3 groups. Patients with a platinum free interval of more than 6 months are considered to be platinum sensitive and commonly treated with secondary cytoreductive surgery platinum based chemotherapy. Those which respond to primary treatment and relapse within 6 months are classified as platinum resistant and are treated with non platinum-based chemotherapy. Patients

who progress while on treatment or within 4 weeks of stopping chemotherapy are considered to be platinum refractory [2,26-28].

By implementing novel treatment strategies for ovarian cancer may further improve the patient's life expectancy. Targeted therapy is a newer approach that uses molecular targeted agents which specifically identify (cell receptors, signal transduction pathways, cell cycle regulators, angiogenic mechanisms etc) and kill cancer cells while doing little damage to normal cells.

Bevacizumab is one of the most promising molecular targeted drugs in ovarian cancer. This 149-kDa recombinant humanized monoclonal IgG1 anti-VEGF antibody was the first drug approved by the US Food and Drug Administration to target angiogenesis. VEGF and its receptors are essential for angiogenesis and are overexpressed in epithelial ovarian cancer. Bevacizumab monoclonal antibody inhibit the VEGF pathway by binding the VEGF ligand [27,29]. Recently, a couple of phase III trials in high risk or advanced ovarian cancer patients demonstrated that by giving carboplatin-paclitaxel plus bevacizumab as a first line treatment is able to prolong progression-free survival compared to standard carboplatin-paclitaxel alone [29,30].

1.12 Biomarkers for Ovarian Cancer

Biomarkers have been applied to the management of ovarian cancer in several different ways. These include monitoring response to treatment, distinguishing malignant from benign pelvic masses, estimating prognosis, predicting response to individual drugs, and detecting primary disease at an early stage. Among the biomarkers for epithelial ovarian cancer, CA125 has received the most attention to date. From the perspective of point-of-screening biomarkers, markers present in biological fluid have a great potential in detecting early stage of ovarian cancer. Recent developments in genomic and proteomic research have identified a number of candidate biomarkers in the management of ovarian cancer. They can be used for global screening purposes would enhance preventative cancer care at an early stage of ovarian cancer as well as to monitor the clinical follow up. Some of the potential biomarkers for the purpose of early detection and screening ovarian cancer are listed in table 2 with a high diagnostic and prognostic value [24, 31-35]. Table 3 shows the potential diagnostic-prognostic biomarkers identified in 1990s to present which can be used for diagnostic purposes but are not currently used in the clinic.

Diagnostic biomarkers for ovarian cancer			
Marker	Full name	Localization	Description
• CA125 • HE4 • Prostatin • IAP	Cancer antigen 125 Human epididymis protein 4 Prostatin Immunosuppressive acidic protein	Serum	Stage-nonspecific biomarkers: diagnosis & follow-up
• hK6,7 • HNF-1 β • WT-1	human kallikrein 6 human kallikrein 7 hepatocyte nuclear factor (HNF)-1 β Wilms tumor 1	Tissue	
• TGF- α • uAS • Mesothelin	Transforming growth factor alpha Urinary angiotatin Mesothelin	Urine	
• CKB	Creatine kinase, brain	Serum & tissue	
• TP	Thymidine phosphorylase	Serum & tissue	Tumor stage-specific biomarkers: later stages
• CLIC4 • VSGP/F-Spondin	Chloride intracellular channel 4 Vascular smooth muscle growth promoting factor	Tissue	Tumor stage-specific biomarkers: later stages
• IAP	Immunosuppressive acidic protein	Serum	Tumor stage-specific biomarkers: later stages Screening of ovarian cancer relapse

Prognostic biomarkers for ovarian cancer			
Marker	Full name	Localization	Description
• hK8	human kallikrein 8	Serum	Prognostic: favorable
• hK13 • hK11 • PR	human kallikrein 13 human kallikrein 11 Progesterone receptor	Tissue	
• hK10 • IGFBP-2 • YKL-40 • tPA	human kallikrein 10 Insulin-Like Growth Factor Binding Protein 2 Chitinase-3-like protein 1 Tissue plasminogen activator	Serum	
• $\alpha_v \beta_6$ integrin • α -V integrin • β III tubulin • CD24 • c-Ets1 • EMMPRIN • GEP • Indoleamine 2,3-dioxygenase • M-CAM • p-glycoprotein • Topoisomerase II • WT-1	$\alpha_v \beta_6$ integrin α -V integrin β III tubulin CD24 molecule c-Ets1 Extracellular matrix metalloproteinase inducer Granulin-epithelin precursor Indoleamine 2,3-dioxygenase Melanoma cell adhesion molecule p-glycoprotein Topoisomerase II Wilms tumor 1	Tissue	Prognostic: unfavorable

Table 2: Diagnostic and prognostic biomarker for ovarian cancer: List of potential biomarkers for the purpose of early detection and screening ovarian cancer [2].

Ovarian Cancer Diagnostic-Prognostic Markers				
Marker	Full name	Diagnostic/ prognostic	Localization	Description
B2M	β 2-microglobulin	Diagnostic	Serum	Suitable tool to monitor course of disease when used in combination with CA125
CA54/61	Mucin-type glycoprotein antigen	Diagnostic	Serum	In case of mucinous cystadenocarcinoma Sensitivity 65% (compared with 36% of CA125)
CA72-4	Cancer antigen 72-4/ TAG-72	Monitoring/ diagnostic	Serum/tissue	Discriminates negative serous adenomas from positive serous carcinomas
CA125 II	Cancer antigen 125 II	Diagnostic	Serum	More precise than CA125
CA602	Cancer antigen 602	Diagnostic	Serum	100% sensitivity in serous adenocarcinoma 67% of sensitivity in mucinous adenocarcinoma

caGT	Cancer-associated galactotransferase antigen	Diagnostic	Serum	8/9 in clear cell carcinoma
Cathepsin B	Cathepsin member B	Preoperative differential diagnosis	Serum	Serum level is fairly proportional to FIGO stage; serous > endometrioid tumors (p < 0.001)
CD34	CD34 molecule	Prognostic	Tissue	Blood vessel count related to lower overall survival (p = 0.022)
COX-1	Cyclooxygenase-1	Diagnostic	Serum	Serum level is proportional to tumor progression
GAT	Glyphosate N-acetyltransferase	Diagnostic	Serum	Differential diagnosis from endometriosis
IAP	Immunosuppressive acidic protein	Diagnostic	Serum	Early detection of recurrence
M-CSF	Macrophage colonystimulating factor	Diagnostic	Serum	Serum level is useful in detecting ovarian cancer
nm23-H1	Non-metastatic cells 1, protein (NM23A)	Prognostic	Tissue	Inverse association with metastatic potential
TP53	Tumor protein p53	Prognostic	Tissue	p53 expression related to unfavorable prognosis
Progesterone	Progesterone	Diagnostic	Serum	Mainly related to nonendocrine ovarian tumor volume
Sialyl SSEA-1 antigen	Sialyl SSEA-1	Diagnostic/ prognostic	Serum	Fair Differential diagnosis with other markers
TNF receptor	p75/p55	Diagnostic	Ascitic fluid	Proportional to peritoneal fluid quantity and stage of disease
HOXB7	Homeobox7	Diagnostic	Serum	Their expression have found to promote growth and development of ovarian carcinomas
SIK3	Salt-inducible kinase 3	Diagnostic	Ascitic fluid	promotes G1/S cell cycle progression when overexpressed and cytoplasmic localization specifically in the tissue obtained from ovarian cancer patients
Osteopontin	Osteopontin	Diagnostic	Serum	Their presence in higher levels were found in the serum of patients with epithelial ovarian cancer, including early stage disease
LPA	Lysophosphatidic acid	Diagnostic	Ascite fluid	Elevated total LPA levels were detected in the plasma of 80% of early stage ovarian cancer patients
VEGF	Vascular endothelial growth factor	Diagnostic	Ascite fluid/ serum/ tissue	A panel of five markers that included VEGF could detect ovarian cancer with a sensitivity of 84% at 95% specificity
IL-6 and IL-8	Interleukin 6 and 8	Diagnostic		A combination of 5 markers including IL6, IL8 and CA125 achieved a sensitivity 84% and a specificity of 95% for early stage disease.
STAT3	Signal Transducer and Activator of Transcription 3	Prognosis	Tissue	Expression of phosphorylated STAT3 form is increased in primary ovarian cancer and its nuclear localization is associated with a poor prognosis
LPAAT-β	LPAAT-β enzyme	Prognosis	Tissue/serum	An increase of enzyme expression has been correlated to a poor prognosis and is associated with a minor survival
MMP	Matrix metalloproteinase	Prognosis	Tissue/serum	In stromal cells, high levels of MMP-2, MMP-9 MT1-MPP, (a subgroup of no soluble enzymes, connected to cellular membrane) are linked to a poor prognosis in patients with EOC.
MIF	Macrophage migration inhibitory factor		Serum	Higher levels of serum MIF were found in ovarian cancer patients with sensibility of 77,8% and specificity of 53,3%

Table 3: Potential ovarian cancer biomarker currently not used in clinics [3].

Due to the fact of the complex nature of the pathogenesis and of the tumor-host interaction in ovarian cancer, several studies relied to use a panel of markers on multiplex platforms. This permits simultaneous analysis of multiple markers with very small volumes of serum.

Mathematical techniques have been incorporated to discover many combinations of marker levels to high sensitivity and improve specificity for early-stage disease (Table 4). This however requires prospective validation [24, 32-34,36].

Panel of biomarker for ovarian cancer		
Marker Panel	Sensitivity (%)	Specificity (%)
CA125/IL-6/IL-8/VEGF/EGF	84 %	95%
CA125/IL-6/G-CSF/VEGF/EGF	86.5 %	93%
Leptin/Prolactin/Osteopontin/IGF2	95 %	94%
Leptin/Prolactin/Osteopontin/IGF2/MIF/CA125	95.3 %	99.4%
CA125/HE4/Glycodelin/PLAUR/MUC1/PAI-1	80.5 %	96.5%
CA125/ HE4/ Mesothelin	78% 68-82% 31-44%	98%
CA125/ CA19- 9 /EGFR /CRP/Myoglobin/APOA1/APOC3/MIP1A/ IL-6/IL-18/Tenascin C	91.3 %	88.5%
CA-125/OVX1/M-CSF	84%	84%
CA125/M-CSF/ OVX1/ LASA/ CA15–3/ CA72–4/CA19–9 and CA54/61	94.3%	90.9%
CA125/ CA72–4/ CA15–3 and LASA	79%	87.5%
CA125/ HE4/ sEFGR/ sVCAM-1	90%	98%

Table 4: Panel of Biomarker: Different combinations of ovarian cancer biomarker producing varying range of sensitivity and specificity [4].

2. Ascitic Fluid

Ascites is the excess accumulation of fluid in the peritoneal cavity. The term derives from the Greek word askites, meaning bag-like. It is caused by many pathologies including malignancy which accounts for 10% of all ascite formation. While ovarian cancer alone accounts for 38% of malignant ascites occurring in women during the course of their disease. Malignant ascites are capable to develop secondary and distant metastasis such as breast, liver, lungs or other organs located outside the peritoneal cavity [27,37-39].

Malignant cells secrete proteins, cytokines, growth factors such as vascular endothelial growth factor (VEGF), vascular permeability factor (VPF), and matrix metalloproteinases (MMPs) play an important role in the malignant ascites formation, metastasis and influence the aggressiveness of neoplastic cells. They are responsible for neovascularization, angiogenesis and an increased vascular permeability of small blood vessels. These together with lymphatic obstruction by tumor invasion are the main factors leading to an increased production and accumulation of ascitic fluid in the peritoneal cavity (Fig 4) [37-39]. Newer strategies to prevent the formation of ascites,

including anti-vascular endothelial growth factor (VEGF) therapy, are proving promising to overcome platinum resistance in ovarian cancer [27, 29, 38,39].

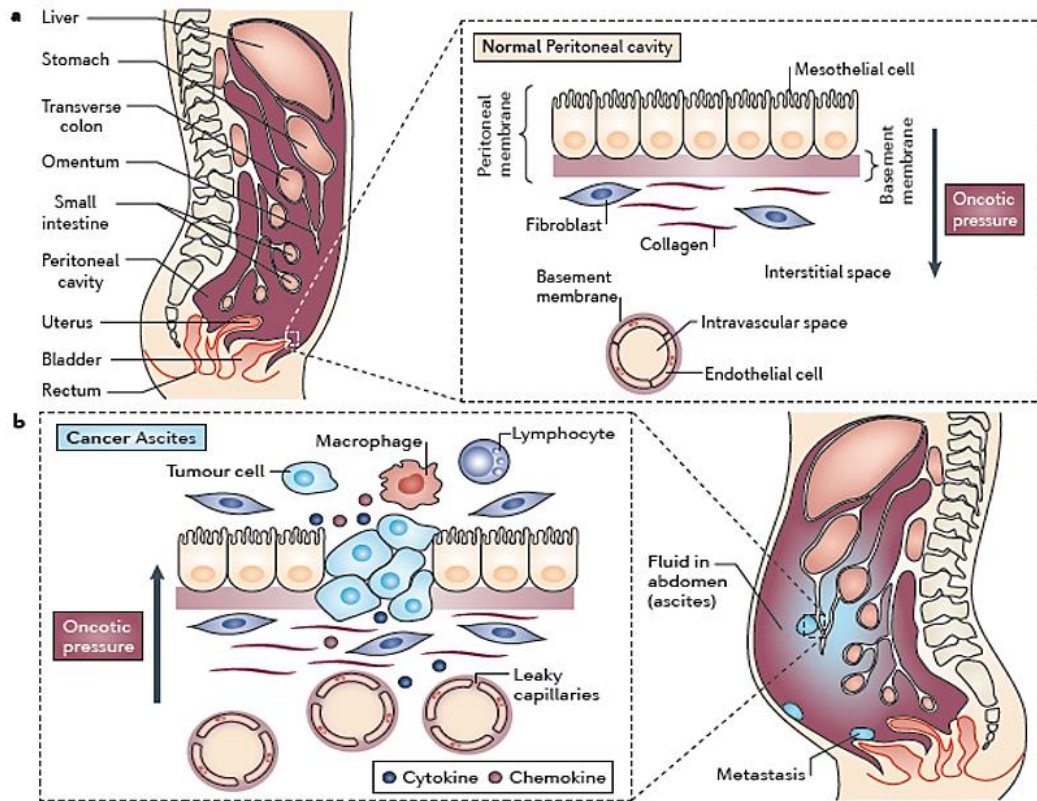


Figure 4: Pathophysiology of malignant ascite. a) Peritoneal cavity of a normal healthy person and the peritoneal membrane covers the visceral organs, as well as the abdominal and pelvic cavities. b) In patients with tumors in the abdominal cavity, the cross-sectional area of microvessels lining the peritoneal cavity is increased, and this results in an increased filtration surface for fluid. In addition, malignant ascites has a high protein concentration that is secondary to increased capillary permeability. Inflammatory cytokines and chemokines, as well as reduced lymphatic flow, all contribute to alterations of the peritoneal membrane. These changes decrease the plasma to peritoneal oncotic pressure difference, so the direction of flow of fluid is into the peritoneal cavity. This leads to the build up of pathological volumes of fluid in the peritoneal cavity [4].

Malignant ascites typically comprised of variable proportions of suspended cells that includes tumor cells, mesothelial cells, fibroblasts, macrophages, white blood cells, red blood cells and debris depending on the pathogenesis. 37% lymphocytes, 29% mesothelial cells, 32% macrophages and less than 0.1% adenocarcinoma cells have been reported to be present in ascitic fluid collected from ovarian cancer patients [38, 40]. In addition, ascitic fluid contains secreted proteins, antibodies against the proteins or peptides secreted or leaked from tumor tissue, soluble growth factors that have been associated with invasion and metastasis, and chemokines are present

[41-43]. Thus making ascitic fluid an excellent reservoir to study various biological aspects of the underlying tumor and equally important for the identification of prognostic and predictive biomarkers and for molecular profiling analysis of various tumors including ovarian cancer.

2.1 Complement System in Ascitic Fluid.

The complement (C) system is an essential component of innate and adaptive immunity. It plays an important role as cytotoxic effector arm for both immunological surveillance in the host defense against infectious pathogens and mAb-therapy. The complement system consists of some 30 soluble molecules / proteins synthesized locally by many cell types, including macrophages, fibroblasts and endothelial cells and several neoplastic cells. The components of this system in circulating blood plasma can easily reach the tumor site and diffuse inside the tumor mass is an advantage over other effector systems. Most of these protein components of the complement cascade are activated upon cleavage by a protease, which leads to each component's becoming, in its turn, a protease. Three pathways are involved in complement attack upon pathogens: i) classical pathway ii) alternative pathway and iii) mannose-binding lectin pathway (MBL -MAPS). These results in the release of chemotactic factors and cell-activating anaphylatoxins (C3a, C4a and C5a), deposition of opsonic fragments and formation of the membrane attack complex (MAC) [44,45]. It was also evident from previous studies that the deposition of C components in various tumor masses indicative of complement activation and its subsequent pathogenetic effects [46,47].

L Bjørge et al investigated complement system in ascitic fluid from ovarian cancer patients. The characterization revealed that most of these ascitic fluids were involved in the haemolytic activity either by alternative and classical pathway. While, the lack of MAC on the malignant cells isolated from the ascite samples was probably due to the expression of C membrane regulators on the tumor cells. The higher concentrations of soluble forms of C1 inhibitor and the alternative pathway inhibitors however did not affect the capability of ascitic fluid causing complement mediated killing of ovarian carcinoma cells. They also described the utility of C system as an effector mechanism in therapy with intraperitoneally administered mAbs, especially if the intrinsic C regulators are neutralized [48-50].

3. Proteomic Technology for the Study of Diseases

Ovarian cancer has been referred to as very complex and heterogeneous. Because of this, tumors with the same histological features that arise in different patients may display diverse alterations with different patterns of oncogene activation or tumor-suppressor gene loss, thus complicating determination of the importance of an individual gene's alteration. Currently, many genomic tests used to diagnose ovarian cancer or guide its therapy do not decrease women's risk of dying from this disease or do not improve their quality of life (QoL) [24,179,180].

Over the past decade, high-throughput technologies has stimulated their use in many bio-medical applications. In this field, proteomics has emerged as a powerful technology providing a central opportunity for the rapid identification and development of novel detectable biomarkers as well as tumor-associated antigens. It denotes the large-scale characterization of proteins, including complicated features like isoforms, modifications, interactions, and functional structures. Large varieties of proteins are known to be produced by the cancer that can be identified in the biological fluids of patients. Thus, protein biomarkers may be more specific in respect to cancer type and status than gene-based biomarkers. For diagnostic applications, protein-based biomarkers in body fluids provide easy-access as well.

In cancer biomarker discovery, various methods like two dimensional gel electrophoresis, mass spectrometry (MS), and protein microarrays as well as combination of different technology as a single platform such as serological proteome analysis (SEPPA), serological analysis of recombinant cDNA expression libraries (SEREX), phage display have become powerful tools to identify proteins markers. These methods could be used to study differential expression of hundreds and thousands of protein simultaneously. However, each approach has strengths and limitations.

Two-dimensional gel electrophoresis is a traditional approach that separates proteins according to two distinct protein characteristics, size and charge [181]. The usefulness of this approach was demonstrated in past studies to differentiate ovarian cancer sample proteome from healthy controls [182,183]. In recent years, improvements were made to overcome the major drawbacks of 2DE by the introduction of fluorescent two dimensional differential in-gel electrophoresis (2D-DIGE). 2D-DIGE facilitated accurate protein separation, detection, and quantitation and hence became an important tool for biomarker discovery of cancers, including ovarian cancer [184]. The main disadvantage these 2DE is that they are highly vulnerable to reproducibility and comparability.

Mass spectrometry (MS) is one among the major technique widely used for the discovery of cancer biomarkers, which can determine the precise mass and charge of proteins, and thus identify the actual precursor proteins or protein profiles. There are two basic approaches to utilize these data for early detection of ovarian cancer. One method attempts to identify a distinctive signature or pattern of protein expression that distinguishes healthy individuals from cancer patients. Surface-enhanced laser desorption and ionization (SELDI) or matrix-enhanced laser desorption and ionization (MALDI) have been used to detect novel patterns of low-molecular-weight moieties in ovarian cancer sera from all stages with controls. SELDI patterns have reported a sensitivity of 95% or more at 95% specificity for early detection of ovarian cancer [185]. The second approach employs SELDI to identify putative markers proteins and peptides that provide the greatest discriminatory power and develops individual bioassays to analyze each protein [186]. However, mass spectrometry technology have some limitations, while they are used for protein profiling of complex diseases such as ovarian cancer, as the data are difficult to reproduce and that they may be biased by artifacts in sample preparation, storage and processing, and patient selection [187].

Another proteomic based approach Serological Proteomics Analysis (SERPA) took advantage of combining the classical 2-DE with Western blotting to screen patient sera for autoantibodies against cancer specific antigens, and it precedes a further step involving MALDI-TOF MS analyses, which identifies the nature and abundance of the total proteins in sample analyzed. The group of Francesco Novelli have successfully demonstrated the utility of this technique to prediction early stages of pancreatic ductal adenocarcinoma (PDAC) by detection of autoantibodies against Ezrin [188]. In general, limitations of detecting autoantibodies by SEPRA arise from the inherent limitations of 2-DE. Those are the potential loss of small (<15 kDa), very large (>200 kDa), very acidic (pI < 3), very basic (pI > 10) and very hydrophobic proteins as well as the inability to detect TAA with conformational epitopes due to the denaturing conditions.

Whereas both phage display system and SEREX utilizes cDNA libraries for the expression and detection of antigens that elicit a humoral immune response in patients. To this end, mRNA extracted from appropriate tissue or cell line is converted to cDNA by *in vitro* methods and subsequently cloned into a bacteriophage for infection of *Escherichia coli* (*E. coli*). Contrasting to phage display system, SEREX adopts a lytic infection of the host bacteria; the recombinant proteins are expressed and can be blotted onto a nitrocellulose membrane for antibody screening

with sera. Seroreactive proteins can then be identified by sequencing the phage cDNA from positive plaques. SEREX has been useful for identifying several tumor specific antigens that generate a humoral immune response in cancers such as those from the kidney, lung, breast and colon [189, 190]. Likewise, SEREX immunoscreening was utilized to identify a set of novel tumor antigens that are associated with ovarian cancer and may prove useful for the early detection and treatment of this disease [191,192].

As underlined before, the great advantage of such approach stays in the fact that conventional methods require the preparation of a large number of membrane filters to be screened and that patients sera are usually available in limited quantity. Phage display technology permits the enrichment of reactive proteins by selection with very small amounts of serum, leading to a low number of clones to be screened. In general, the combination of SEREX-based techniques (that, although useful, in its original form presents severe methodological limitations) with novel tools, allowing the creation of large functional libraries, ensuring the ability to manage them with the appropriate systems, and integrated with innovative techniques for the sensitive and specific detection of analytes of interest, would represent a major breakthrough in this field of study. ORF selection, phage display, protein arrays, new proteomic technologies, and so on, are all suitable candidates for the development of these new integrated systems. The reports on the use of these technologies in profiling ovarian cancer are limited.

4. Expression Library

Expression library represents an important approach for the study of the expression profiles of biological systems. This methodology provide a direct physical association between the protein under analysis and the gene encoding these proteins. Expression cDNA libraries are the most common source of DNA for screening approaches. They offer valuable strategy for the identification of disease markers, new therapeutics and targeting agents for focused therapy. They are prepared from total single-strand mRNA extracted from whole organisms such as yeast or from various tissues, encompassed of greater variety of genes that are specifically expressed. Later, this isolated mRNA is converted into double-strand DNA copy (cDNA) by means of reverse transcriptase enzyme. Once cloned into an appropriate plasmid, the final population of recombinant vectors obtained represents the entire set of genes expressed by the source of starting

mRNA. Various formats are used for expression of eukaryotic proteins; of them bacterial system is most favorable one for its ease of use and high yield of protein. Although eukaryotic systems, such as the baculovirus system [52,53], can also be used.

cDNA or genomic DNA libraries can be used in many different applications such as PCR, DNA hybridization [54], two-hybrid systems [55], enzymatic activity [56], high-throughput structure determination [57] and by recognition with antibodies. This study focus on its application to identify tumor associated antigens (autoantigens) which specifically recognizing immunoglobulins present in ascitic fluid from ovarian cancer patients, and will be discussed in detail in chapter 2.

To this end, with an intention to enhanced expression and exposition (in display systems) of polypeptides, fragmented cDNA libraries are preferred. cDNA can be fragmented by means of physical methods (sonication), chemical or enzymatic methods (DNase) [58] and PCR-based methods [59]. Fragmented cDNA libraries increase chance to identify restricted binding sites and epitopes. Moreover, high degree of heterogeneity among the polypeptide sequences can be achieved.

It is important to enrich the library for potentially reactive proteins, in order to limit the number of proteins to be screened. These results in the need for: a) a system to remove non functional DNA sequences from the library, to decrease the library size; b) a system to select proteins of interest from the high original complexity. Both problems could be overcome by ORF selection systems and display/selection techniques described in section 4.5 of this chapter.

5. Display systems

Display technology refers to a collection of methods for creating libraries of modularly coded biomolecules that can be screened for desired properties in a high-throughput format on a global scale. This innovative approach has facilitated large-scale analyses of protein–protein/protein–substrate interactions, rapid isolation of antibodies (or antibody mimetics) without immunization, and function based protein analysis. The concept of expression library can be readily applied to the display systems: by means of recombinant DNA technology, wide collections of different particles displaying polypeptides can be generated and through specific selections strategies, providing a progressive enrichment of such complex libraries based on their specific reactivity. Two main advantages of this system are: first, the selected protein can be immediately characterized and identified by a simple DNA sequencing reaction; secondly, the gene encoding

the protein of interest can be manipulated with all the tools provided by molecular biology and genetic engineering techniques. Thus, allowing isolation and identification of specific proteins and related genes from a background of billions of unreactive clones [63].

There are three main formats or display platforms:

i) Peptide-on- DNA/RNA display: These are cell-free display systems where DNA or RNA are capable to bind its own coded peptide. Thus, permitting a screening of a large pool of complexes and identify the interactors by isolation and sequencing of nucleotide sequences of either DNA or RNA.

ii) Viral (Phage) display: It is one of the most commonly used display system. Here the gene of interest is cloned into the coding sequence of viral coat proteins and expressed as fusion with a surface protein of the phage. These fusion protein exposed on the surface of the phages allows the selection and isolation of novel interactors for its binding property to a given protein from a collection of billions of phages. Several different viral systems have been used to display peptides, including lysogenic filamentous phages, and lytic lambda phage, T7 bacteriophage, and T4 bacteriophage. We have employed this approach using filamentous phage for our study and will be described in much depth.

ii) Cell based display: Here the cDNA library encoding various proteins is recombinantly expressed in cultured cells and selected for binding to a specific ligand on the cell surface. Yeast two hybrid system is the most popular among this category due to the high efficiency of transformation.

5.1 Phage Display

Phage display is a system for the high throughput analysis of protein interactions by selecting peptides, proteins, or antibodies with specific binding properties from a pool of variants. This technique uses bacteriophage for the coupling of phenotype to genotype. Here, cDNAs libraries from appropriate tissue sources are expressed as fusion proteins with one of the phage coat proteins and exposed on the surface of the phage. Thus, allowing the selection and isolation of novel interactors for its binding property to a given protein from a collection of billions of phages [64-70]. Characterization by DNA sequencing to identify these unknown interacting proteins is relatively easy and straightforward step.

The concept of displaying proteins or peptides or polypeptides on the surface of filamentous M13-derived bacteriophage (phage) was first introduced by G.P. Smith in 1985 [71]. Smith demonstrated that phages could be manipulated in their genome level by inserting a foreign DNA into the gene encoding phage coat protein, retaining their infectivity and displaying a specific fusion protein on its surface. These fusion proteins in their immunologically accessible form could be isolated for its binding property by biopanning against immobilized immunoglobulins thereby enabling over a 1000 fold enrichment of the epitope binding sites of the antibodies.

Depending on the particular application, many types of phage have been used for phage display including Ff filamentous phage, Lambda and T7. The Ff filamentous phage family (M13 and its close relatives fd and fl) have been widely adopted since they provide a robust and highly flexible platform for display. Among them, filamentous bacteriophage M13 have been used as the source of the majority of successful screenings and best characterized library display vector by far [72,73]. M13 is a filamentous bacteriophage contains a circular single stranded DNA (6407 base pairs long) encapsulated by approximately 2700 copies of the major coat protein pVIII and capped by five copies each of pVII and pIX at distal end. While, the proximal end is composed of four to five copies each of pVI and pIII. (Fig. 5) The protein pIII has been identified as the one responsible for phage infection and for release of the phage particle following assembly. It has two N-terminal domains (N1 and N2) and a C-terminal domain (CT). Infection of *E.coli* host is mediated by the interaction between phage coat protein pIII through its N2 domain (one of the two N-terminal domains of pIII) and the F-pilus. This in turn, brings TolA protein (a membrane protein in *E. coli*) into close proximity and interacts with N1 (second N-terminal domains of pIII), leading to the deposition of phage circular ssDNA into the cytoplasm and later converted to dsDNA bacterial enzymes. The C-terminal domain of pIII known as 'CT' terminates phage assembly in the periplasm and release phage from the cell membrane. These filamentous phage infected *E.coli* cells do not get lysed, instead they replicate and are released from the cell membrane without killing the host as in contrast to Lambda and T7 [74].

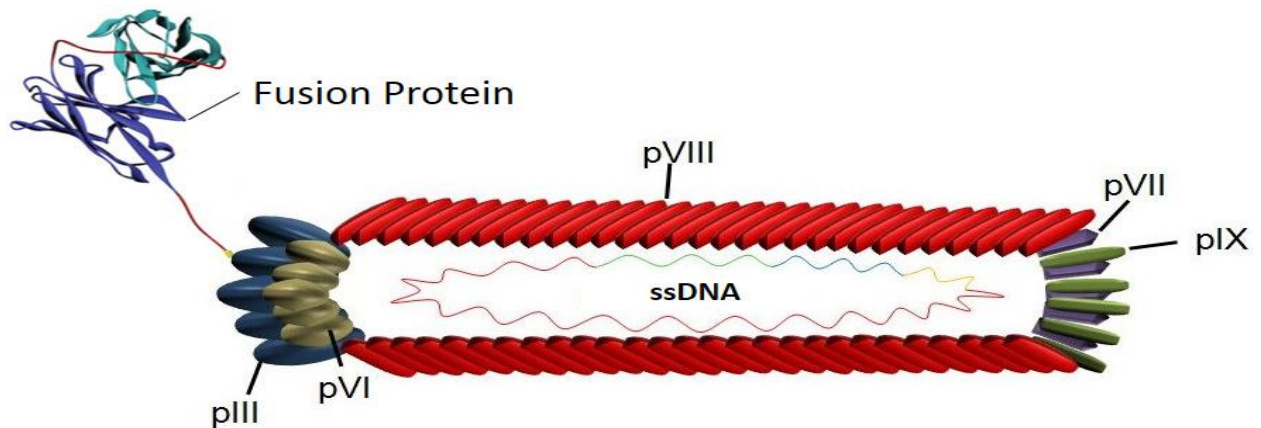


Figure 5: M13 filamentous bacteriophage displaying fusion protein [5].

Although all five M13 phage coat proteins have been demonstrated to be utilized, mostly pIII followed by pVIII and rarely pVI are used for phage display with respect to the number of fusion proteins displayed per phage and stability of the fusion proteins. Three different types of phage display exists by far that includes a) phage system, b) hybrid system and c) phagemid system (fig 6).

Generally, in phage system, the insert DNA are cloned upstream to the gene encoding the pIII or pVIII and are present as a single copy. A large numbers of smaller proteins (upto 2700 copies) may be displayed if pVIII is chosen as a fusion partner. Whilst pIII efficiently displays a fewer numbers of larger proteins [72,73,75].

In Phagemid system, the virion contains the phagemid that carries an antibiotic resistance marker, bacterial and phage origins of replication, the phagemid DNA containing a phage promoter upstream of the sequence encoding the fusion protein which is to be displayed, and a phage packaging signal. The transformed bacteria with this phagemid are later infected with packaging-defective helper phage providing all the proteins necessary for phage assembly. Infection with helper phage initiates the assembly preferably using phagemid DNA carrying a fully functional packaging signal. Thus, drives the expression of fusion library on phage coat proteins and carry the phagemid encoding that sequence. In hybrid system, the phage genome contains two copies of phage coat protein gene, one with a fusion partner and a wildtype. Specially designed promoters for these two genes allows a higher expression of wildtype as compared to the fusion protein [72,76].

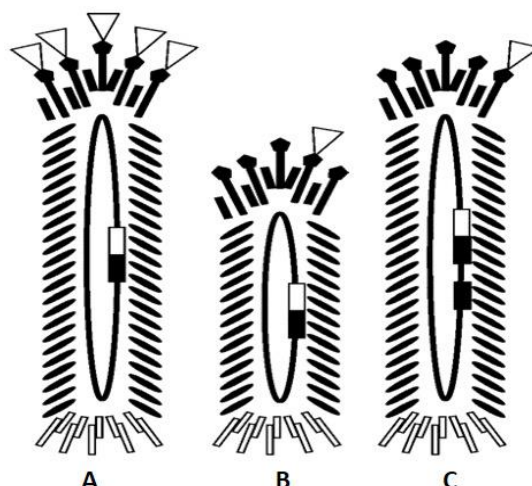


Figure 6. The three types of phage display. (A) Phage systems. The phage genome contains only one copy of pIII (black), and the displayed sequence (white) is fused to that copy. Consequently, every pIII displays the same fusion protein (triangle). (B) Phagemid systems. Instead of a phage genome, the virion contains the phagemid, which is generally smaller. Infection with helper phage drives the expression of phage proteins, and the phagemid expresses the pIII fusion library. (C) Hybrid systems [6].

5.2 Phage display Selection

Unlike the other conventional immunoscreening approaches, phage display technique is much faster as well as more cost and labour effective, requiring no special equipment. Once a phage display library has been constructed, successive rounds of selection based on affinity selection permits the enrichment and isolation of less abundant interacting proteins from a library with large diversity. Selection strategy generally involves the following steps (Fig. 7):

1. Library amplification and phage particle production
2. Enrichment by immunoprecipitation of phage particle with immobilized target.
3. Washing step to remove the unbound phages
4. Elution and amplification of bound phages by infecting host bacteria.

These biopanning rounds are repeated at least three to six times to achieve a sufficient enrichment of binding peptides. The selected peptides are then identified by sequencing their corresponding DNA [75,76].

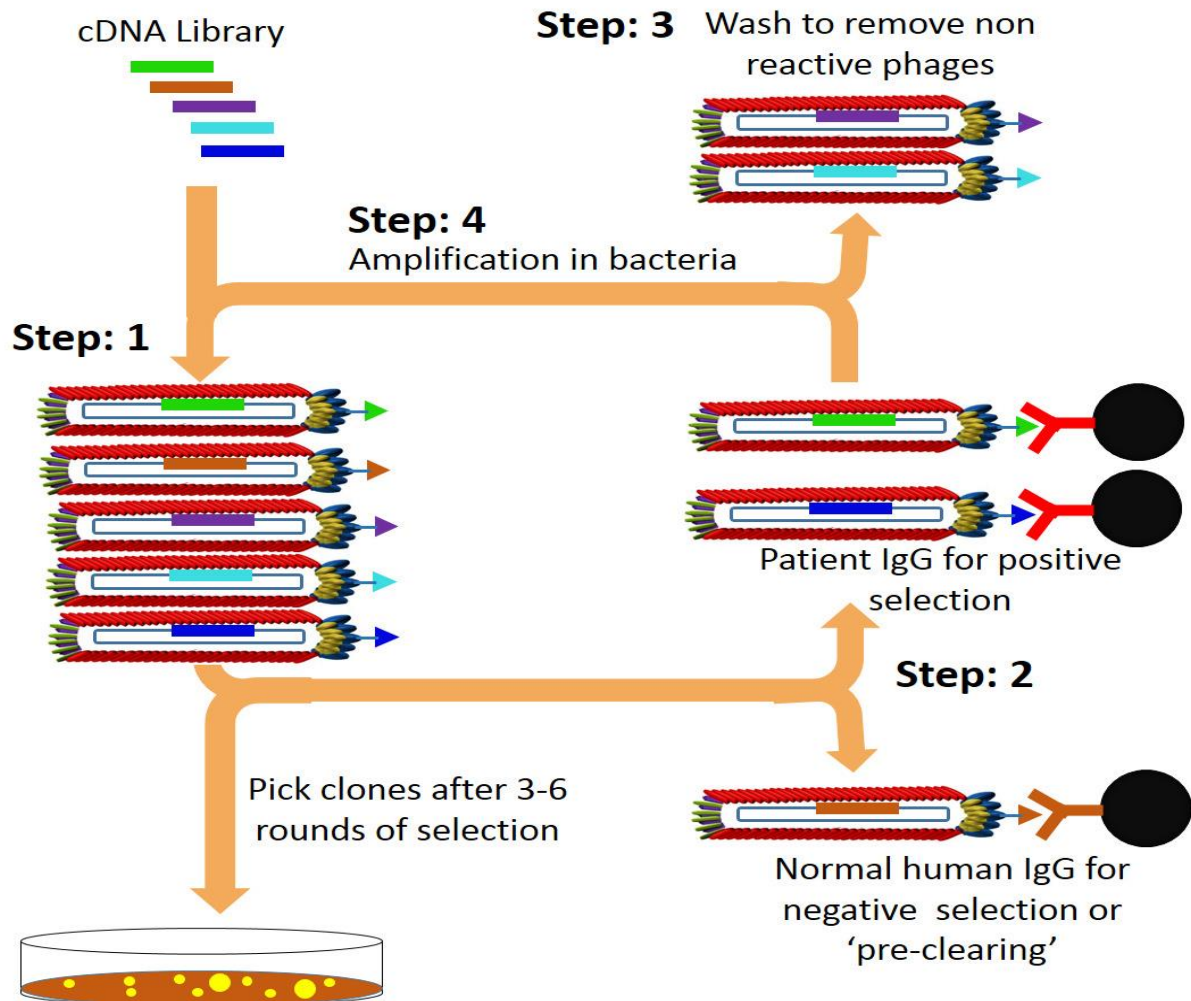


Figure 7: Phage display selection cycle. Binding protein selection from phage display libraries. Step 1: Libraries of proteins are displayed on phage particles as fusions to coat proteins. Each phage displays a unique protein and encapsulates the encoding DNA. Highly diverse libraries ($>10^{10}$) can be represented as phage pools. Step 2: Antigen-specific clones can be selected by binding to immobilized antigen followed by step 3: washing to remove nonbinding phage. Step 4: Retained phage can be amplified by infection of a bacterial host, and the amplified pool can be cycled through additional selection rounds to further enrich for antigen-binding clones. Individual binding clones can be subjected to DNA sequencing to decode the sequences of the displayed proteins [7].

5.3 Application of Phage display

5.3.1 Identification of protein-protein interactions in vitro

Over 80% of cellular proteins may work in complexes with other proteins and their protein-protein interactions are regulated by several mechanisms [63,77]. Phage display has been employed in numerous studies of protein-protein interactions. Peptide libraries have been used to determine the epitope to which an antibody binds [78]. Various strategies including genomic scale screening by

construction of fragmented whole genome and gene fragment phage display libraries allowed an in-depth characterization of the protein region involved in the interaction [79].

Phage display have also proved as a useful tool in mapping the interacting domains of the binding proteins. For instance, this technique was used to map protein-protein interaction sites between c-myc proto-oncogene product and its coactivator CBP [80]. Again, Fuh et al in 2000 successfully demonstrated the carboxyl-terminal phage display as a powerful new method for mapping PDZ domain binding specificity [81]. Phage libraries were used to identify the structural motifs recognized by major histocompatibility (MHC) molecules and could be used to determine the binding motifs of other MHC class II alleles and isotypes [82].

The capability of this approach is not limited to protein or peptide interactors, phage display have been reported to be used in identifying binding proteins for non-protein molecules like phosphatidylserine [83]. The possibility of using phage display technique in identifying protein-DNA interactions was well highlighted in the work done by X.Cheng et al. [84]. Carbohydrate-protein interaction is an important process in cell to cell recognition. Peptide phage display biopanning facilitated a positive selection of carbohydrate binding peptide [85]. In addition, Wang *et al.* 2003 demonstrated its usefulness to isolate the peptides interacting with carbon nanotubes [86]. Human bcl-2 was identified as the binding partner of a small chemical compound taxol using phage display [87].

Phage display has been used in enzymology to determine their substrate. Novel peptide inhibitor of the enzymatic activity of Human kallikrein 2 (hK2), a serine protease was identified by screening their exposed enzymatically active site of the enzyme against phage display peptide library. These peptides are potentially useful for treatment and targeting of prostate cancer by modulating pathways involving hK2 [88]. Using a combination of phage display selection and highthroughput screening methods, Wirsching and colleagues generated variants of hirudin, a thrombin-specific inhibitor, with increased protease resistance that may prove useful for hematologic disorders [89].

5.3.2 Phage display selection on live cells

Over the past decade, approaches to efficiently select phage libraries against molecules expressed on cultured cells and mouse and human tissues have evolved. Selection on living cells can be done on either monolayers of adherent cells or on cells in suspension. The basic procedure involves the

removal of unbound phage by washing and phage recovery is done by bacterial infection. In a study conducted by Doorbar et al, human platelets were used directly as targets for the selection of a peptide antagonist of the thrombin receptor [90].

In 2001 Giordano and colleagues described a new approach for the screening, selection and sorting of cell-surface-binding peptides from phage libraries. Biopanning and rapid analysis of selective interactive ligands (BRASIL) allows separation of complexes formed by the cells and bound phage from the remaining unbound phage still in the suspension. This method is based on differential centrifugation in which a cell suspension incubated with phage in an aqueous upper phase is centrifuged through a non-miscible organic lower phase. The same group further evaluated this approach by screening human endothelial cells stimulated with vascular endothelial growth factor (VEGF), constructed a peptide-based ligand-receptor map of the VEGF family and validated a chimeric ligand-mimic that binds specifically to VEGF receptor-1 and neuropilin-1 [91]. More recently, phage display selection approach was successfully applied to in vitro co-culture model of human umbilical vein endothelial cells (HUVECs) and gastric adenocarcinoma cell line resulted in the identification of peptides targeting vascular endothelial cells in gastric cancer [92].

5.3.3 In vivo phage library selection

This technique involves intravenous administration of a phage-displayed random peptide library into animals and letting them to circulate for a certain period of time to allow distribution of the clones. Then organs or tissues are collected and examined for phage bound to tissue-specific or differentially expressed disease markers. This method was first described by Pasqualini and his colleagues in 1996, to isolate peptides that are capable of mediating selective localization of phage to brain and kidney blood vessels in vivo [93]. This approach was latter used to isolate peptides recognized by the repertoire of circulating tumor-associated antibodies purified from the serum of prostate cancer patient [64]. Many more studies have used this technique to identify receptors for peptides homing to the vasculature of the lung, breast [94], placenta, white adipose tissue, pancreas, muscles, intestines, uterus and other organs. The first in vivo screening of a peptide library in human was introduced in 2002 by Arap et al [95].

5.3.4 Antibody phage display

Phage display of antibody fragments has been used successfully in generating target specific antibodies which can be useful in multiple applications including proteomics, specific drug delivery and in analysis of intracellular processes. The major advantages in using phage display is for generating antibodies with high affinity, specificity and stability which is completely independent in its nature for not immunizing any animals, especially humans and uses an in vitro selection process [96]. During the past decade, phage display library screening techniques have been developed to isolate monoclonal antibodies (mAbs) for therapeutic applications. Human antibody, Adalimumab (tradename Humira) a human IgG1 specific for human tumor necrosis factor (TNF) was the first fully human antibody used for clinical practice is an example of such antibodies approved for therapy [97-101].

5.4 Recent innovations in phage display technology

Several noticeable developments on phage display application to map protein-protein interactions were eventually implemented. Selectively-infective phage (SIP) is a novel methodology for the in vivo selection of interacting protein-ligand pairs. This is a method that eliminates the need for physical separation of specific and unspecific binders, therefore providing an efficient and rapid procedure for selection of high-affinity interactions [102]. Bacteriophage vectors have potential as more efficient gene transfer and vaccine delivery vectors because of their low cost, safety and physical stability. The attractive features offered by this system have paved the way for various attempts to develop phage as a vector for gene therapy applications [103- 106]. Another important advancement is their feasibility to use phage display technology for targeted chemotherapy to treat cancer [107].

4.5 Selection of Open Reading Frames

In such complex library, apart from cloned genes that encodes protein, there are large number of non-functional clones present. Eliminating out-of-frame DNA sequences has become desirable, and sometimes even essential for an increasing number of applications in protein engineering and genomics. Pre-screening a library to remove frame-shifted variants is an effective way to reduce the amount of molecular diversity to be assessed in subsequent steps, while simultaneously enriching for useful diversity and therefore increasing the probability of identifying a clone with

the desired function. The concept of filtering DNA for the presence of open reading frames (ORFs) was necessarily introduced to the library we used for this study (Fig 8). Most innovative among all filtering approach was to clone DNA fragments upstream of the β -lactamase gene in an appropriate vector and clones produced were selected for ampicillin resistance. This ORF enriched library was then digested or filtered based on Cre-lox mediated recombination by replacing β -lactamase gene with another gene (like phage coat protein gene) encoding ORF as their fusion partner [60, 61,178]. While these systems have proven efficient at removing frame-shifted library members, they also inevitably impart selection pressure for the folding and solubility of the protein of interest, and as it is impossible to quantify the degree of selection pressure for folding imparted by the existing systems, the risk is that functional variants will be eliminated in the course of preselection for reading frame. Systems have been described also for open reading frame selection without a prerequisite for the folding and solubility [62].

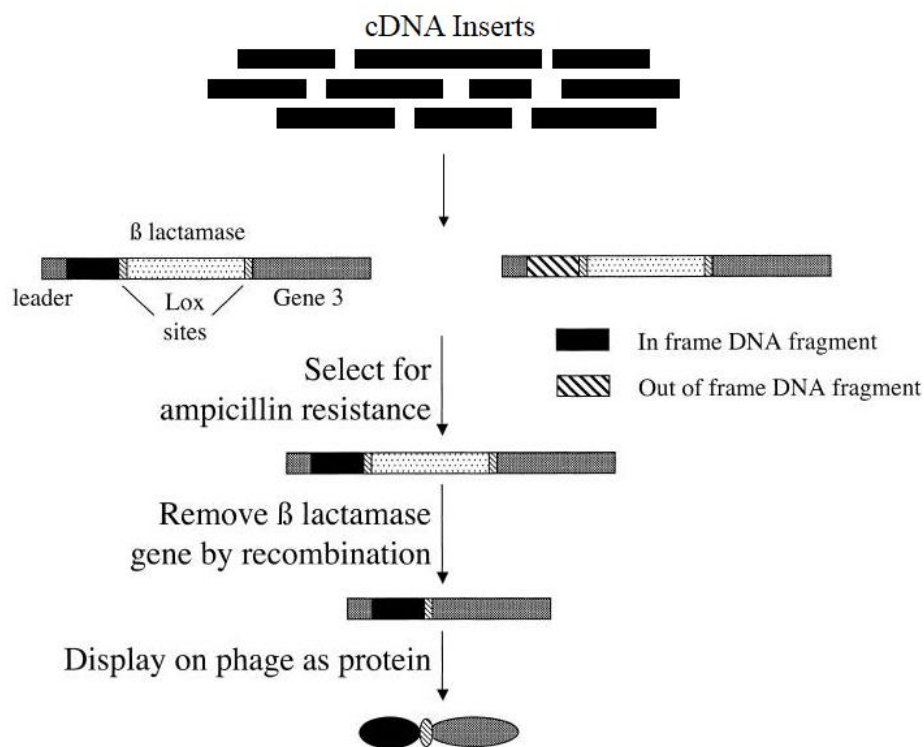


Figure 8: Schematic representation of ORF filtering: Random fragments are cloned upstream of a β -lactamase gene. Those fragments that are ORFs permit readthrough into the β -lactamase gene and confer ampicillin resistance. Those that are out of frame, or contain stop codons, do not survive. After selection on ampicillin, the β -lactamase gene can be removed by passage through bacteria expressing Cre recombinase. The selected ORF can then be displayed on phage [8].

5.6 Phage display for cancer biomarker

Expression library screening especially phage display of cDNA libraries from appropriate tissue sources has proved to be a useful strategy for identification and isolation of novel interactors. They have been relied for studies of many different cancer types including ovarian cancer. Here, the selection involves biopanning of a phage display library using immunoglobulins purified from biological fluids (such as serum or ascitic fluid) of an ovarian cancer patient as bait. Thus, allowing the identification of autologous antibodies targeting tumor antigens as a sensitive biomarker. There are limited number of reports on the use of these technologies in ovarian cancer of them most marked ones are described (Table 5).

Honami Naora and colleagues utilized phage display screening to isolate and identified tumor antigen encoded by the homeobox gene HOXB7. An up-regulation of HOXB7 expression was found to promote growth and development of ovarian carcinomas [108]. In 2004, Claudia I Vidal et al described methodology where antibody fingerprinting is a combinatorial screening in which phage display random peptide libraries are selected on in vitro pools of immobilized ascitic immunoglobulins from ovarian cancer patients. They identified the heat-shock protein 90 kDa (HSP90) as the native antigen mimicked peptide and evaluated their immune response is restricted to a subset of patients with advanced disease [109]. Later, Chatterjee et.al. used a combination of high-throughput phage display selection and protein array based serologic detection of many potential antigens and validated autoantibodies present in the sera of patients as biomarkers for ovarian Cancer. Forty-five unique antigen biomarkers where found to solely interact with ovarian cancer patients IgG but not with patient having benign gynecologic syndromes. These includes some known antigens, RCAS1, signal recognition protein- 19, AHNAK-related sequence, nuclear autoantogenic sperm protein, Nijmegen breakage syndrome 1 (Nibrin), ribosomal protein L4, Homo sapiens KIAA0419 gene product, eukaryotic initiation factor 5A, and casein kinase II, as well as many previously uncharacterized antigenic gene products having a known or suspected association with cancer. The experiment resulted in an average sensitivity of 55% and specificity 98% with all the identified antigens. While, an average sensitivity and specificity of 32% and 94% respectively was resulted from the top 6 of the most specific clones [110]. More recently, an in vitro screening approach by phage display library was used to isolate a novel peptides ZP1 (sequence SVSVG MKPSRP) which specifically bound to its target human ovarian tumor cell line SK-OV-3 and therefore suggests its potential for targeted drug delivery in ovarian cancer

therapy [111]. In the same year, S.Charoenfuprasert et.al identified salt-inducible kinase 3 (SIK3) as a TAA through screening of a random peptide library in the phage display system. This novel ovarian TAA promotes G1/S cell cycle progression when overexpressed and shown to have a cytoplasmic localization specifically in the tissue obtained from ovarian cancer patients. Clinical study on this antigen resulted in survival advantages to cancer cells for growth and correlates the clinicopathological conditions of patients with ovarian cancer [112].

Technique	Antigen Source (cDNA Library)	Autoantibody Source	TAA	Ref
Phage Display	Human ovarian cancer cell line	Serum	HOXB7	[108]
	Random peptide library	Ascite	HSP90 mimic peptide	[109]
	Human ovarian cancer cell line	Serum	RCAS1	[110]
			Signal recognition protein-19	
			AHNAK-related sequence	
			NASP	
		Nijmegen breakage syndrome 1		
		Ribosomal protein L4		
		Homo Sapiens KIAA0419 gene product		
		Eukaryotic initiation factor 5A		
		Casein kinase II		
		Chromodomain helicase DNAbinding protein 1		
	12-mer phage display random peptide library	Human ovarian tumor cell line. to isolate cell surface-bound peptides binding specifically to SK-OV-3 cells	SVSVGMPKPSRP	[111]
	Random peptide library	Ascite	SIK3	[112]

Table 5: Biomarker for ovarian cancer identified by phage display [5]

6. Protein Microarray

Protein arrays provide a powerful tool to examine interactions between proteins (including antibodies), peptides, DNA/RNA or chemical compounds on a large scale. Here, such arrays would contain collections of microscopic analyte spots at high density usually between 500 up to a million different proteins are immobilized in an orderly manner to a solid surface. Further, by applying conventional hybridization processes, expression levels or interaction events are measured [113].

There are three general types of protein array (Fig 9):

i) Functional protein microarrays, constructed by immobilising large sets of purified proteins or an entire proteome are screened for a wide range of biochemical functions, such as protein-protein, protein-DNA, protein-small molecule interactions and enzyme activity, and to detect antibodies and demonstrate their specificity. It comprises protein/peptide/antigen microarrays.

ii) Analytical microarray, where primarily antibodies, antibody mimics, affinity reagents, but may also be nucleic acid aptamers are arrayed and used to evaluate the presence and concentrations of proteins in a complex mixture such as plasma/serum or tissue extracts. It comprises antibody microarrays.

iii) Reverse-phase microarrays employ the complex samples such as tissue lysates are printed on the surface (the bait) to capture antibodies (the prey). In the case of lysates from cancer tissue or cell lines as source of the bait, proteins require liquid phase fractionation, incorporating isoelectric focusing and reverse-phase liquid chromatography (LC), prior to printing onto an array support. It comprises lysate microarrays.

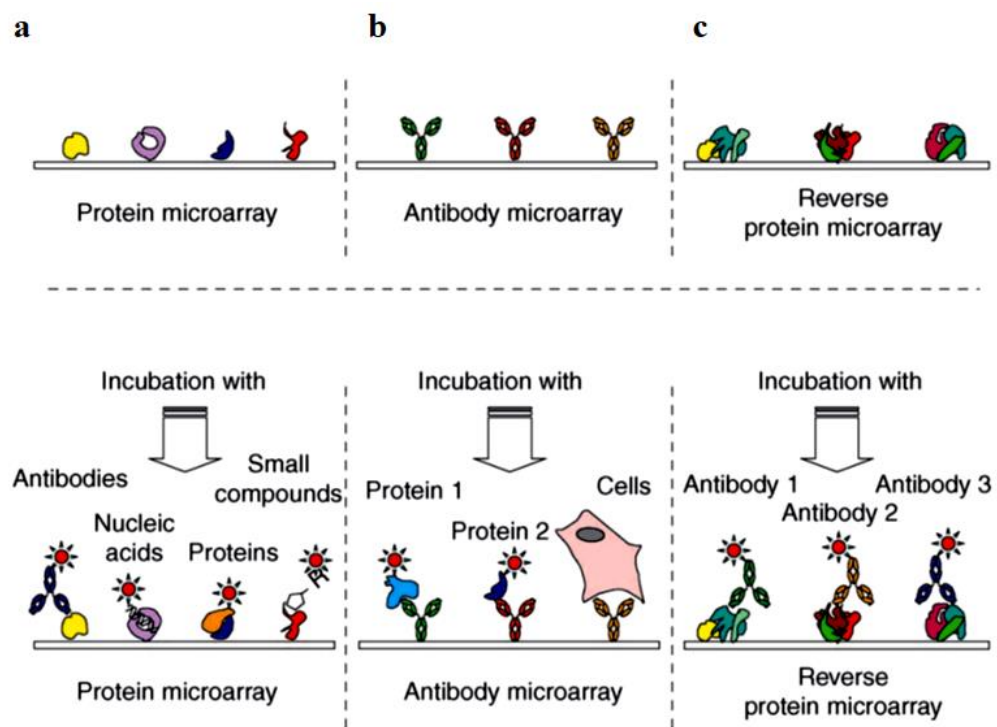


Figure 9: Types of protein microarrays and their possible applications. a) Protein microarrays (PMAs), consisting of individual recombinant proteins; b) antibody microarrays (AMAs), consisting of antibodies or fragments; and c) reverse protein microarrays (RPMAs), consisting of whole or fractionated protein lysates/extracts. All the three types of arrays are screened for their ability to bind with known or putative directly labeled interaction partners [9].

6.1 Protein microarray production

There are several concepts to be taken into consideration when manufacturing or analyzing a protein array.

6.1.1 Printing methods

To generate protein microarrays, materials have to be spotted or deposited at defined xy coordinates onto the substrate of choice, generally a glass slide which has been modified or coated in some manner. This process has to be highly precise ($\pm 2 \mu\text{m}$) and robotics are typically used to transport solutions from sources (e.g., 384 well plates) to slides. The amount of solution deposited per spot is typically a few nanolitres and thus 10 μL of a solution will provide sufficient material for over 2000 chips or microarrays. The fact that such tiny amounts of material are required is one of the major advantages of microarrays. Protein microarray production is typically achieved in one of these ways: contact printing [114,115], inkjet and bubble-jet printing [116,117], piezoelectric [118], electrospray deposition [119], photolithography [110-112]. All these systems provide environmental controls, which includes temperature and humidity as well as maintaining all parameters such as contact time, distance between spots etc.

6.1.2 Protein immobilisation considerations, formats and surfaces

The right choice of the proper substrate is important when setting-up a protein array system. There are some crucial features that are needed to be fulfilled while choosing a slide. The best surface requires optimal binding conditions to conserve the protein functionality during immobilization enabling protein in their correct orientations and maintaining their three-dimensional structural conformation. A high binding capacity with low unspecific background to accommodate proteins of varying composition will be an advantage [123]. To meet the requirements of protein microarrays, several surfaces have been proposed, which can be divided into three major groups as shown in table 6 [124]

	Surface chemistry	Surface coating
2D slides	Amine slides	Amine groups
	Aldehyde slides	Aldehyde groups
	Epoxy slides	Epoxy groups
	Mercapto slides	Mercaptopropyltrimethoxysilane groups
	MaxiSorb slides	Polystyrene-based modified surface
3D slides	Hydrogel slides	Modified polyacrylamide gel
	Agarose slides	Agarose gel
	Polyacrylamide gel	Polyacrylamide gel
	FAST slides	Nitrocellulose-based matrix
	SuperProtein slides	Hydrophobic polymer
Other	PEG-epoxy slides	Polyethylene glycol layer with reactive epoxy groups
	Dendrimer slides	Dendrimer layer with reactive epoxy groups or carbonyldiimidazole
	BSA-NHS slides	Bovine serum albumin activated with <i>N</i> -hydroxysuccinimide
	Ni-NTA slides	Nickel-nitrilotriacetic acid complex
	DMA-NAS-MAPS slides	<i>N,N</i> -dimethylacrylamide, <i>N,N</i> -acryloyloxysuccinimide, [3-(methacryloyl-oxy)propyl]trimethoxysilyl copolymer
	Streptavidin slides	Streptavidin
	Avidin slides	Avidin

Table 6: Different types of protein microarray surfaces [6]

6.1.3 Detection methods

The detection methods available to detect interactions are generally depend on the microarray format and substrate. They are basically divided into two: i) Labelled probe method: they are conventional methods that usually use fluorescent, chemiluminescent, colorimetric or radioactive detection. Fluorescence is used primarily for its high sensitivity and excellent dynamic range to produce quantitative results [125,126]. ii) label-free methods, including mass spectrometry (MS) [127], surface plasmon resonance (SPR) [128], atomic force microscopy (AFM) [129], microelectromechanical systems (MEMS) [130] and quartz-crystal microbalance analysis (QCM) [131]. Although label-free detection technologies are highly desirable, their availability and sensitivity have not been high enough to have come into common use for functional protein microarrays. Many new strategies have been developed, in particular to achieve higher levels of sensitivity. For example, Rolling circle amplification (RCA) generates a localized 1000 fold higher fluorescent signal via amplification of an oligonucleotide circle carried by the secondary antibody [132, 133].

6.2 Applications of Microarray

All array types have uses in diagnostics (biomarkers or antibody detection) and discovery research. Protein microarrays allow the detection of specific antibodies in biological fluids such as serum or ascitic fluid against a very large number of targets simultaneously. Typically, a complex mixture would be applied to arrays of possibly thousands of specific binders, and the individual bound analytes detected in parallel by appropriate labelling and scanning. In proteomics, array can be used for expression profiling to compare the levels of proteins in different samples. Arrays can also be used as high throughput platform to determine patterns of antigens recognized by autoantibodies during the course of diseases, such as autoimmunity or cancer, as well as a way to characterize the repertoire, so called ‘autoantibody signatures’ that may represent disease subgroup or to monitor immune responses in healthy individuals. Here, the samples to be analysed themselves will find their target depending on the binding properties and screened for cross reactivity against many proteins, which can also be done in a multiplex array format against multiple protein targets.

6.3 Application of protein array in discovery of autoantigens in cancer

In the field of oncology, protein arrays offer huge potential as tools for the identification of cancer biomarkers, in particular auto-antibody/antigen markers. The identification of tumor associated antigens (TAAs) recognised by the patient's immune system represents an exciting approach to identify novel diagnostic cancer biomarkers and to contribute towards a better understanding of the molecular mechanisms involved. Circulating autoantibodies have not only been used to identify TAAs as diagnostic/prognostic markers but to determine their potential as therapeutic targets (Table 7). In a study conducted by Xiaoju Wang et al, identified a panel of 22 phage derived peptides was identified, discriminating autoantibody signatures in prostate cancer compared to the control group with a sensitivity of 88.2% and 86.1% specificity. Autoantibodies against peptides derived from prostate-cancer tissue could be used as the basis for a screening test for prostate cancer [134]. Tumor-associated antigen arrays represent an excellent platform to profile autoantibody for the enhanced detection of early stages of tumors and permit monitoring of the efficacy of treatment [135].

In earlier studies of Gil Mor et. al reported to identify 4 serum protein markers for early diagnosis of ovarian cancer. A combination leptin, prolactin, osteopontin, and insulin-like growth factor-II

initially analyzed by microarray and eventually these potential biomarkers were evaluated by ELISA, as alone as well as in combination. Finally evaluated with a different cohort and analyzed by multiple statistical approaches in a blind manner and resulted in sensitivity of 95% and specificity 95% when used in combination. They claimed to discriminate between a healthy and EOC patients, including patients diagnosed with stage I and II disease, with high efficiency (95%) [132].

In a similar study conducted by M A Hudson et al in 2007, used protein microarray (V3.0, Invitrogen) with 5005 human proteins to identify proteins aberrantly expressed in ovarian cancer when probed with sera from various stages of ovarian cancer patients. Lamin A/C, SSRP1, and RALBP1 were found to be candidate tissue markers and exhibit an increased expression in the cancer tissue relative to controls when immunostained. Suggesting, these are useful marker for biopsies but not for routine screening of fluid samples from patient [136]. Later, C.G Gunawardana and colleagues used protein microarray technology to identify autoantibody signatures in ascitic fluid collected from ovarian cancer and fifteen potential tumor-associated antigens were discovered. Among all, AASDHPPT showed the strongest signal-to-noise ratio [126].

Conversely, Gnjjatic and colleagues used a commercially available protein microarray (V4.0, Invitrogen) with 8277 human proteins to identify autoantibodies in ovarian cancer and pancreatic cancer sera. Of the arrayed proteins, 202 proteins demonstrated a greater immunoreactivity and stronger fluorescent signal in ovarian cancer patient sera compared to 29 in pancreatic cancer, with few overlaps. They also determined correlates of autoantibody signatures as potential good or bad prognostic antibody responses against different combination of antigens [125].

More recently, array defined autoantibody reactivity towards nucleophosmin, cathepsin D, p53, and SSX were identified as common antigens for patients at each stage (I–IV) of ovarian cancer were significantly higher than for controls when compared to healthy or benign ovarian disease. Furthermore, mean autoantibody level against placental-type alkaline phosphatase, TAG 72, survivin, NY-ESO-1, GRP78 and Muc16 (CA125) was significantly different and allowed the differentiation between Stage III/IV and early stage ovarian cancer [137].

The success rates of phage display methods were critically improved with the introduction of protein microarray screening as concluding steps of phage selection. Here, selected phage derived proteins were arrayed on slides and immunoscreened by protein microarray to identify antigens specifically recognized when challenged with patient samples. These recent developments permit

a drastic reduction in the large collection of protein derived from phage expression systems and to focus on several hundred to a few thousand which were identified with high potential and validate these in larger cohorts of patients using protein arrays. This was very well demonstrated in a study to identify autoantibody signature in prostate cancer [134]. In 2006, Chatterjee et.al successfully used this same approach to evaluate the potential of a large panel of tumor antigens as biomarkers for a serum-based screening test that can detect the presence of epithelial ovarian cancer. The author also describes this as a global approach to antigenic profiling, epitomics, has applications to cancer and autoimmune diseases for diagnostic and therapeutic studies [110].

As summary, protein microarrays are suited for detecting autoantibody responses. Moreover, their ease of use, the low amounts of reagents and sample required and the number of molecules that can be tested per array make them ideal for multiparametric testing.

Technique	Array Format	Autoantibody Source	TAA	Ref
Protein Microarray	169 protein in RCA Microarray	Serum	leptin, prolactin, osteopontin, and insulin-like growth factor-II	[132]
	protein microarray (V3.0, Invitrogen) with 5005 human proteins	Serum	Lamin A/C, SSRP1, and RALBP1	[135]
	ProtoArrays® Invitrogen	Ascitic fluid	L-aminoadipate-semialdehyde dehydrogenasephosphopantetheinyl transferase (AASDHPPT)	[126]
	V4.0, Invitrogen) with 8277 human proteins	Serum	202 Autoantigens	[125]
	Phage derived Peptide/protein	Serum	RCAS1 Signal recognition protein-19 AHNAK-related sequence NASP Nijmegen breakage syndrome 1 Ribosomal protein L4 Homo Sapiens KIAA0419 gene product Eukaryotic initiation factor 5A Casein kinase II Chromodomain helicase DNAbinding protein 1	[110]
	Ovarian cancer cell line (exosome derived) dot blot array	Serum	Nucleophosmin, cathepsin D, p53, SSX Placental-type alkaline phosphatase, TAG 72, survivin, NY-ESO-1, GRP78 and Muc16 (CA125)	[137]

Table 7: Autoantigens in ovarian cancer identified by Protein Microarray.

7. Rationale of the project

Ovarian cancer is the fifth most common cancer among women and is major causes of death from gynaecologic cancer. Each year, approximately 238000 (3.7% incidence of all cancer cases) new cases of ovarian cancer were diagnosed worldwide (as estimated by GLOBCAN project in 2012) accounting for more than 151000 (4.3% of all cancer mortality) deaths in women [1]. This is due to the lack of reliable and effective early detection methods, since majority of early-stage of these cancers are asymptomatic and are detected at later stages, after they have invaded the surrounding tissues [23]. Most often, metastasis of ovarian cancer occurs through the cells which they shed into the peritoneal cavity. Since there is no anatomical barrier exist in peritoneal cavity, these tumor cells metastasize once they are embedded/implanted to peritoneal surface and advance to pelvic organ (Stage II), the abdomen (stage III) or beyond the peritoneal cavity (stage IV) [14,21]. Only 25% of ovarian cancers are diagnosed in the early stage (Stage I) while they are confined to the ovaries. Up to 90% of stage I ovarian cancer patients can be cured by currently available therapy. The cure rate become narrowed down to less than 20% when diagnosed at an advances stages of this cancer [23]. These numbers mentioned above clearly support the need for new efficient biomarkers for early diagnosis.

Although the diagnosis, treatment and survival of this heterogeneous, genomically unstable and highly lethal disease in women is based on clinical features such as tumor size, histological subtypes, FIGO stage, differentiation grade and the presence of genetic markers (Such as BRCA1 mutations) or proteins markers in biological fluids. The response to the treatment greatly varies among the patients even though they presents similar clinical features. The major detection approaches for ovarian cancer includes transvaginal ultrasonography (TVUS), serum markers and a combination of the two [21]. Cancer antigen-125 (CA-125) is the most extensively investigated and currently been used for the serum based screening of epithelial ovarian cancer (EOC). Although CA-125 is well characterized tumor biomarker specific to EOC, they have a limited ability to detect early stage of this disease and hence used to monitor the effectiveness of the treatment [138,139].

In past years, studies have revealed the presence of circulating autoantibodies specific to a number of tumor-associated antigens (TAAs) in human [64,140]. These tumor-associated antigens absent in a normal cell may elicit a very early host immune response in course of tumor development, this feature could be made use to develop biomarkers which can detect autoantibodies which are

stable and abundant even at the early stage of tumor [110]. Thus, identification of these TAAs could lead to the discovery of important molecular pathways involved in the development of ovarian cancer, and may give insights regarding the onset of tumorigenesis and therapeutic strategies. Moreover, TAAs have been already demonstrated to be an effective and sensitive means of cancer screening and diagnosis [112]. Using TAAs as biomarker for cancer could be superior of choice, since they are capable of measuring varying level of immune response in reasonably short time. Despite from all these advantages, these TAAs can be used for targeted immunotherapeutic treatments and might require for vaccine development in the far end of this study [65]. Very few tumor-associated antigens have been identified to-date, offering a promising area yet to be explored.

Accumulation of ascitic fluid in peritoneal cavity is a characteristic feature of ovarian cancer. Since it remain in closer or direct contact with the disease site, ascetic fluid is an optimal source containing secrete proteins, antibodies against these secreted or leaked proteins or peptides from tumoral tissue, soluble growth factors that have been associated with invasion and metastasis. Thus making ascitic fluid an excellent reservoir to study various biological aspects of the underlying tumor and equally important for the identification of prognostic and predictive biomarkers and for molecular profiling analysis of various tumors including ovarian cancer. To date, there exist no systematic analysis to characterize ovarian carcinoma ascites.

The recent advance in the field of discovery technologies made it possible to profile molecular signature in any autoantibody/autoantigen related pathologies including cancer and autoimmune disease simultaneously during the progress of the disease. In this study, we utilized a combination of technologies that combines phage display selection and immunoscreening protein microarray allowing a highthroughput analysis of a large set of analyte. Our laboratory have already demonstrated the usefulness of this approach in the identification of molecular targets in various autoimmune diseases [141]. An extensively characterized cDNA phage library was used in this study consists almost every genes present in the human genome. More information about the library is described in the result section of this thesis. To this extend, we applied our technological platform for the high-throughput profiling of ovarian cancer ascites with an intention to overcome the difficulty to detect their molecular targets or tumor antigens, which are present in lower abundance and consequently increased the specificity to a few fold magnitude.

8. Objective of the research

After completion of the sequencing of the human genome, scientists shifted their attention to the products of the genome, the proteins, in the hope of development of personalized medicine and diagnosis. The term “proteome” was coined as a linguistic equivalent to the concept of “genome”; it is used to describe the entire set of proteins expressed by genome of the cell, tissue or an organism at a particular time or throughout the lifetime. The proteome is highly dynamic by nature with complex molecular system that requires accurate methodologies to study the interactions between this large numbers of components and which is referred to as the “proteomics”. Advances in proteomic technologies allow the large-scale determination of gene and cellular function directly at the protein level in a highthroughput format. The field of proteomics is a collection of various technical disciplines, leading to a sensitive analysis of complex interactions network such as those established during the immune response [142].

With the intention to profile ovarian cancer antibody repertoire in a systematic manner, we propose a novel approach by combining different technological platform which enables the identification of the interactors/molecular signature of disease from a high degree of complexity and present in low abundance with high sensitivity. In addition, to determine the clinical implications of identified interacting antigen specifically expressed by tumor cells as a prognostic tool to predict the cancer survival. The key steps involved in highthroughput profiling of ovarian cancer ascitic fluid are:

- Characterize ascitic fluid collected from various disease conditions based on their antibody response against antigens present in ovarian carcinoma cells.
- Isolation and identification of immune reactive antigen
- Validation of the novel antigen and their clinical correlation
- Surface targeting antibody and CDC mediated regulation of tumor growth

9. Project Summery

In this study, we present a systematic and in-depth profiling of ovarian cancer ascites. Thus, to isolate and identify the antigens recognized by ovarian carcinoma ascites antibodies. In addition, to validate and evaluate these selected antigens for their clinical correlation in the disease. The ascites represents an optimal source for molecular profiling of ovarian cancer. We ranked ascitic fluid for its reactivity by characterizing them for their antibody response against cellular antigens in ovarian cancer. The most reactive ascites were chosen for further investigation. To this extent, we utilized a highthroughput protein expression and screening platform that combines cDNA phage display library selection and proteins microarray approach were used to profile ascitic fluids. Phage libraries of open reading frame (ORF) fragments created from mRNA derived from various tissues were used. Here, cDNAs are expressed as fusion proteins with one of the phage coat proteins and exposed on the surface of the phage thus allowing the selection with antibody present in ascites collected from ovarian cancer patients, which were identified as most reactive [64-69, 108-112]. Successive rounds of biopanning allowed the patient antibodies to select their own ideal binding peptide and isolation of these less abundant interacting proteins from a library with large diversity. Phage display selected peptides were further screened for their immunoreactivity by protein microarray analysis. Further, microarray identified antigens were validated by indirect ELISA, since these immunological techniques are able to detect the presence of specific antibody even at very low concentration [143]. Subsequently, correlates of autoantibody signatures with known tumor expression of corresponding antigens, prognostic value and patient survival outcome were examined. Moreover, we demonstrate the presence of autoantibody in ascites targeting cell surface antigens expressed by tumor cells and determined its role in controlling tumor growth by activating complement system.

Chapter 2

10. Results

10.1 Introduction to results

To date, there is no systematic analysis of the antigens recognized by ovarian carcinoma ascites antibodies. To address this issue we designed a comprehensive discovery and validation strategy, outlined here (Fig 10):

- 1) **cDNA library construction from human tissues:** The cDNA is filtered to retain only clones encoding Open Reading Frame (ORF) fragments which are then displayed on filamentous phage.
- 2) **Characterization based on autoantibody response:** This involves an initial examination of the ascites from cancer patients using tissue culture cells or their extracts as source of antigens in Western blotting, whole cell ELISA, cell lysate ELISA assay and by indirect immunofluorescence on whole cells. With these immunotechniques, we identify ascites which have high-titer fluorescent staining or strong signals to cell extracts and subsequently use the purified antibodies to isolate ORF displaying Phages.
- 3) **Selection of immunoreactive antigens:** Phages displaying proteins are immunoprecipitated with ascites antibodies from ovarian cancer patients through cycles of selection and amplification.
- 4) **Immunoscreening by protein microarray:** Putative antigens are cloned and expressed as GST-fusion proteins and immunoscreened by independent sets of cancer and control antibodies by protein microarray.
- 5) **ORF sequencing:** The antigens, screened by protein array were identified by sequencing.
- 6) **Validation by ELISA:** ELISA was performed to determine whether the antibodies present in the ascitic fluid from the ovarian cancer patients were specifically recognized by the selected peptides derived from the screenings.
- 7) **Clinical correlation:** Clinical correlation of overall survival of the patients with the presence of specific antibodies against the identified novel antigens was determined.

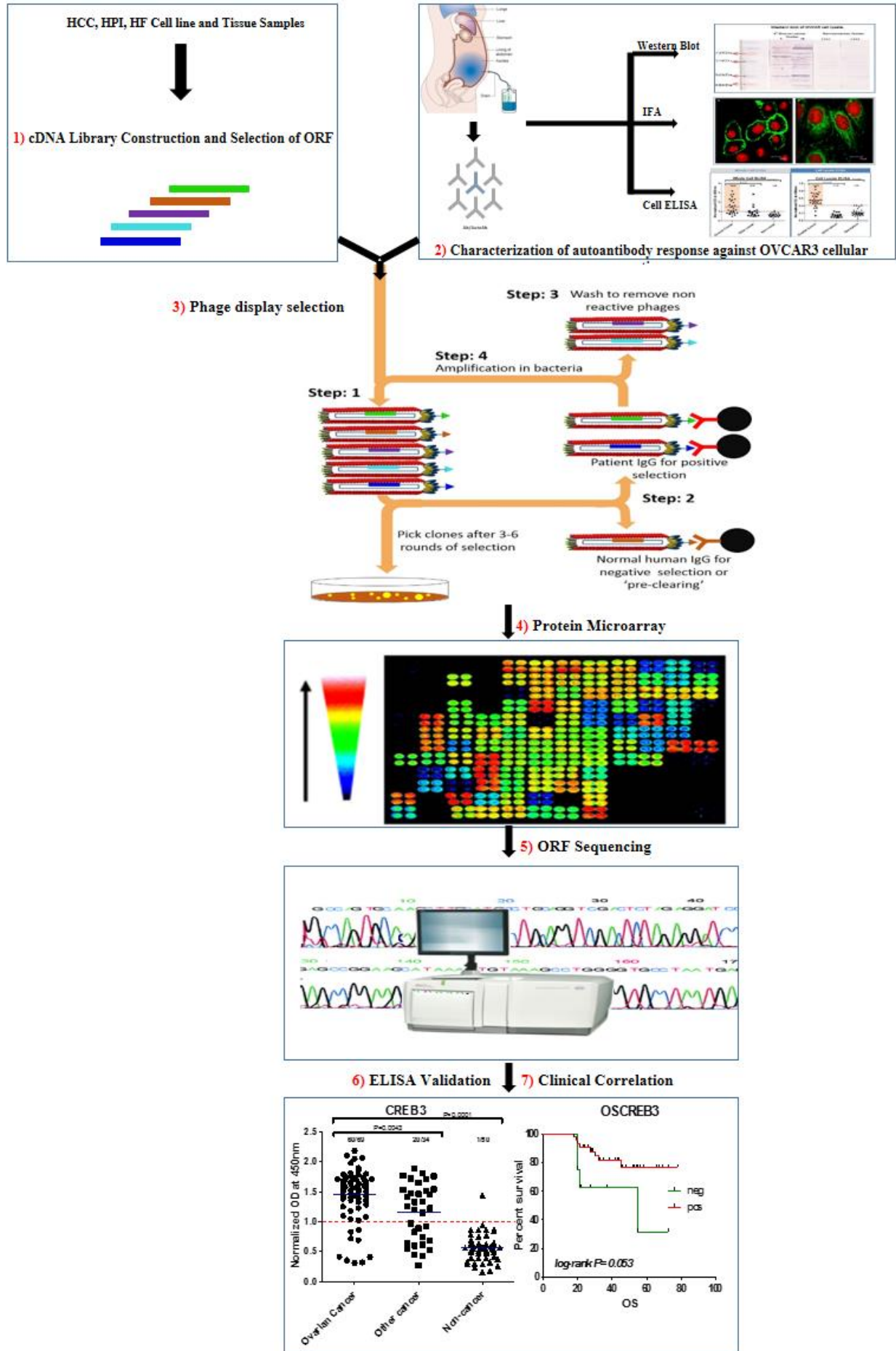


Figure 10: Workflow of the project. 1) construction of cDNA library from appropriate tissue or cells followed by filtration of cDNA to retain only clones encoding Open Reading Frame (ORF) fragments which are then displayed on filamentous phage. 2) Characterization of ascitic fluid base on the autoantibody response against ovarian carcinoma cellular antigens. 3) Most reactive ascites antibodies were used for phage display selection to immunoprecipitate the interacting peptides displayed on filamentous phages. 4) Protein microarray approach to immunoscreen a large set of phage-selected peptides expressed as fusion protein simultaneously with ascitic fluid from various disease conditions. 5) Cancer specific antigens immunorecognised by protein microarray were identified by sequencing corresponding antigenic clones. 6-7) Novel putative antigens were validated by ELISA and their clinical correlation was determined.

10.2 cDNA Library construction and characterization

The cDNA phage library used in this study was constructed and extensively characterized as described in Di Niro et al [60]. The library was constructed using cell lines and tissue samples from three different source: colon carcinoma (HCC), fibroblasts (HF) cell lines (representing intestinal cell components) and isolated pancreatic human beta cell (HPI). mRNA from three different source (HCC, HF and HPI) was isolated and mildly fragmented by optimal heating to obtain calibrated fragment length ranging from 100 to 700 bp with an average of 350 bp prior to reverse transcription with an ideal concentration of random primers. The resulted single-stranded cDNA was then normalized individually with a corresponding mRNA. Later asymmetric adaptors with BssHII or NheI restriction site at 5' or 3' end, respectively was added. This step ensures a correct sense orientation of these cDNA fragments. Finally, the cDNA library was cloned upstream of the beta lactamase gene of pPAO filtering vector and clones encoding ORFs were filtered out using ampicillin selection. Consequently, cDNA library of approximately 2×10^6 clones was generated. This ORF enriched library was endured to Cre-lox mediated recombination by replacing β -lactamase gene with phage coat protein gene, thus encoding ORF as their fusion partner and used to perform selection. The genetic composition of the selected library was characterized by 454 sequencing to assess both quality and diversity: more than 21,000 genes were found to be represented with an efficient normalization of gene abundance.

Total Number of Sequences	1.5 million
Average Length	245
Genes	More than 21,000

Table 8: Gene abundance. cDNA fragments from selected phagemids were identified and ranked by 454 sequencing. The reads were mapped onto the human genome reference sequence using GMAP software and sequence and the corresponding mapped genes were identified.

10.3 Sample preparation

Ascites were collected from 153 patients representing various disease conditions that includes:

- Ascites from patients diagnosed with ovarian cancer (69),
- Other cancers (34) and
- Non-cancerous control ascitic fluid (50) from female patients with no known history of cancer (Table 9).

Sets of Ascitic fluid	Classification	Application Used	No: Used
Ascitic Fluids (153 samples)	<ul style="list-style-type: none"> - Ovarian cancer (69) - Other cancer (34) - Non-Cancerous control (50) 	Western Blot	20 samples
		IFA	10 samples
		Cell lysate ELISA	74 samples
		Whole cell ELISA	74 samples
		Phage display Selection	7 samples
		Protein Microarray	17 samples
		ELISA Validation	All 153 samples

Table 9: Summary of ascetic fluids used: A total of 153 ascitic fluids used were further classified into three groups based on the patients from they were collected; ovarian cancer, other cancer and non cancerous conditions. Numbers in brackets indicate the number of patients for each group. The number of ascites used for all different application are also indicated.

In our preliminary experiments using ascitic fluid in its natural state, we observed a hindrance due to presence of abundant proteins such as human serum albumin. Hence, the IgG fractions of the ascitic fluids samples were affinity purified with Protein A. Figure 11A gel loaded with equal volume of unpurified ascites shows presence of high concentration of HSA (66.5KDa) in comparison with immunoglobulins (50KDa heavy chain and 25KDa light chain). Affinity purification with protein A resin enabled to remove serum albumin (HSA), the major component and other components including cell debris (Fig 11B). Purified IgGs were quantified and check on a SDS-PAGE gel [Fig 11 A-B]. From the quantification, it can be seen (Fig 11 C) that various samples shows considerable variability in their concentration of IgG ranging from 8 to 1 μ g/ μ l with an average of 3 μ g/ μ l. Quantified IgG were normalised to 1 μ g/ μ l (Fig 11 C-D) and were used for the proceeding experiments.

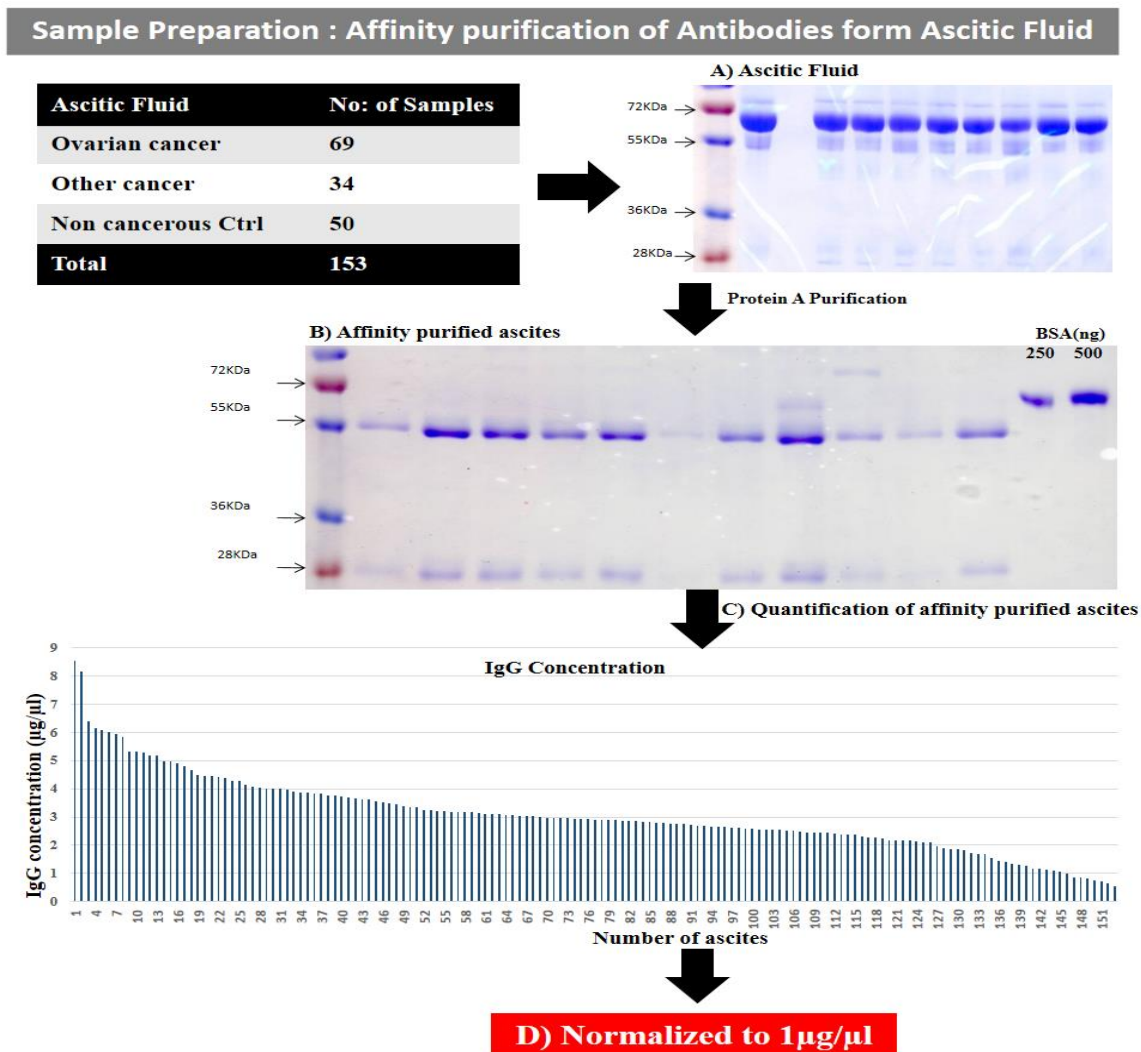


Figure 11: Affinity purification of immunoglobulins: A) SDS-PAGE gel shows ascitic fluid prior to purification. B) Gel showing the immunoglobulins obtained after purification of ascites using protein A agarose. C) The graph shows the varying range of purified IgG concentration after purification. D) All IgG purified from ascites were normalized to a concentration 1µg/µl and were used for all proceeding experiments. group of samples of IgG.

Ovarian cancer ascitic fluid represents stage I-VI collected from both platinum sensitive and resistant patients with grade ranging from G1-G3. Cancer other than ovarian cancer includes cancer of lung, liver, colon, fallopian tube, breast, gallbladder, pancreas, rectum, lymph nodes, lymphoma, various mesothelioma including peritoneal lining, adenocarcinoma of pulmonary, gastric and other organs. While, non-cancerous ascites collected from patients having conditions such as cirrhosis caused by various reasons, pulmonary fibrosis, cholestatic liver diseases, pneumonia, accumulation due to various transplantations, heteroplasia, inflammation etc.

10.4 Characterization of ascitic fluid based on autoantibody response

To identify the presence of an anti self-antibody signature in the samples from cancer patients and controls were analyzed by Western blotting and ELISA (using extracts of tissue culture cells as source of antigens) as well as by indirect immunofluorescence on whole cells.

10.4.1 Western blot of ovarian cancer cell lysate

The occurrence of antibodies targeting proteins in OVCAR-3 cell extract was investigated initially by Western blotting. An equal amount of OVCAR cell lysate was loaded into each well and later transferred to a nitrocellulose membrane. Recognition of the antigen was compared between twenty IgG purified and normalized ($1\mu\text{g}/\mu\text{l}$) cancerous ascites and controls. In figure 12 four representative nitrocellulose membrane strips incubated separately with purified ascites, two each from ovarian cancer (#3, #18) and noncancerous control (#1201, #1202). The result (Fig 12) shows that cancer derived ascites recognized a higher number of antigen present in OVCAR3 cells compared to controls, verifies the presence of tumor specific antibodies targeting ovarian carcinoma cellular antigens. Although, the ascites #3 and #18 collected from ovarian cancer, pattern of antigen recognized are very different from each other with few common bands in varying intensity. Therefore, a more quantitative and reproducible methods was adopted to better understand the immunoreactivity of the full panel of purified ascites using a minimal volume as possible.

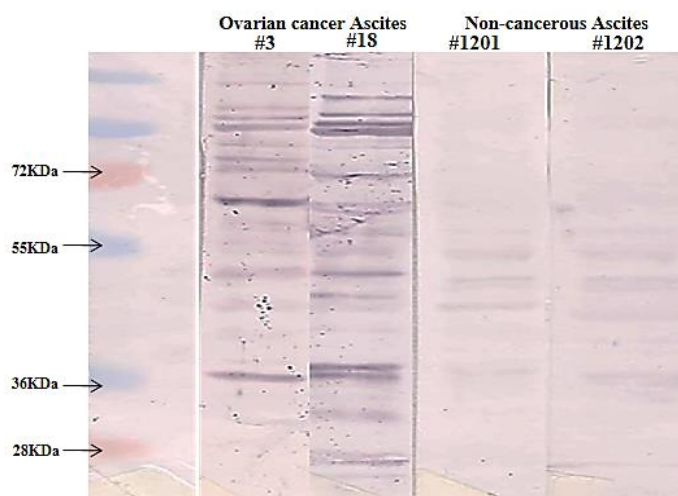


Figure 12: Western blot of OVCAR3 cell lysate. Each strip contains equal amount of OVCAR3 cell lysate and were incubated separately with IgG purified ascites. Ascites #3 and #18 from ovarian cancer patient. #1201-#1202 are non cancerous controls. The immunoreactivity detected with anti human IgG AP conjugated secondary Ab.

10.4.2 Ovarian cancer whole cell ELISA

Whole cell enzyme linked immunosorbent assay is convenient method that can accurately quantify both soluble as well as insoluble intracellular proteins/ tumor associated antigens in cultured adherent cells as well as a possible alternative to immunohistochemical characterization of tumors [144]. OVCAR-3 cells were grown and fixed on a 96-well plate. Targets of interest are detected by primary antibodies purified from ascitic fluid, which are in turn are quantified with α -human immunoglobulin labeled secondary antibody. The cell-ELISA experiments were performed in triplicate for each sample and the results were reproducible. For each experiment, the cut-off value was calculated as cumulative mean + 2 SD (standard deviation) of the absorbance from non-cancer control samples. As shown in figure 13, eighteen out of twenty-eight IgG samples from ovarian cancer gave a signal above the cut-off value, indicating that they do recognize targets present in OVCAR3 cells. While IgG samples from other cancer types were less reactive as only 6/18 were above the cut-off. Only 1 out of 28 non-cancerous samples was positive, others were shown to be below the cutoff value and indicating the absence of tumor specific antibody.

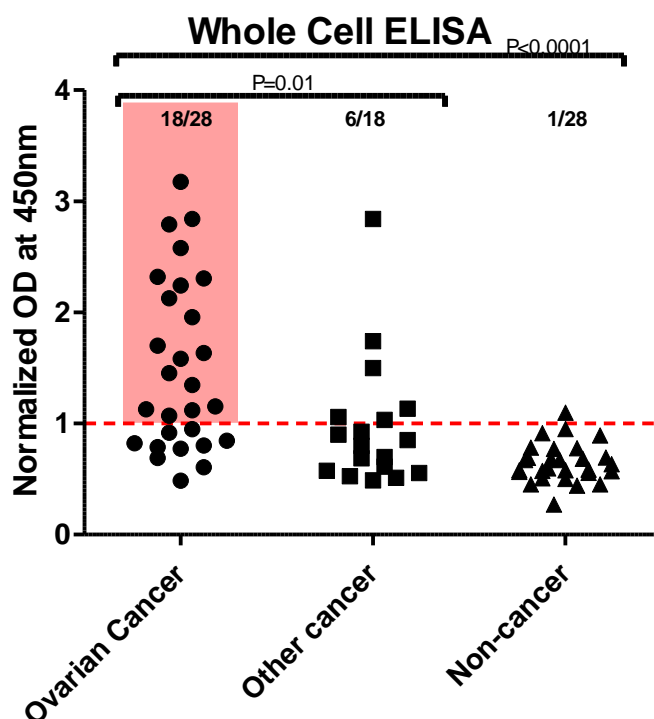


Figure 13: Ovarian cancer whole cell ELISA: Fixed and permeabilized 80% confluent OVCAR cells were incubated with 1:100 dil of purified IgG from Ovarian cancer ascites, other cancers and non-cancerous controls. 1:2000 dil of detection antibody α hIgG-HRP was added. Developed using TMB substrate and stopped with 1N H₂SO₄. OD was measured at 450nm.

10.4.3 Ovarian Cancer Cell Lysate ELISA

In addition to the whole cell ELISA, we also performed a total cell lysate ELISA with OVCAR-3 cells to examine the prevalence of antibodies present in test and control sample targeted against soluble intracellular proteins/ TAA's in OVCAR3 cells. The cell extract was prepared under non-denaturing conditions and the soluble fraction was quantified by BCA. The microtiter plate coated with the soluble fraction of OVCAR3 cell extract were challenged with 1: 50 diluted human IgG (1 $\mu\text{g}/\mu\text{l}$) from 28 ovarian cancer patient, 18 patients having other cancers and 28 non-cancerous control. Figure 14 shows the results from the cell lysate ELISA. We observed the presence of antibodies particularly in ovarian cancer sample (23/28) which recognizes TAA's as compared to other cancer or non-cancerous control (0/18 and 3/28 respectively). It is evident that cell lysate ELISA detects more number of sample as positive as compared to whole cell ELISA. This may be due to the antibodies in ascitic fluid gets more access to find their target when cell lysate is used. Unlike whole cell ELISA, this assay contains only soluble antigen in the lysed fraction and thus detected none of the other cancer as positive.

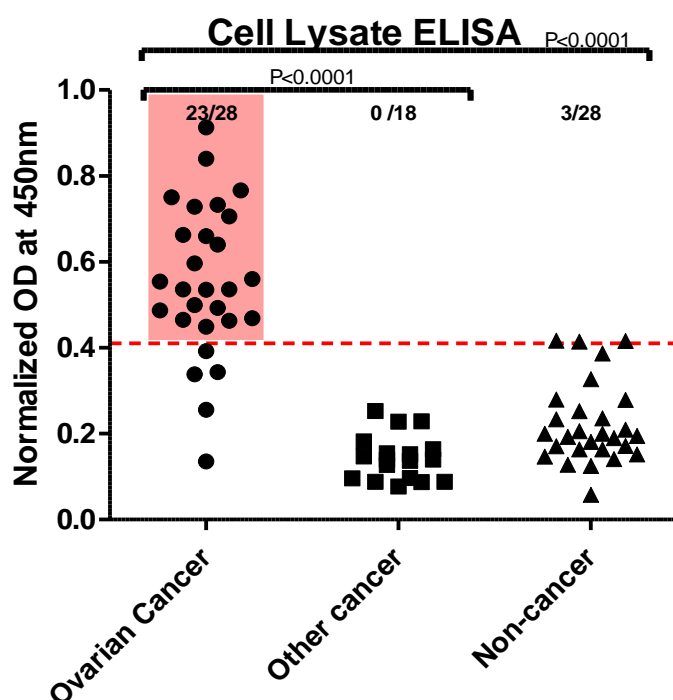


Figure 14: Ovarian Cancer Cell Lysate ELISA: .OVCAR3 cell lysate were prepared in a non-denaturing condition. Microtiter palate was O/N coated at 4° C with OVCAR3 cell lysate. Blocked with 2% BSA in PBST (0.05%). Incubated with 1: 50 diluted purified primary IgG for 1 hr 30min at 30° C. 1hr at 30° C with 1:5000 diluted secondary α IgG-HRP was added to each well. Added TMB substrate and stopped with 1N H₂SO₄. Read at 450nm.

Result from both these cell based ELISA tests provided a quantitative information, clearly differentiating ovarian cancer from non-cancer patients ($P < 0.0001$ for both whole cell and cell lysate ELISA) and other cancerous conditions ($P = 0.01$), ($P < 0.0001$) for whole cell and cell lysate ELISA respectively) and hence permitted to rank patients with elevated tumor specific antibody levels in ascitic fluids.

10.4.4 Immunofluorescence Assay on OVCAR3 Cells (IFA)

Further, antibody response was analyzed by immunofluorescence assay on OVCAR3 Cells. In order to observe various localization, staining of live ovarian cancer cells was performed to detect cell surface antigens. Simultaneously, the cells were fixed and permeabilized, thus permitting more access for ascite antibodies to find their intracellular target. Live OVCAR-3 cells were incubated with ascite antibodies for 2 hrs. To exclude the possibility that cellular uptake of antibodies, incubations were performed at 4°C which, only resulted in binding to the cell membrane since cellular uptake does not occur at this temperature. In figure 15, image A and B represents the cell surface localization of tumor specific antibody was detected with α -human immunoglobulin conjugated to Cy5 (in green). Nuclei were stained with Propidium iodide (in red). Live OVCAR-3 cells when incubated with cancer ascite #44 (image A) shows a prominent signal of cell surface staining as similar to the positive control (image B). The mAb MOV18 (humanised α -Folate antibody) directed against the isoform α of the folate receptors which are over expressed by endothelial ovarian cancer cell on their cell surface was used as positive control for this assay [145,146]. Other localization of target antigen was observed when the same cells were fixed and permeabilized. Image C shows nuclear localization (with cancerous ascites #18) while cytoplasmic (C) localization was clearly observed when incubated with control IgG #1385. Cells incubated with either ascitic fluid from non-cancerous patient or healthy human IgG (image F) failed to produce any signal of binding.

Taken together the results suggest that the presence of tumor specific antibody targeting cancer proteins and help us to identify ascites which have high-titer fluorescent staining or strong signals to ovarian cancer cellular antigens and subsequently use them to isolate ORF clones by Phage Display.

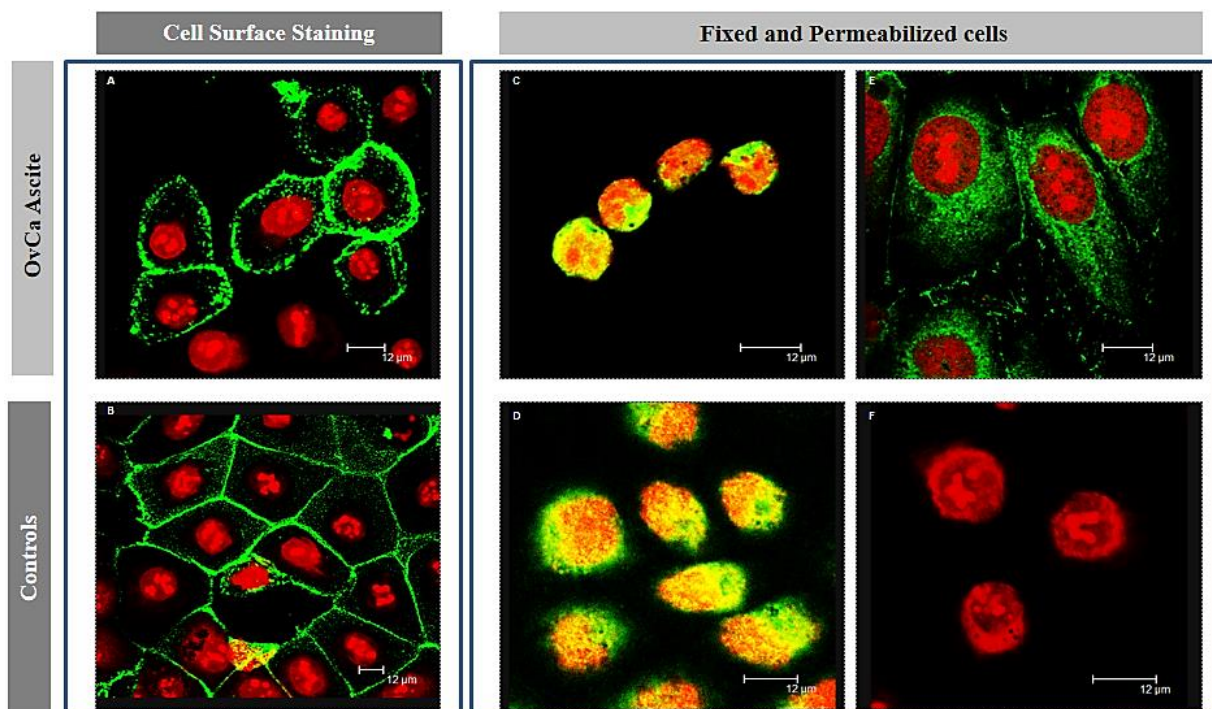


Figure 15: Immunofluorescence assay on OVCAR3 Cells. Cell Surface Staining: (A, B) Image A represent cells incubated with cancerous ascite (#44). (B) Positive control humanised α -Folate antibody. Fixed and Permeabilized cells (C,D,E and F) were separately incubated with either cancerous ascites (Image C and E: incubated with ascite #18 and #1385 respectively) , (F) Cells incubated with non Cancerous ascite (1206) or Anti BCOR antibody (D). The intracellular localization of tumor specific antibody was detected with α -human immunoglobulin conjugated to Cy5 (in Green). Nucleus were stained with Propidium iodide (in red). Image A-B shows the surface localization. Nuclear (C-D) and cytoplasmic (E) localization were clearly observed. Cells incubated with either acitic fluid from non-cancerous patient or healthy human IgG failed to produce any signal of binding.

10.5 Selection of ORF Phage Display Library

The Phage Display technology approach was used to identify novel TAAs. A phage library of open reading frame (ORF) fragments created from mRNA derived from various tissues were used [60, 147]. This library comprised of nearly all genes present in human genome. Characterization by massive sequencing of this library confirms that it represents more than 21,000 different genes or gene fragments.

The following step are briefly summarized for the selection of polypeptides from the cDNA libraries (Fig 16), with the purpose of isolating clones reactive to antibodies of interest, purified from ascitic fluid, from the background represented by all other phage clones.

1. Library amplification and phage particle production: The ORF filtered cDNA library was expressed and collected as a phage population.
2. Enrichment by immunoprecipitation of phage particle with immobilized target: Purified ascitic antibodies were immobilized G-protein functionalized magnetic beads were then incubated with the population of phages resulting from the cDNA libraries. A negative selection or 'pre-clearing' step was introduced before each round of selection. Phages were incubated with antibodies purified from healthy donors and unbound phages were collected and used for selections. Later, beads functionalized with antibodies from ovarian cancer patients were incubated with pre-cleared phages.
3. Washing steps: Extensive washes were performed to remove unbound phages.
4. Elution and amplification of bound phages by infecting host bacteria: Bound phages were eluted with DH5 α F' bacterial culture and planted onto agar plates.

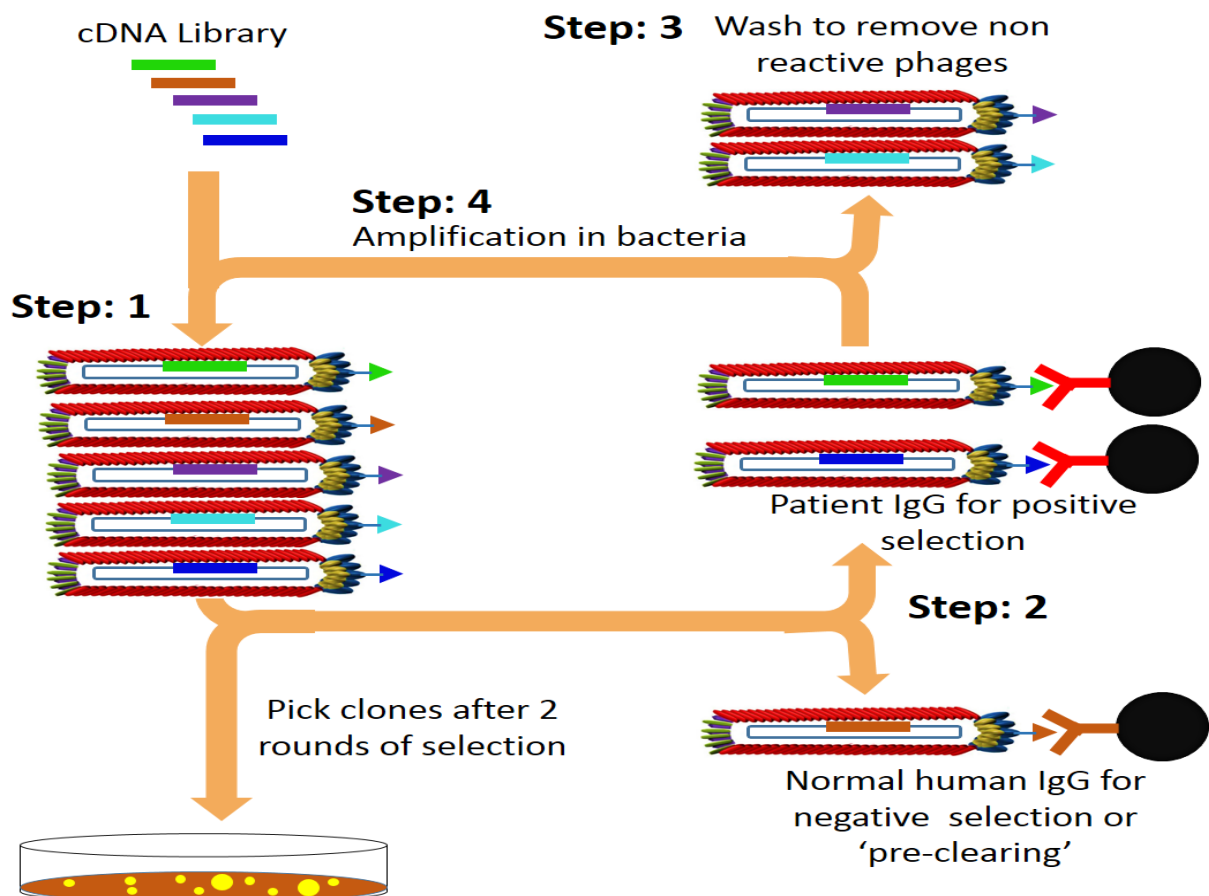


Figure 16. Schematic representation of the four steps followed for the selection of phages selection.

ORF displaying phages were selected with ascitic fluid collected from patients diagnosed with ovarian cancer, which has already been characterized as most reactive based on the result obtained from the initial immunological assays (Table 10).

Ascite ID	Stage	Grade	Age at diagnosis	Cells in ascites	Histology	Sensitivity to platinum
44	I	G2	51	Numerous	Non Serous	Sensitive
49	II	G3	61	Rare/some	Serous	Sensitive
61	II	G3	64	Rare/some	Serous	Sensitive
3	III	G3	60	Rare/some	Serous	Resistant
18	IIIC	G3	69	Absent	Non Serous	Resistant
1385	IIIC	G3	68	Numerous	Serous	Resistant
51	IV	G2	43	Numerous	Non Serous	Resistant

Table 10: Purified ascites used for phage display selection. These ascites were chosen from the ranking list based on initial immunocharacterization for there reactivity towards antigen present in ovarian carcinoma cells.

We performed seven independent screenings using the seven most reactive ascites. Two successive rounds of selection based on affinity selection permitted the enrichment and isolation of less abundant interacting proteins from a library with large diversity. Before each round, a “pre-clearing step” was introduced by incubating phages with sera/immunoglobulins from healthy blood donors with an intention to eliminate the polyreactive clones. The stringency of washing steps were progressively increased between different cycles. In all cases, about 10^{11} phages were the input of the selections. Whereas, the output titre was variable, in the range of 10^5 - 10^6 . The bound phages were eluted with DH5 α F’ bacterial culture and planted onto agar plates. Output data of the three selection cycles are reported in Table 11:

Ascite ID	1 st IN	1 st OUT	2 nd IN	2 nd OUT
44	10^{11}	2×10^6	10^{11}	10^6
49	10^{11}	10^6	10^{11}	2×10^5
61	10^{11}	3×10^5	10^{11}	10^5
3	10^{11}	5×10^6	10^{11}	10^6
18	10^{11}	10^6	10^{11}	2×10^6
1385	10^{11}	10^6	10^{11}	5×10^5
51	10^{11}	4×10^5	10^{11}	10^6

Table 11: Input and Output of phage populations for each selection round with different ascitic fluid. For each selection, patient ID (indicated as a number) Input (IN) and Output (OUT) phages are shown.

The first round of selection was performed with all the seven ascites at the same time. The input for this initial round was the NS library [60]. The second round was performed in similar manner for each single ascites individually but with the input as library obtained after the first round of selection.

In order to evaluate the absence of any possible bias (i.e. short fragments) introduced throughout the selection process, the input and the output of each selection was screened and the variability of the fragments selected was determined.

14 random clones from the input and output phages were checked by PCR by using specific primers for the phagemid vector. The length of the insert was determined by running of a 1% agarose gel.

Figure 17 shows the variability of 28 random clones, the first 14 derived from the NS library represents the input for the first round of selection and the others 14 were the output of the first round of selection for the ascite #44. For all the input and output fragments analyzed the mean length was 350bp with a range between 150bp and 700bp. No clear enrichment or specific fragments were shown, meaning that the process was not introducing bias for short fragments throughout the selections.

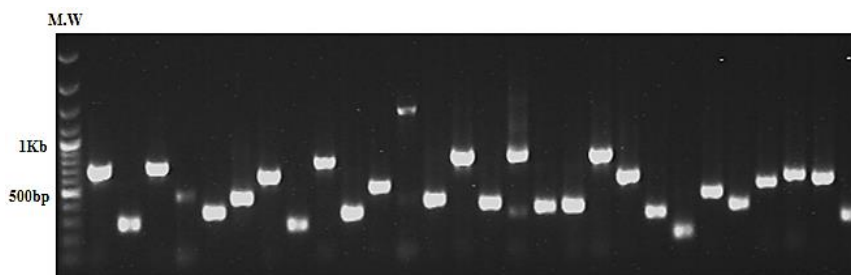


Figure 17: Random clones checked for the input and the output of the selections. PCR products of 28 random clones loaded on agarose gel screened for variability.

10.6 High-throughput protein production of the selected clones

After two rounds of selections, the immunoscreened phages were sub cloned into an expression vector, modified pGEX Vector: pGEX 4T- 1 mut BssHII NheI (Fig 18). After subcloning, they were amplified in the host bacteria BL21 (DE3) RIPL cells for enhanced protein production. 95 single clones from each of the 7 selections were randomly picked from agar plates and inoculated into 96 deep well plates in order to produce GST fusion protein. This modified vector was constructed with BssHII and NheI restriction sites and fusion tags, the N-terminal fusion with

GST, a highly soluble protein and C-terminal FLAG protein was introduced to improve the quality of protein by permitting better folding of the downstream polypeptide thereby avoiding inclusion bodies formation and to monitor the degradation. In addition, GST fusion proteins facilitate the purification by affinity separation (Fig 19).

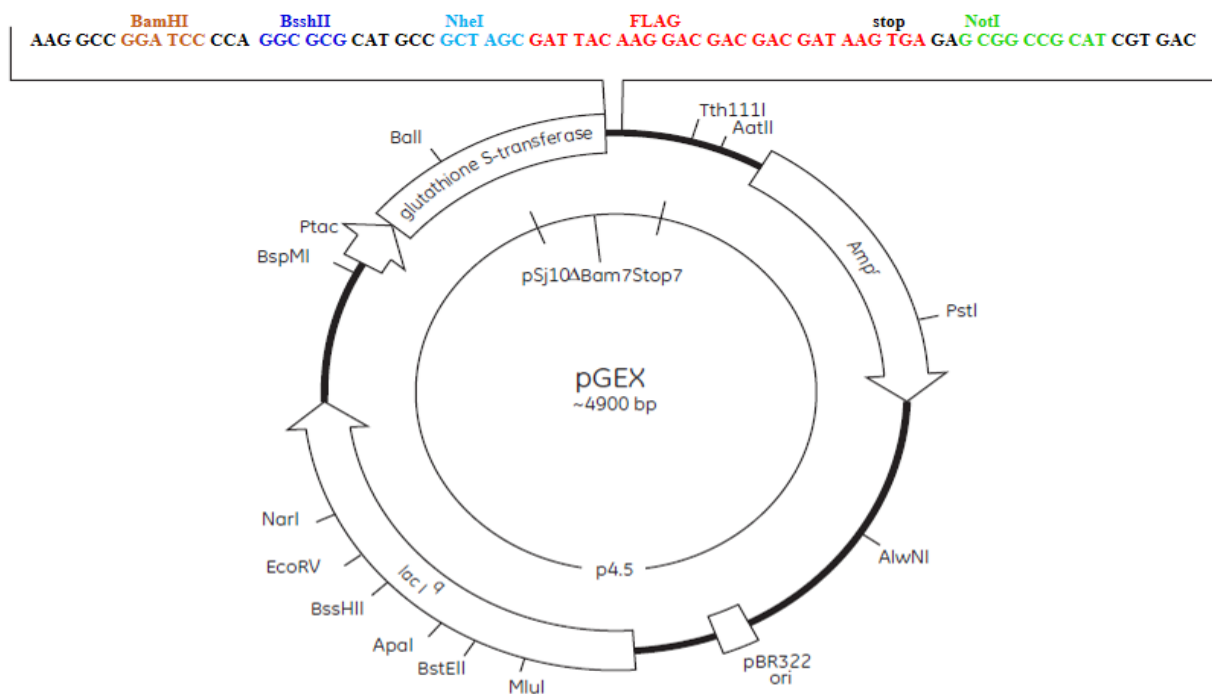


Figure 18: pGEX 4T- 1 mut BssHIII NheI Vector Map

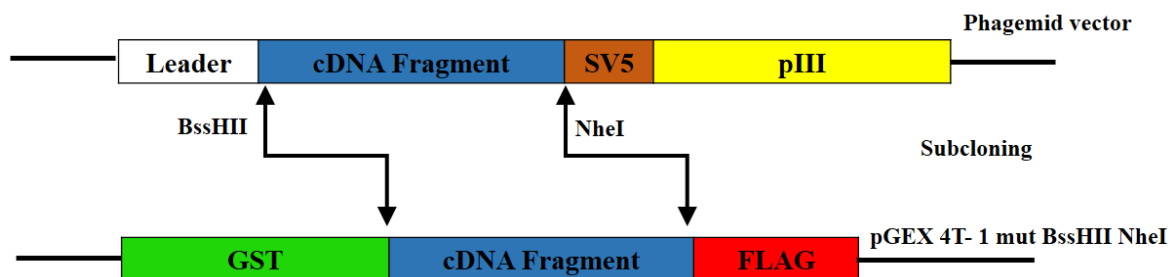


Figure 19: Subcloning of the selected cDNA fragments from phagemid vector into modified pGEX vector. cDNA fragments were cloned into BssHIII and NheI sites of pGEX vector; the library was plated in ampicillin to select ORF. 95 single clones from each of the 7 selections (95 x 7) were randomly picked from agar plates and recombinant proteins were produced in a hightthroughput format.

The presence of the insert was confirmed by PCR analysis before they were cloned into a pGEX expression vector (Fig 20). These immunoprecipitated ORF clones were expressed as GST-fusion proteins by transforming BL21 (DE3) RIPL cells with this expression vector.

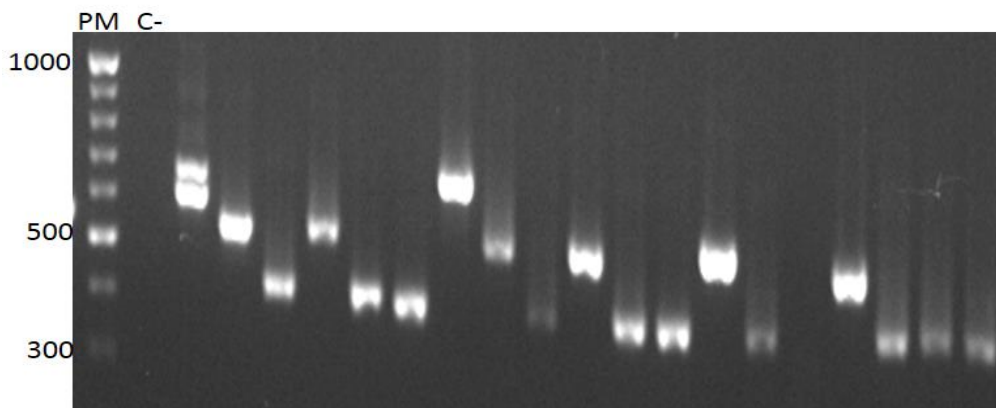


Figure 20: PCR confirms the presence of insert. These PCR fragments were cloned into pGEX 4T-1 mut BssHII NheI.

A bacterial expression system using *E. coli* in a 96 deep well plate allows high-throughput production and screening of recombinant proteins from the selected cDNA library. It is very convenient system to work with, as well as non-expensive and consequently yielding good quality purified protein in small amount for protein array screening. In this account, an automated mini-fermenter (Fig 21) based on inflation of air developed in our laboratory was used for a better bacterial growth and improved protein production compared to the standard shaking or agitation method. This system consist of a compressor as a source of air which is connected to a circuit formed by a pressure gauge , a computer that regulates the entry of air through an electric valve and an incubator, maintained at a constant temperature in which 96 well plate can be placed. The air flow is directed to a plastic case, containing multiple layers of grid like gauges designed to equally distribute the air pressure through each of the 96 hollow stainless needle at the bottom of the plastic case. The plastic case can be connected to the 96 deep well plate with this needle dipped into the culture medium. This allows inflation of air into each well of the 96 well plate in which the bacteria grow. All the condition such as the air pressure, inflation rate per minute, diameter of the needle etc. were previously been optimized.

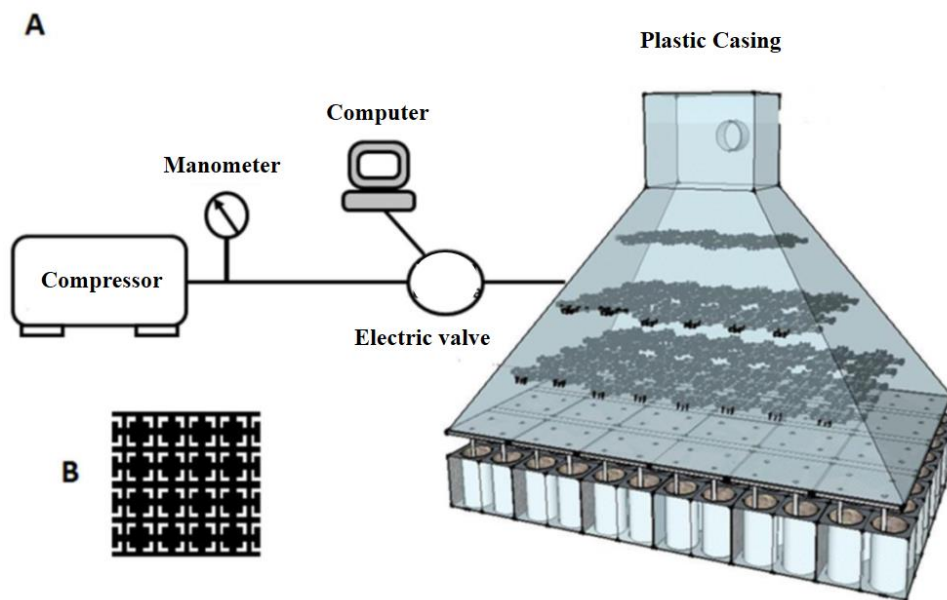


Figure 21: Mini-fermenter: A) Schematic representation of the mini-fermenter, B) The grid inside the plastic casing.

Subsequently, a high-throughput system developed by Studier in 2005 [148] and previously been optimized in our laboratory was adapted for the expression and purification of 700 random clones. Here an autoinduction medium for protein production in Lac promoter expression system was taken into account. This optimized medium allows bacterial growth without the activation of the genes coding for the recombinant proteins before the bacteria have reached the desired optical density. Induction of Lac promoter of the bacteria causes the production of T7 polymerase thus leading to the transcription of cDNA fragment located downstream of the T7 promoter in pGEX vector and an enhanced protein production. This resulted in a synchronized growth and simultaneous induction of 700 different clones at the same time producing comparatively equal amount of proteins.

A robust protocol for the multiplexed purification of recombinant proteins generated by our laboratory was used to purify several hundred proteins in a 96 well format at considerable speed. Each single step of the procedure was previously optimized to get an acceptable yield and quality of the purified proteins. The most important steps in this procedure are summarized in figure 22 and briefly explained. In order to avoid centrifugation step of the culture plate to have cell pellets, a choice was made to use a commercially available lysis buffer (FAST Break, Promega) that acts pretty well on the cells on culture. Later, the GST-fusion proteins were affinity purified with magnetic beads coated with reduced glutathione (GSH). Purification steps was

performed by means of magnetic devices. GSH-magnetic beads were used in that representing a good tool for the high-throughput processing: no need for centrifugation or filtration steps were required; volumes used were easily scaled in order to optimize yields with a reduced reagents consumption; by means of a magnetic plate and a 96-plexed manifold, washing steps and elution were performed in a short time.

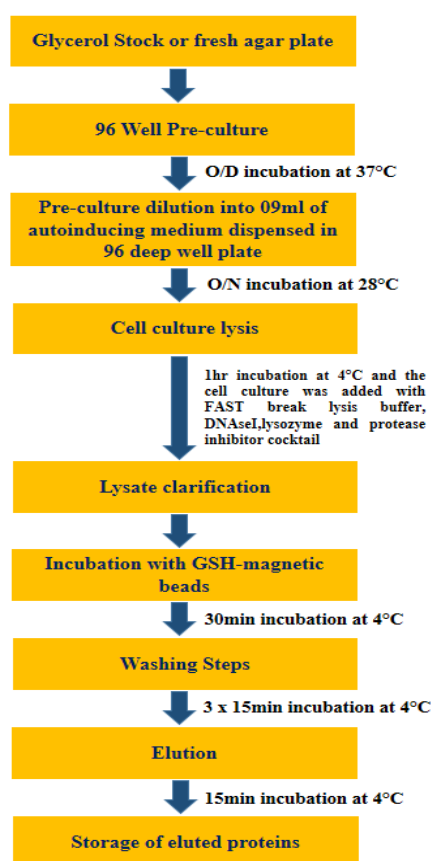


Figure 22: Workflow of the high-throughput protein production and purification protocol.

To ensure a proper production, a few random selected proteins were denatured and loaded on a gel for SDS-PAGE. The coomassie stained gel shown in figure 23, a final concentration in the eluted sample ranging from 0.1 up to 1 $\mu\text{g}/\mu\text{l}$. The quality of proteins produced was generally good: an acceptable level of a slight contamination of known co-purified high molecular weight bacterial proteins was observed. Western blot (with anti-GST and anti-FLAG primary antibody) was carried out to check whether the expressed proteins were full length fusion protein. A variable degree of degradation was moreover observed, but full-length proteins were always present in the sample (data not shown).

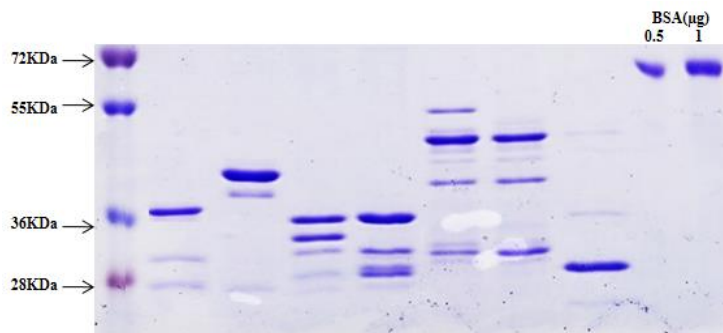


Figure 23: Coomassie staining of GST-fusion proteins produced by high-throughput approach. 2 μ l of each protein sample were loaded. Dilutions of a BSA sample (amount: 0.5 and 1 μ g) were introduced as calibrator.

The procedure led to the production of 96 recombinant proteins/day, with the quality and the amounts required for the production of a high density protein microarray to be screened with purified ascites.

10.7 Immunoscreening of the selected antigen by protein microarray

ORF displaying phages after successive and stringent rounds of selection were initially validated for their immune recognition by protein microarray. Protein microarrays are very reliable and extensively been used for the identifying novel antigens in cancer [68,110,125,126,135,137]. Besides their ease of use to analyze a large set of biomolecules, they require less amount of sample and reagent, making them a choice of interest. 96 bacterial clones from each of the 7 screenings were randomly selected and proteins were expressed and purified in a 96 deep-well (1.2 ml liquid culture) format, yielding approximately 700 independent GST fusion proteins. Purified proteins were spotted onto nitrocellulose slides along with controls and calibrator IgGs and screened for their immunoreactivity. Protein microarray is a high throughput approach, which simultaneously can analyze all these selected proteins. To ensure the proper printing of full-length proteins on slides, an array was incubated with anti-GST (Fig 24A). Later, each array were challenged individually with 17 different ascitic fluid collected from patients representing different disease conditions:

- 13 ascitic fluid out of 17 were collected from patients suffering ovarian cancer,
- 2 from cancer patients other than ovarian and
- 2 ascitic fluid collected from non-cancerous conditions.

The reactivity was revealed with anti-human IgG antibody as shown in figure 24 where each antigenic protein are printed as duplicate spots and normalized for signal intensity by using the IgG calibration curve. A cut-off value was calculated using the signal intensity produced when incubated with non-cancerous ascitic fluid. Here identical arrays show difference in immunorecognition when incubated with ovarian cancer ascites (Fig 24 B) in comparison with non-cancerous ascites (Fig 24 C). Seventy three highly positive antigens found to have a threshold values for determining reactive clones were arbitrary established at Signal to Noise (S/N) ratio greater than 3. These identified antigens were specifically reactive towards ovarian cancer ascites in contrast to non-cancerous ascites for their immunoreactivity.

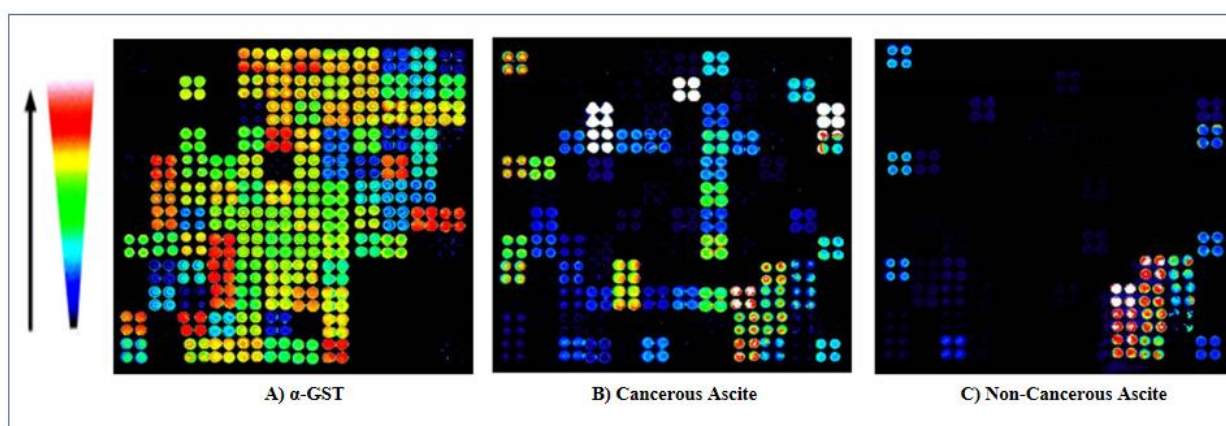


Figure 24: Immuno-screening by protein microarray: Fluorescent signal from arrayed antigen. A) Array challenged with α -GST as positive control for expression of full length recombinant proteins. Image B and C: Fluorescent signal from array screened with cancerous ascitic fluid and noncancerous control respectively. All the printed proteins were challenged against 1:50 dilution of 17 different Ascitic fluid collected from patients representing different disease conditions including control.

10.8 Identification of novel putative tumour-associated antigens (TAA) by sequencing

The plasmids encoding the genes of these 73 identified proteins were extracted and the cDNA were amplified by PCR and sequenced with the Sanger method. All the 73 immunoreactive clones were PCR amplified with pGEX primers and were run on a 1% agarose gel (Fig 25).



Figure 25: PCR of immunoreactive clones amplified with pGEX primers. Amplified fragments have shown to have a size ranging 150-800bp

It was observed from the gel that the size of the amplified fragments vary between 150-800bp, which complies with the initial dimension of the cDNA fragments (this size range will be correctly displayed by the phage on the capsid) used for the construction of phage display library. Fragments representing each size were further purified and subjected to sequencing.

Gene fragment display suffers from the problem that only one clone in 18 is functional, due to the orientation of the fragment and the reading frame in which they are translated. It has been noticed from the result that majority of the fragments are composed of 3N bases suggesting the cDNA library was well ORF filtered. From the sequencing result, we matched our sequences to the genetic sequences available in blast database and later translated to identify the protein expressed by this cDNA. Hence, decided to evaluate only the 'genic ORFs' ie those cloned fragment with 3N bases,+1 reading frame of translation carrying both the BsshII and Nhe I restriction sites. The mimotopes or the nongenic ORFs were removed from the list. Following the sequencing, we observed that many clones constituted ORFs encoding different fragments of the same protein. Among the identified proteins, we decided to initially validate those which were positive with all the ovarian cancer ascitic fluids analyzed (Table 12).

Name	HUGO Name	Subcellular Location	Function	Length (bp)
Homo sapiens cAMP responsive element binding protein 3	CREB3	Nucleus, Cytoplasm	Transcription factor	303
Homo sapiens mitochondrial ribosomal protein L46	MRPL46	Mitochondrion	Hydrolase activity	231
Homo sapiens exosome component 10	EXOSC10	Cytoplasm, Nucleus	rRNA Processing	204
Homo sapiens BCL6 corepressor	BCOR	Nucleus	Transcriptional corepressor	228
Homo sapiens huntingtin interacting protein 1 related	HIP1R	Cytoplasm, Perinuclear region	Receptor-mediated endocytosis	396
Homo sapiens high mobility group nucleosomal binding domain 2	HMGN2	Nucleus, Cytoplasm	Chromatin organization, Regulation of transcription	261
Homo sapiens olfactomedin 4	OLFM4	Secreted, Mitochondrion	Cell adhesion	129
Homo sapiens KIAA1755	KIAA1755			156

Table 12: Identified novel putative tumor associated antigens selected for validation. The table summarizes the cellular localization and function of each of the identified genic antigens.

10.9 Large Scale Production of Novel Putative Antigens

The antigens screened by protein array and identified by sequencing were produced in higher quantities in order to be validated by ELISA. The recombinant proteins were purified by affinity chromatography, using the GST- tag. All the expressed and purified proteins were quantified and were analysed by Coomassie staining (Fig 26 A) and Western blot with both α FLAG (Fig 26 B) and α GST (Fig 26 C) primary antibody, to ensure the full-length protein production and to monitor the level of degradation.

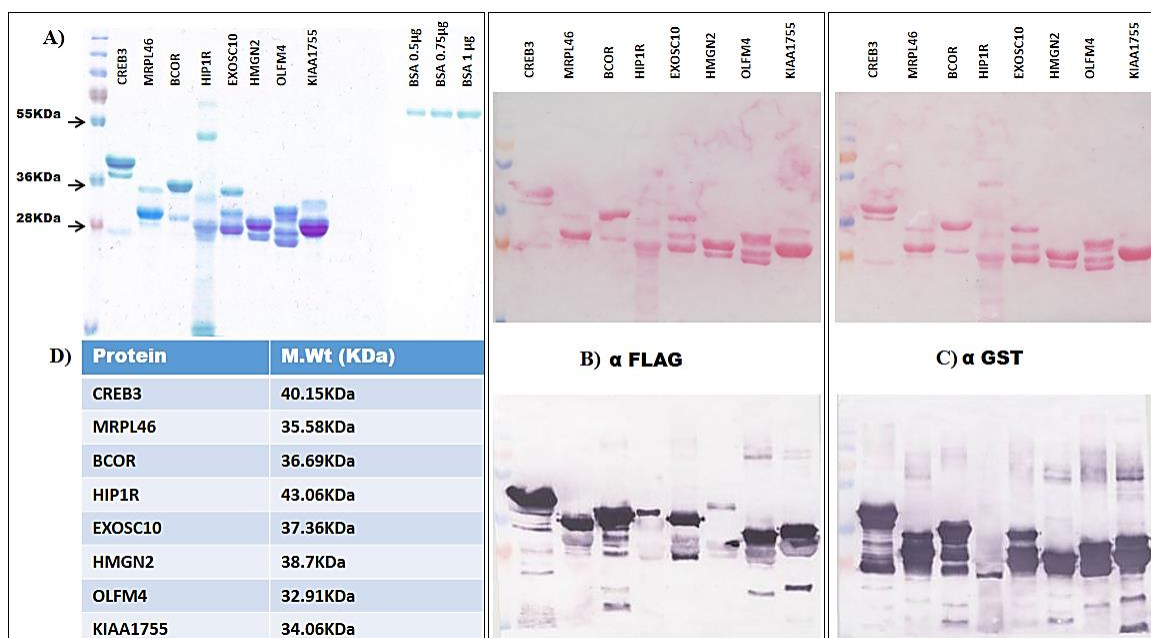
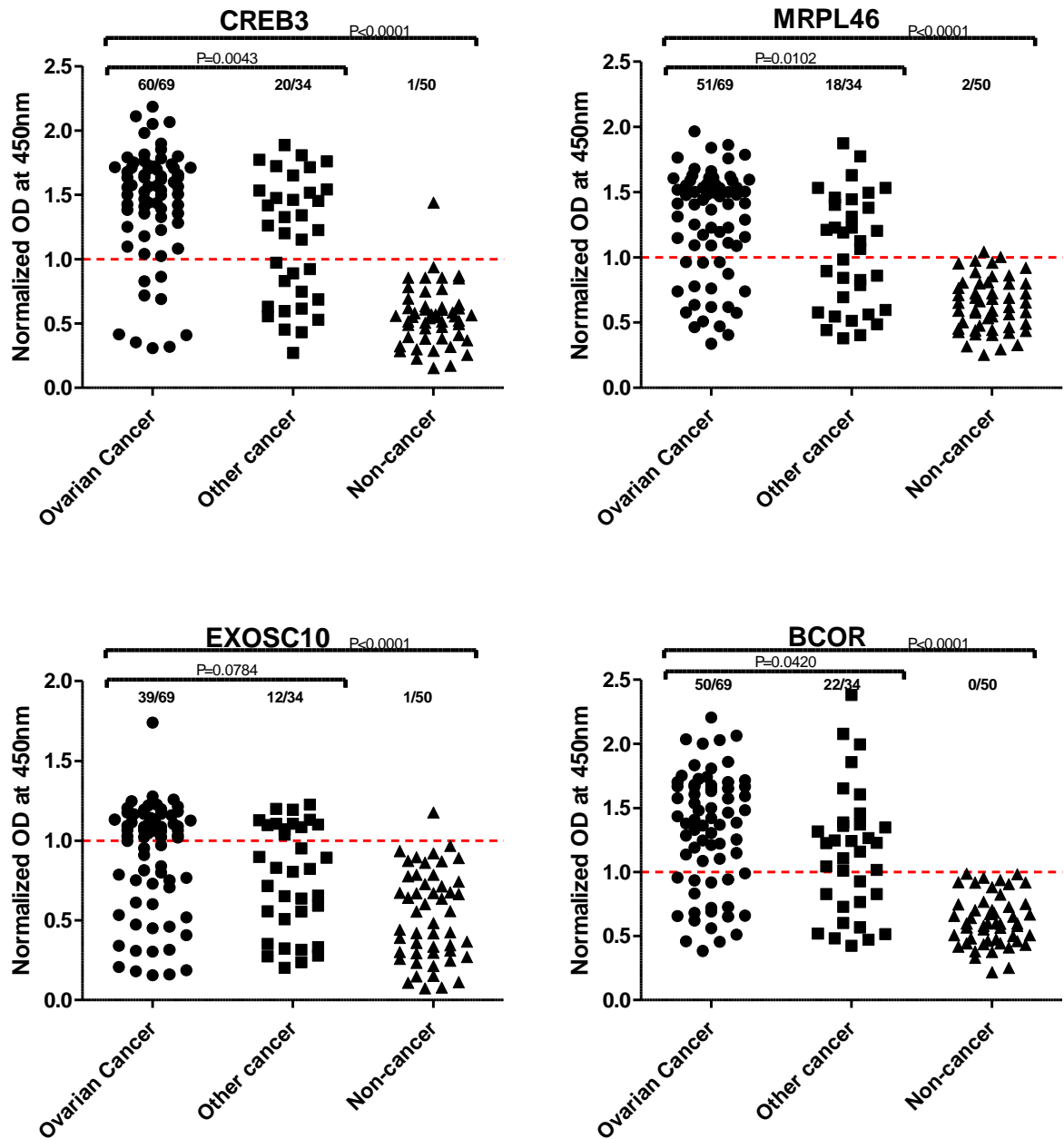


Figure 26: Expression and Purification of Antigens: A) Coomassie staining, molecular weight and western blot of all predicted antigens with B) α -FLAG antibody, C) α -GST antibody and the respective membrane stained with ponceau. D) Eight top antigens with their corresponding molecular weight in kilo Dalton.

10.10 Validation of Putative Antigenic Protein by Indirect ELISA

ELISA was performed to determine whether the antibodies present in the ascitic fluid from the ovarian cancer patients were specifically recognized by the selected peptides derived from the screenings. This techniques offer a higher level of sensitivity to measured autoantibodies even at a very low concentration. Each well of ELISA plate was coated with $1\mu\text{g}$ recombinant protein in $100\ \mu\text{l}$ PBS. Each antigen was validated separately by ELISA against a set of 153 protein A purified ascites from various disease conditions (Table 9). First tested with a set of ascites which includes 69 ovarian cancer, 34 other cancer and 50 noncancerous cancerous controls (Fig 27). The sixty-nine ovarian cancer ascitic fluid includes stage I-VI collected from both platinum sensitive and resistant patients with grade ranging from G1-G3. Out of all antigens tested, eight showed a statistically significant difference in immunoreactivity between ovarian cancer and non-cancerous control ascites as reported in figure 27 and summarized in table 12. The prevalence of autoantibodies in ovarian cancer patient is described by the P-value, calculated using two tailed unpaired t-test: antigens with $P\text{-value} < 0.05$ are considered significant. These eight identified as novel putative TAAs includes **A**) CREB3 (Cyclic AMP-responsive element-binding protein 3) **B**) MRPL46 (Mitochondrial ribosomal protein L46) **C**) BCOR (BCL-6 corepressor) **D**) HMG2

(High mobility group nucleosomal binding domain 2) **E**) HIP1R (Huntingtin interacting protein 1 related) **F**) EXOSC10 (Exosome component 10) **G**) OLFM4 (olfactomedin 4) and **H**) KIAA1755. The full-length production and purification of these antigens are shown in figure 26.



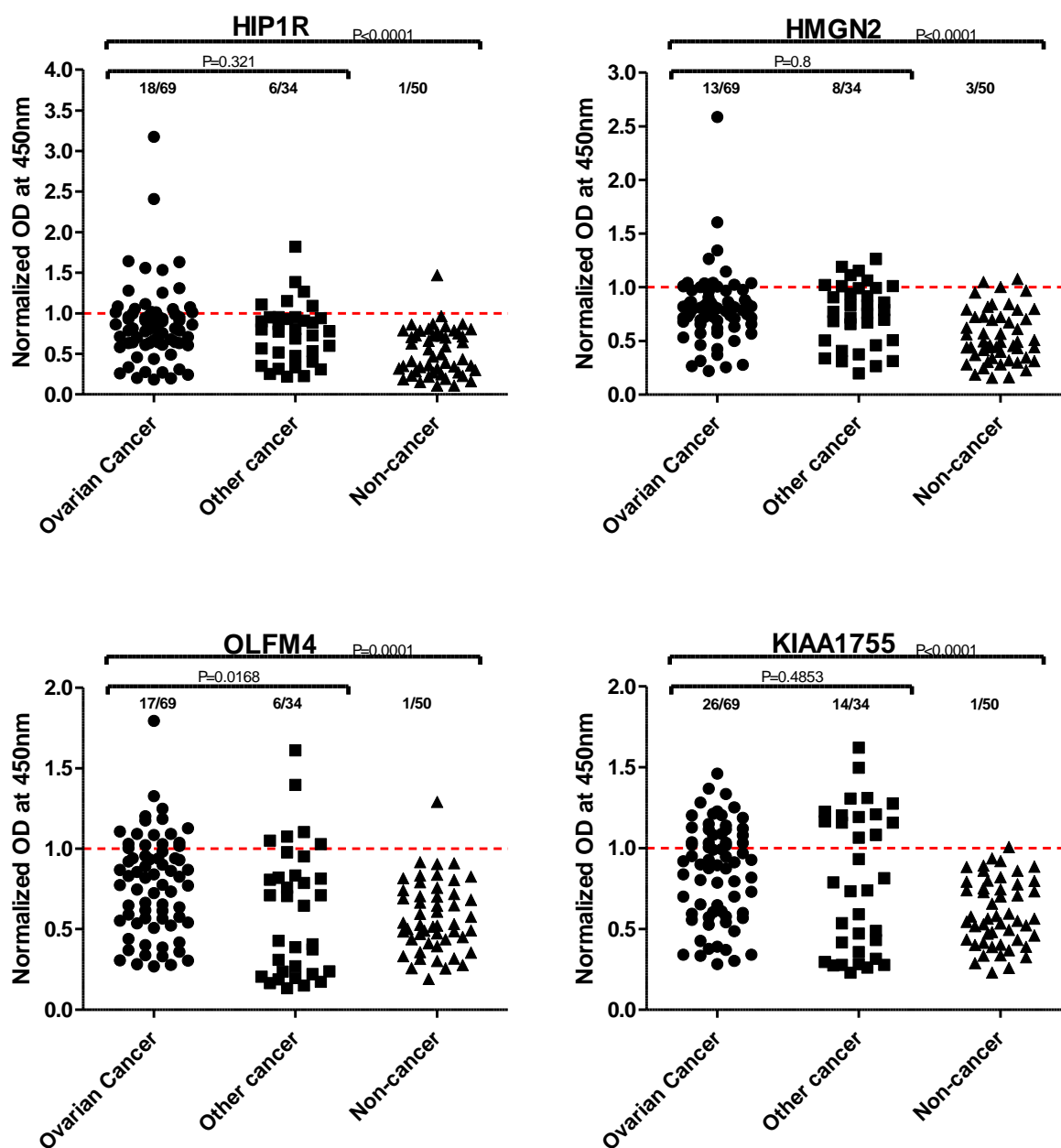


Figure 27: Validation of antigenic protein by ELISA. Each antigen was challenged with 1: 50 dilution of a total 153 IgG purified ascites ($1\mu\text{g}/\mu\text{l}$) which further is divided into 3 different groups i) Ovarian cancer (69) ii) Other cancer (34) iii) Non-cancerous control (50). Cut-off value was calculated separately for each antigen as mean + 2(standard deviation) of the OD from all non-cancerous control wells. Significance for ELISA data obtained for each antigen are reported. The prevalence of autoantibodies in ovarian cancer patient is described by the P-value, calculated using two-tailed unpaired t-test: antigens with P-value<0.05 are considered significant.

Concerning the reactivity, each of the eight antigens have shown to produce a varying range of immunorecognition with different group of ascites. CREB3, MRPL46, BCOR and EXOSC10 were proved to be most sensitive and can detect 60/69, 51/69, 50/69 and 39/69 ascites derived from

ovarian cancer patients as positive. Were as, KIAA1755 detected 26 out of 69 as positive. 18/69 and 17/69 were predicted to be above the cutoff by HIP1R and OLFM4 respectively. HMGN2 was the least sensitive among the panel and predicted 13/69 to be positive. However, among all eight antigens, only four antigens namely CRB3, MRPL46, BCOR and OLFM2 were capable to differentiate ovarian cancer from patients suffering other cancer with a P-value<0.05. The sensitivity and specificity of each antigen in detecting ovarian cancer are summarized in table 13.

Name	Sensitivity	Specificity
CREB 3	86.95%	98%
MRPL46	73.91	96%
EXOSC10	56.52%	98%
BCOR	72.46%	100%
HIP1R	26%	98%
HMGN2	18.84%	94%
OLFM2	24.63%	98%
KIA1755	37.68%	98%

Table 13: Sensitivity and specificity of detection. Sensitivity and specificity of each antigen in detecting ovarian cancer.

Many previous studies on the use of a panel of markers have reportedly shown that combinations of multiple marker improve sensitivity and specificity for early-stage disease detection [24, 32-34,36].

10.11 Analysis for the prognostic potential of the novel antigens and their clinical correlation

A significant association of autoantibody responses with better clinical outcome was found by comparing differences between curves with the log-rank method. Subsequently, clinical data of the corresponding patients were analyzed after the experimental phase of this study was completed. Patients with at least 18 months follow up details were used for the overall survival analysis. Figure 28 shows Kaplan–Meier analyses of overall survival of ovarian cancer patients according to the presence of antibody response to these three identified antigens. A log-rank method was used to evaluate their significance. Which resulted in a significant difference in survival time between patients producing surplus protecting antibody and non-producing patients against CREB3 (log rank p value = 0.05), MRPL46 (log rank p value = 0.006) or EXOSC10 (log rank p value = 0.05). Our data clearly implies that patients who overexpress any of the three antigen or produce high titer of antibody against CREB3, MRPL46 or EXOSC10 have a prolonged overall survival. None of the other identified antigens showed any significant clinical correlation with the disease.

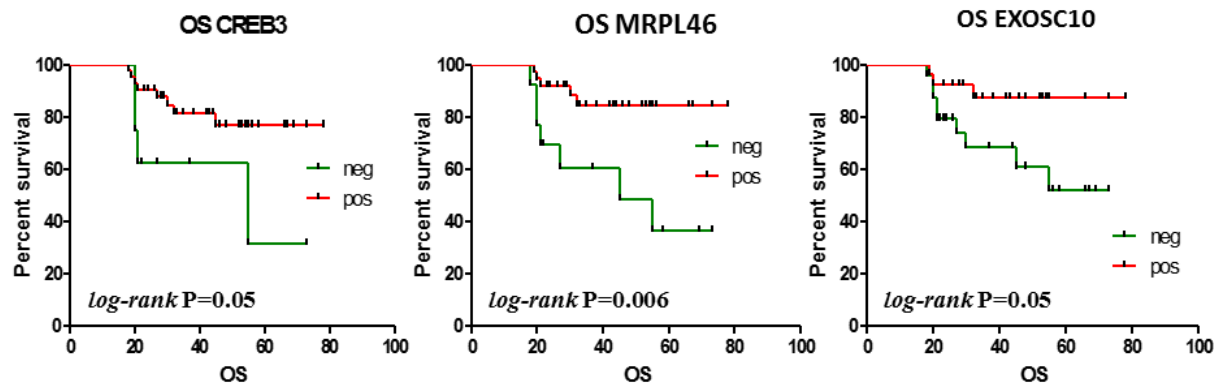


Figure 28: Antigenic markers with potential prognostic value. Kaplan-Meier analyses of overall survival of ovarian cancer patients according to the presence (positive) or absence (negative) of antibody response to CREB3, MRPL46 and EXOSC10. Patients showing immune response to these antigens (pos) are represented as red line. Whereas patients who do not produce immune response (neg) are indicated as green. A prolonged overall survival (in months) of the antigen positive patients was the outcome of this analysis as compared to antigen negative group of patients.

10.12 Verification of Cell Surface Targets by Cell Surface ELISA on Live OVCAR-3 Cell Line

Cell surface antigens represent only 1% of the total cellular protein (Fig 29) [149-151]. The presence of tumor specific antibody targeting surface antigens present on ovarian carcinoma cell line already been demonstrated by our immunofluorescence assay performed on live ovarian cancer cells (Fig 15).

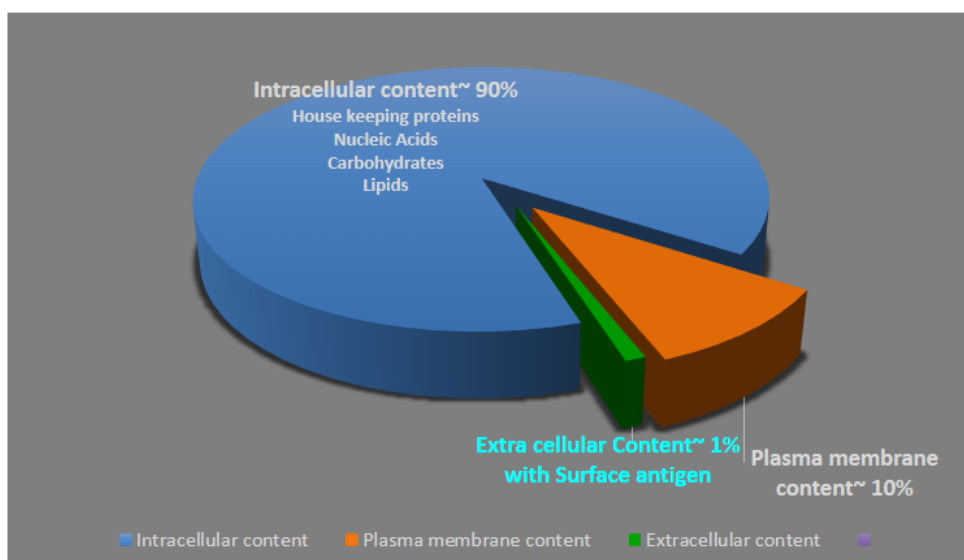


Figure 29: The ratio of surface targets which are accessible for humoral and cytotoxic immunity and remaining intracellular content [10].

Subsequently, a cell surface ELISA was performed on live OVCAR-3 cells to determine the presence and to quantify the amount of immunoreactive antibody present in ascitic fluid directed against cell surface tumor antigen. 80% confluent live OVCAR-3 cells were incubated with 1:50 dilution of primary antibody (affinity-purified antibodies from ovarian, other cancer and non-cancerous control). Later detection antibody was added to determine the presence of cell surface antigen. This assay was performed as triplicate and the average value of 3 wells were considered to be the OD of individual sample. The cut-off value was calculated as 'sum of (cumulative mean + twice the standard deviation) of the absorbance from non-cancerous control wells.

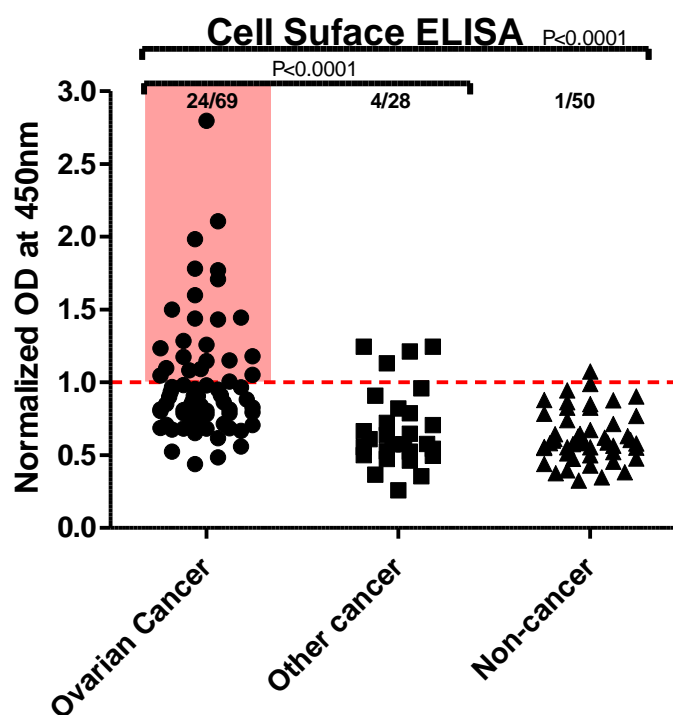


Figure 30: Ovarian Cancer Cell Surface ELISA. Scatter plot representing cell surface ELISA performed on live OVCAR-3 cells. Each spot represent a mean OD value obtained from a triplicate wells. The cut-off value was calculated as 'sum of (cumulative mean + twice the standard deviation) of the absorbance from non-cancerous control wells.

Figure 30 shows the cell surface result for set of 147 ascitic fluid. 34.78% (24/69) of ascitic fluid from patients with ovarian cancer are shown have significantly higher signal for the presence of specific antibodies against cell surface tumor antigen as compared to 4/28 ascitic fluid from other cancer patients. Except 1 out of 50, none of the noncancerous controls (49/50) were unable to produce any signal, leaving them below the cut off. Cell surface ELISA facilitated to determine

the amount of immunoreactive antibody present in ascitic fluid directed against cell surface tumor antigen. In addition, this assay provides a highly specific in differentiating ovarian cancer patients from non-cancerous patients as well as patients having cancer other than ovarian with P -value <0.0001 for both the cases.

10.13 Role of Cell Surface Antigen Interacting Antibodies in Tumor Regulation by Complement Dependent Cytotoxicity (CDC)

Our data confirm the presence of tumor specific antibodies in ovarian cancer ascites targeting surface antigen. To understand if these tumor specific antibodies when interact with cell surface antigen are capable to activate complement pathway and regulate tumor growth by complement dependent cytotoxicity. Ascitic fluids have previously been characterized by L Bjørge et al and are known to contain all the components required for complement activation [48]. Additionally, based on the interesting findings from two independent studies demonstrating that the two chimeric mAbs cMOV18 and cMOV19 against α isoform of the folate receptor (FR) which recognizes two different epitopes that are highly expressed on EOC cell surface are known to cause antibody-dependent cell cytotoxicity (ADCC) and Complement dependent killing of various EOC cell lines including OVCAR-3 [51, 148]. These findings prompted us to investigate the presence of specific ascitic antibody collected from ovarian cancer patients and evaluate their ability to activate the complement system.

To this extent, confluent OVCAR cells were incubated individually with ascitic antibody or mixture of cMOV18 and cMOV19 or no antibody control (diluted in DPBS supplemented with $\text{Ca}^{2+}/\text{Mg}^{2+}$). Further NHS containing complement factors were added to the cells to activate complement pathway which resulted in formation of membrane attack complex (MAC) on their cell membrane and lead to complement dependent cytotoxicity (CDC). The residual viable cells as well as number of cells killed was estimated by the MTT assay (3-(4,5-dimethylthiazol-2-yl)-2,5-diphenyltetrazolium bromide assay). The resulting purple solution is spectrophotometrically measured at 570nm and can be directly related to the number of viable (living) cells. The absorbance was measured at 570nm. Considering the cells with only NHS ('no antibody') as 100% living cells, the percentage of dead cells was calculated as: % of dead cells = $100 - [100 \times (\text{average of cells} + \text{Abs}) / (\text{Average of cells} + \text{NHS})]$. As expected, a 25-30% of killing of OVCAR3 cells was attained by the mixture of cMOV18 and cMOV19 via complement activation was entirely in

agreement with Paolo Macor et. al [51]. Normalization of this assay was made by considering the percentage of killing obtained with the mixture of cMOV18/19 as 100% and any killing above 10% caused by CDC were considered to be over the cutoff value.

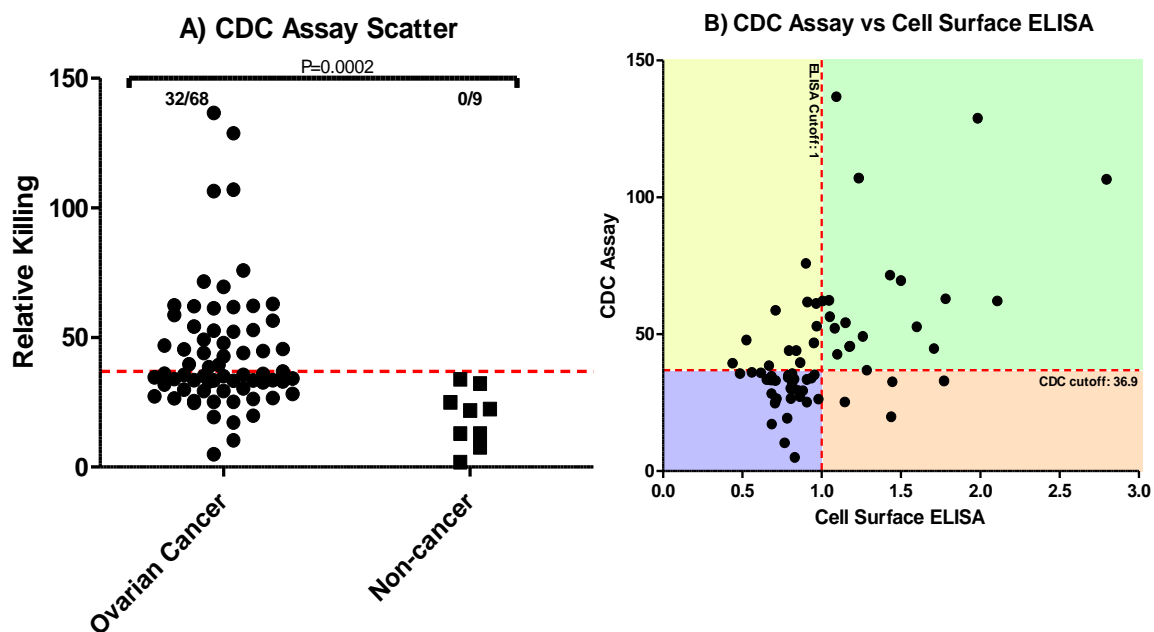


Figure 31: A) Complement dependent Cytotoxicity Assay of ascites from ovarian cancer and non-cancer patients B) comparative analysis of CDC assay versus cell surface ELISA of all ovarian cancer ascites

As in figure 31A, 32 out of 68 ascitic fluid from ovarian cancer patients shown to have presence of tumor specific antibody which are capable to activate C system leading to the killing. None of non-cancerous sample IgG were able to cause killing, indicating the absence or presence of these specific antibody in very low concentration. Later, a comparative analysis was made between CDC assays and cell surface ELISA to understand their correlation. Scatter plot (Fig 31 B) shows 75% of cell surface ELISA positive ascites are capable of mediating complement dependent killing of the ovarian carcinoma cell line.

Chapter 3

11. Discussion

11.1 Background

Ovarian cancer is the seventh most common cancer among women and is the leading cause of death from gynecological cancers in women worldwide, accounting for more than 151,000 deaths. This is due to the lack of reliable and effective early detection methods, since majority of early-stage of these cancers are asymptomatic and are detected at later stages, after they have invaded the surrounding tissues. Up to 90% of stage I ovarian cancer patients can be cured by currently available therapy. However, Only 25% of ovarian cancers are diagnosed in the early stage (Stage I) while they are confined to the ovaries. Ovarian cancer is characterized with the accumulation of ascitic fluid in the peritoneal cavity. These body fluids are excellent reservoir to study various biological aspects of the underlying tumor and equally important for the discovery of prognostic and predictive biomarkers. Because ascitic fluid persist in closer or direct contact with the tumor site and may contains many cells of tumor origin in addition to tumor secrete proteins, antibodies against these secreted or leaked proteins or peptides from tumorous tissue, soluble growth factors that have been associated with invasion and metastasis.

To my knowledge, the study presented in this thesis represents the first systematic analysis to profile ovarian cancer antibody repertoire in ascitic fluid using a high-throughput proteomic based methodology. The proteome of this heterogeneous, genomically unstable and highly lethal disease in women represents a complex molecular system: the major goal of present-day proteomics is to analyze proteins in their interactions with each other in a complex networks, which constantly changing over time and under different stimuli. Thus, requires methodologies allowing sensitive and simultaneous analysis of a large number of components. The first challenge to overcome was the necessity of a high sensitive tool to detect these low abundant molecular targets or tumor proteins with an increased specificity. Secondly, the proteomic tool should have high multiplexed capability, to allow the analysis of the huge number of molecules underlying biological processes.

In this work, the immune system has been used as a model of complex biological systems, where the analysis of its complexity and interactions could give new important insights into the biology of the system, insights that were not possible if studying single components. In a same vein, significant practical applications could be found, for example in the development of novel, highly sensitive diagnostic and prognostic tools.

Through the advent of the SEREX technology (serological identification of antigens by recombinant expression cloning procedure), the direct identification of immunogenic proteins by means of antibodies/autoantibodies present in body fluids derived from cancer patients was proven [189-192]. SEREX allowed the detection of novel antigens that could become potential candidates for diagnostic/prognostic tools, or probes for vaccination. Although extremely effective in identifying antigenic proteins, SEREX approach is a labour intensive procedure and requires a reduction in the panel of candidate antigens to be analyzed.

With regard to characterize ovarian cancer ascitic fluids, we employed a technological platform that combines a selection of a phage display cDNA library followed by protein microarray. This innovative approach could help the simultaneous screening of a huge number of proteins, in order to identify novel autoantigens/tumor associated antigens involved in the disease; secondly, a molecular dissection of the immune response involved in such disease. Thus, to produce large datasets in a sensitive and reproducible manner, with reduced demand for time and reagents. Identified targets were validated and evaluated for their clinical correlation with the disease as well as prognostic potential to predict the patient survival outcome were examined.

11.2 Immunoproteomic approach in the identification of TAAs

Currently there are no efficient screening and detection methods available for ovarian cancer; thus still remains a challenge for the cancer researchers. By early detection, a tremendous decrease in mortality can be achieved. Keeping this as our fundamental objective, we have identified a set of TAAs with very high prognostic potential for ovarian cancer.

Our strategy initially characterized ascitic fluids from various disease condition (ovarian cancer/ other cancer and non-cancerous sample) for their antibody response targeted against soluble, insoluble intracellular proteins present in OVCAR cells using various immunological assay which

includes western blot, whole cell ELISA, cell lysate ELISA on OVCAR cell line. This screening was done in order to identify the most reactive sample that could be used for phage display selection to screen out those interacting peptide displayed phages. Western blot analysis of OVCAR cell extract has proven to show the occurrence of cancer specific antibodies. The prevalence of antibodies present in cancerous and non cancerous sample targeted against soluble/insoluble intracellular proteins in their non denatured form present in OVCAR cells were examined by whole cell ELISA and was confirmed by cell lysate ELISA on OVCAR3 cells. This data indicates that the ascitic fluid from ovarian cancer patients contains tumor specific antibodies which are absent in non-cancerous samples.

Our immunofluorescence assay illustrates the presence of tumor specific surface antigen on live ovarian cancer cell line. The cell surface staining performed at a low temperature with same set of antibodies on live OVCAR3 cells. The result we obtained implies the presence of IgG determinants on cell surface such as surface antigens or receptors. Antibodies binding to these specific receptor gets internalised by endocytosis or pinocytosis [196,197]. Another possibility could be some of the intracellular antigens or proteolytic fragments of intracellular target might get externalised and displayed on the surface of cancer cells by unconventional secretion [152], enabling the antibodies to bind and trigger immune responses. The indirect immunofluorescence double staining performed on fixed and permeabilized OVCAR3 cells when incubated with cancerous ascites shows nuclear and cytoplasmic localization. As a control, cells incubated with either ascitic fluid from non-cancerous patient or healthy human IgG did not produce any signal.

These results provide the first verification of tumor specific anti-self antibody signature present in ascitic fluid from ovarian cancer patients. The immunoreactivity of these antibody repertoires to same target antigen varies considerably in patients having ovarian cancer. Patients with cancer other than ovarian or having a non-cancerous condition lacked these antibodies targeting ovarian cancer cellular antigen. With these immuno-techniques, we identified and ranked patients according to elevated tumor specific antibody levels in their ascitic fluids having a high immunoreactivity to cellular antigen and subsequently use the purified antibodies to isolate ORF clones by Phage Display. The precise mechanism by which these antibodies produced against intracellular antigens have to be further investigated

Phage display expression libraries provide a simple and efficient approach for the identification of novel antigens, by allowing the screening of cDNA libraries created from appropriate tissues directly with antibodies contained in ascitic fluid from ovarian cancer patients. The cDNA phage library used in this study was constructed and extensively characterized as described in Di Niro et al [60]. Various important strategies were incorporated while the construction of this library. The concept of cDNA filtering by applying the pPAO display system developed by our laboratory was successfully introduced. DNA fragments were cloned upstream of the beta lactamase gene in this vector and clones produced were selected for ampicillin resistance. This resulted in elimination of out-of-frame DNA sequences in an effective way to reduce the amount of molecular diversity to be assessed in subsequent steps, while simultaneously enriching open reading frames (ORFs) corresponding to real genes with biological significance and desired functions. This ORF enriched library was then fused with phage coat protein gene by Cre-lox mediated recombination, thus encoding ORF as their fusion partner and used to perform selection. A deep characterization of the non selected (NS) library by massive sequencing approach has revealed efficient normalization of gene abundance with the presence of good diversity of cDNA [60,141]. More than 21,000 genes were identified to be present in this library. In addition, that 90 % of the clones were determined to be open reading frame (ORFs) sequences, which are correctly expressed as a fusion partner on the phage surface. These remarkable features of our library offers a rational advantage to be utilized for the selection of novel proteins potentially involved in the autoantibody response of patients suffering from ovarian cancer.

Two rounds of selection were performed with magnetic beads functionalized with antibodies purified from ovarian cancer ascites which were found to be the most immunoreactive by initial immuno characterization. Thus, to screen out those peptide displayed phages which are recognized by immobilized antibodies present in the ascitic fluid from ovarian cancer patients but absent in healthy controls. The advantage of using phage display is that the selection of binding polypeptides leads at the same time to the isolation of the corresponding gene, allowing its manipulation and engineering and all downstream applications described in this work.

A large set of clones selected by successive rounds of ORF phage display screening were expressed as GST-fusion proteins. Unlike the conventional immuno assay techniques, protein microarrays represent a novel approach for large-scale characterization of antibodies directed against these

large set of target simultaneously from a single experiment maintaining the same specificity and sensitivity with respect to standard immunoassay. Besides their ease of use to analyze a large set of biomolecules, they require less amount of sample and reagent, making them a choice of interest. In this work, we have demonstrated the applicability of this method for the multiplexed characterization of complex antibody responses. This approach was strongly enhanced by the combination of high-throughput production and purification of proteins in 96 well plate format. Approximately 700 different purified GST fusion proteins along with controls and calibrator IgGs were spotted onto nitrocellulose slides with the aid of a robotic system. These arrays of large set of proteins were immunoscreened by independent sets of cancer and control antibodies in microliter volumes; immunoreactivity was detected as fluorescent signal. The result (Fig 24 B-C) we obtained clearly indicates the specificity of this assay to distinguish potential antigens for their immunorecognition from identical arrays when incubated with ovarian cancer ascites (Fig 24 B) in comparison with non cancerous ascites (Fig 24 c). The quantitative data about the antibody reactivity of many ascitic fluids to a high number of proteins provided by this sensitive assay enabled us to isolate seventy-three highly reactive antigenic clones. This signifies microarray as a highly promising tool for the high throughput in profiling complex antibody responses. Moreover, combining protein microarray screening as concluding steps of phage selection permitted a drastic reduction in the large collection of protein derived from phage expression systems and to focus on few numbers of potentially important antigens.

On characterizing these antigenic clones by Sanger sequencing, the most of the fragments selected represent genic ORFs, while a few clones represent alternative reading frames. Some of these non-genic ORF encodes for polypeptide (known as mimotopes) even though having corresponding gene fragment in their incorrect reading frame. The mimotopes mimicking the structure of an antigenic epitope (both linear as well as conformational epitopes) are capable to elicit immune response as similar to antibody response caused by the conformational epitopes of real antigens and were recognized by the ascite antibodies [198,199]. Mimotopes or the nongenic ORFs were excluded from the validation list. While, based on the specific reactivity measured for each protein, eight most reactive antigens were identified to produce a strong significantly different immune response signal between all the ovarian cancer and control ascitic fluids screened by protein array and identified as genic ORFs by sequencing, were produced in higher quantities in order to be validated by ELISA.

11.3 Antigens Identified As Most Immunoreactive

As expected, some of the isolated proteins found were associated previously with cancer and in various cancer related pathologies other than ovarian cancer although not necessarily as tumor antigens, thus confirming the efficacy of the approach and suggesting these antigens shares common pathways in various disease conditions.

cAMP responsive element binding protein 3 (CREB3) gene spans 4669 bps of chromosome 9 at 9p13.3 encodes for 395AA and exists 3 isoform. cAMP responsive element binding protein in 3 (CREB3) is a transcription factor belonging to leucine zipper family of DNA binding proteins. CREB3 subfamily proteins are anchored to the ER membrane in an inactive form. Only upon stimulation, the CREB3 subfamily proteins are translocated by COPII vesicles from the ER to the Golgi apparatus where they will proteolytically cleaved there by site 1 protease (S1P) and S2P sequentially to release the N-terminal fragment, which translocates into the nucleus and might work as homodimers or heterodimers to activate the transcription of genes. [153]. This transcription factors activated upon intramembrane proteolysis (RIP), binds the cAMP via a conserved gene promoter element CRE (cAMP response element), which has the sequence 5'-TGACGTCA-3' and regulates cell proliferation. Nuclear form of CREB3/Luman specifically binds the UPRE consensus sequence and activates transcription [154]. A previous study has demonstrated that HDAC3 selectively represses CREB3-mediated transcriptional activation and chemotactic signalling in human metastatic breast cancer cells [155]. CREB3 was known to be a binding partner of hepatitis C virus core protein. This interaction with the viral oncoprotein might interfere with a tumor suppressive function of CREB3 to promote cellular transformation in hepatocellular carcinoma [156]. Dendritic cells (DCs) are antigen-presenting cells (APC) of the immune system. Recently CREB3/Luman was identified to interact with as a DC-STAMP (Dendritic Cell Specific TrAnsMembrane Protein (DC-STAMP)). Same group also demonstrated that CREB3/ Luman coimmunoprecipitated OS9, DC-STAMP-interacting protein. Suggesting LUMAN and OS9 are part of the same complex and interact with each other at the cytosolic site of the ER. Thus leading to a new proposed Model of DC-STAMP/LUMAN/OS-9 pathway in which DC-STAMP/LUMAN/OS9 complex resides in the ER in immature DC and upon DC maturation, DC-STAMP/LUMAN complex translocates to the Golgi, where LUMAN is subsequently cleaved and its amino-terminal region is liberated, which then relocates to the nucleus. OS9 does not alter their

localization [157]. The CREB3 epitope resulted from library screening fits in activated nuclear region as well as they overlap with a part of minimal region of CREB3/LUMAN needed for DC-STAMP interaction.

The fragment which was pulled down by phage display selection fit within the HRDC domain of human exosome component 10 (EXOSC10). EXOSC10 also known as Polymyositis/scleroderma autoantigen 2 or PM/Scl-100 was identified as 100–110 kDa protein reactive with PM/Scl autoantibodies [158-160] with a high specificity [161]. Approximately 5–8% of the sera from myositis patients, 3% of those from scleroderma patients, and 24% of those from patients with PM/Scl overlap syndrome contain the anti-PM/Scl autoantibody. The autoantibodies that characterize this specificity are predominantly directed against the PM/Scl-100 antigen. Immunolocalization studies showed that the PM/Scl autoantigens are present in the nucleoplasm and, at higher concentrations, in the nucleolus. The nucleolus is the site of ribosome synthesis, which involves the transcription and nucleolytic processing of precursor rRNAs, the nucleotide modification of rRNAs, and the assembly of mature rRNAs with approximately 80 ribosomal proteins into small and large ribosomal subunits. In yeast (*Saccharomyces cerevisiae*), 11 proteins, 10 of which are known or predicted to have 3'-5' exoribonuclease activity. Yeast exosome components, namely Rrp6p are homologous to the PM/Scl-100 autoantigens. Functional studies suggest their presence in the nuclear and cytoplasmic compartments. Exosome is involved in the processing and degradation of several RNA species. The cytoplasmic exosome subfraction is probably involved in the degradation of mature cytoplasmic mRNAs. The human counterpart of the yeast exosome was shown to exhibit 3'-5' exoribonuclease activity [162,163]. The isolated GST fusion protein MRPL46 is a short N terminal fragment of mitochondrial ribosomal proteins L46. Mammalian mitochondrial ribosomal proteins are encoded by nuclear genes and help in protein synthesis within the mitochondrion. Mitochondrial ribosomes (mitoribosomes) consist of a small 28S subunit and a large 39S subunit. This gene encodes a 39S subunit protein [164]. Their expression is enriched in testis.

BCOR was originally identified as a novel corepressor of BCL-6 repressor and selectively potentiate BCL-6 repression. BCOR gene (127514 bps) is located in X chromosome at Xp11.4, encodes for 1755 AA BCL6 corepressor protein and are known to have 4 isoforms produced by alternative splicing. BCL-6 corepressor function as a novel transcriptional corepressor,

specifically inhibit gene expression of B-cell lymphoma 6 (BCL6). BCL-6 encodes a POZ/zinc finger transcriptional repressor that is required for germinal center formation and may influence apoptosis. When BCL6 is aberrantly expressed, it leads to the development of diffuse large B cell lymphomas (DLBCL). The interaction of BCL6 with their novel corepressor suggests a strong correlation between BCOR and the oncogenic mechanism underlying the BCL-6-associated lymphomas [165-166]. BCOR mutations are associated with the X-linked inherited diseases Lenz microphthalmia and Oculofaciocardiodental syndrome [167] as well as in acute myeloid leukemia with normal karyotype [168]. BCOR is ubiquitously expressed in all tissues examined, including the spleen and lymph nodes, where BCL-6 expressing mature B cells are found. The result from our immunofluorescence experiments performed on OVCAR cells is in agreement with the work done by Khanh D. Huynh et.al , 2000 [165] implies their localization in nucleus.

HIP1R is a multi-domain protein consisting of an N-terminal phospholipid binding domain (ANTH) which mediating phosphoinositides-interaction, a central coiled-coil, and a C-terminal actin-binding domain (THATCH). The coiled-coil domains of HIP1R comprise the binding site for clathrin light chains that regulates actin assembly and the clathrin-mediated endocytic machinery in cells. Isolated fragment of HIP1R constitute a region of central coiled-coil domain. Inside the cell, they are mainly localized at the endocytic compartments and in the perinuclear region. HIP1R has been previously described as a specific binding partner of BCL2L10 and induces BAK-dependent Cell Death [169-170]. In 2009, a study conducted at Medical University of Vienna, Austria [171] to define a gene signature in chronic lymphocytic leukemia (CLL) patients with trisomy 12 lead to the identification of HIP1R. HIP1R is considered as the best potential surrogate marker for +12 in CLL. Expression of this gene has a high sensitivity and specificity for detection. HIP1R identified as antigens associated with a colon cancer-related serological response [172], reacted exclusively with serum IgG derived from colon cancer patients but not with serum IgG from normal controls.

In 2002, Kimmo Porkka et.al identified a 31 AA peptide identical to nucleosomal binding domain present in the N-terminal part of HMGN2 protein. When internalized, this peptide binds to the nuclei of tumor cells and tumor endothelial cells in vivo. This nuclear-targeting capability of the peptide could be utilized to deliver anti-cancer drugs that can act in nucleus [173]. Further Xiong Wen-bi and colleagues in 2008 coupled pseudomonas exotoxin domain III with the same HMGN2

fragment. The *in vivo* anti-tumor activity of this recombinant chimeric protein was determined in female Balb/c nude mice bearing HeLa tumor cells. Chimeric protein significantly inhibited the growth of xenograft HeLa tumor in nude mice. Remarkable necrosis and apoptosis of tumors were seen in treated mice. This peptide has the potential to be used as a novel toxin-carrier in the study of cancer targeting therapy [174].

Olfactomedin 4 (OLFM4) gene is located on chromosome 13q14.3. Often deletion of this gene is associated with the progression of human prostate cancer [175]. They has been also reported that OLFM4 promotes the proliferation of pancreatic cancer cells by favoring the transition from the S to G2/M phase. In myeloid leukemic cell lines, inhibits cell growth and induces cell differentiation and apoptosis. It may play a role in the inhibition of EIF4EBP1 phosphorylation/deactivation. It facilitates cell adhesion, most probably through interaction with cell surface lectins and cadherin. OLFM4 was identified as a novel secreted protein in head and neck squamous cell carcinoma (HNSCC). It was found to be overexpressed in 75% the tested cases of HNSCC, thus making them a potential marker of this disease [176]. Aberrant expression of OLFM4 has been primarily reported in tumors of the digestive system as well as association of OLFM4 expression mediated by estrogen receptor signaling was found to promoted the malignant progression of endometrioid adenocarcinoma [177]. The isolated OLFM4 fusion epitope is predicted to be a transmembrane protein. KIAA1755 is an uncharacterized protein.

11.4 Validation of novel putative antigens

We validate each of the eight most immunoreactive antigens (Table 12) individually by ELISA for the presence of anti-antigen antibodies in ascitic fluids collected from patients with various disease conditions. A total of 153 IgG purified ascites that includes ovarian cancer patients (69), other cancer (34) and non-cancerous controls (50) against these identified antigens were tested by ELISA. Each of the eight novel putative antigens has shown to produce a statistically significant difference in immunoreactivity between ovarian cancer patients and controls as reported in figure 27. As observed by protein arrays, the specificity of these eight proteins was very high, ranging from 94% to 100%. Sensitivity was more variable, with the highest value (86.95%) obtained for CREB3, least effective was HMGN2 with 18.84%. The Sensitivity and specificity attained for each antigens individual antigen are summarized in table 13. However, CRB3, MRPL46, BCOR and OLFM2 were the only antigens capable to differentiate ovarian cancer from patients suffering

other cancer. This remarkable feature of these antigens has to be further evaluated for their usefulness to predict metastatic potential of the ovarian cancer or their correlation with metastasis. Our panel of 8 tumor associated antigen were able to detect the majority of samples as positive which originated from ovarian cancer patient at least by once with any of the 8 antigen. It has already been described that a combination of multiple markers can increase the sensitivity of detection. A combined sensitivity of 88.4% with a specificity of 94-100% was achieved from this assay. We have identified and validated eight TAA which have never been reported in the context of ovarian cancer. We currently continue our work to analyze the expression level of these identified antigenic genes in comparison with the level and distribution of protein produced as well as to understand how they are correlated in eliciting immune response. Further studies are required to determine important information on the role played by these molecules and the pathways they are involved in the development and regulation of ovarian cancer.

Moreover, the phage display library screening facilitates enrichment of the clones carrying same cDNA as well as selection of overlapping sequences of varying length sharing same epitopes. As expected, this phenomenon was clearly observed in view of the fact that multiple copies of BCOR clones were immunoscreened. On further analysis of these BCOR clones it was noticed that they occur in varying length with an overlapping epitope in common. All forms of BCOR were expressed and ELISA was performed with BCOR proteins of varying length. D5 Short BCOR was found to be recognized by most number of ascitic fluid [data not shown], leading to the identification of restricted epitopes.

Finally, we confirmed whether any of the top immunogenic antigens had a prognostic value for cancer survival. It was seen that patients who overexpress any of the three antigens or produce high titer of antibody against CREB3, MRPL46 or EXOSC10 have a prolonged overall survival. Our data from the survival analyses stratified for antibody responses against each of these antigens rise the possibility that serologic detection of tumor specific antibody of ovarian cancer patient with favorable prognostic potential. A thorough investigation to exploit the diagnostic potential of these identified TAA's has to be carried out. Validation with serum sample from same set of patients used for this study as well as the diagnostic capability of these antigens to detect of autoantibodies in serum from early stage ovarian cancer patients will have to be assessed. In

addition, the reactivity of autoantibodies from ovarian disease other than cancer should be compared to determine the diagnostic power.

As a matter of fact, all 8 identified antigens are confined inside the cells. This situation may be justified, as cell surface protein accounts for only 1% of the total cellular protein giving a probability to identify 1 surface antigen from 100 isolated clones. In fact, the magnitude for isolation of surface antigen tremendously reduce as 100 clones were randomly picked from 10^5 - 10^6 phage display selected clones. However, intracellular localization of these antigens may have several advantages. These intracellular tumor-associated antigens may elicit a very early host immune response in course of tumor development. This feature of antibody targeting intracellular antigen could apparently be used for cancer vaccines as well as to develop biomarkers that are capable of measuring varying level of autoantibodies which are stable and abundant even at the early stage of tumor in reasonably short time [110]. During tumor progression, cancer cells tend to shed extracellular protein thus making intracellular proteins a better choice for antigen-induced antibody therapies. A reduction in cross reactivity and minimal side effects can be achieved by using epitope based peptide vaccine, thereby increasing the specificity [193].

The interest in using of anti-TAA antibodies as serological markers for cancer diagnosis derives from the recognition that these antibodies are generally absent, or present in very low titers, in normal individuals and in non-cancer conditions [194,195]. Their persistence and stability in the serum of cancer patients is an advantage over other potential markers, including the TAAs themselves, which are released by tumors but rapidly degrade or are cleared after circulating in the serum for a limited time [48]. Furthermore, the widespread availability of methods and reagents to detect serum autoantibodies facilitates their characterization in cancer patients and assay development. However, in contrast to autoimmune diseases, where the presence of a particular autoantibody may have diagnostic value, cancer-associated autoantibodies, when evaluated individually, have little diagnostic value primarily because of their low frequency. We have observed that this drawback can be overcome by using mini-arrays of carefully selected TAAs, and that different types of cancer may require different TAA arrays to achieve the sensitivity and specificity required to make immunodiagnosis a feasible adjunct to tumor diagnosis [144]. The reactivity of autoantibodies against post-translational modified isoforms of these identified

proteins should be evaluated. This assay could be facilitated by 2-dimensional separation of ovarian cancer cell proteome followed by identification of reactive protein by mass spectrometry.

The data presented in our study demonstrates the capability of our approach in biomarker discovery and has a great potential to develop diagnostic marker for the early detection of ovarian cancer. With this approach we have identified and validated eight different tumor associated antigens, which includes CREB3, MRPL46, BCOR, HMG2, HIP1R, EXOSC10, OLFM4 and KIAA1755 with a key role in tumor regulation. We believe that identification of more TAAs could help in better understanding of the molecular pathology involved in cancer development and progression. Understanding the physiological activators, interactors and targets of these identifies TAA's will derive new knowledge in transcriptional regulation and new strategies in the intervention of human diseases. We conclude that the proposed approach represents a valid strategy to high-throughput profiling ascetic fluid from ovarian cancer patients.

11.5 Tumor regulation mediated by cell surface tumor antigen targeting antibodies

The latter part of this project demonstrated the presence of autoantibody in ascites targeting cell surface antigens expressed by tumor cells and verified its role in controlling tumor growth by activating complement. The meaningful targets for immune responses are mainly domains of surface-expressed proteins and glycoproteins that are accessible to antibodies and cytotoxic immune cells [150]. Our immunofluorescence assay illustrates the presence of tumor specific surface antigen on live ovarian cancer cell line. The cell surface staining was performed with the same set of antibodies on ovarian carcinoma cells while incubating them on ice. The result we have obtained implies the presence of cell surface receptor. Antibodies binding to these specific receptor gets internalised by endocytosis or pinocytosis [196,197]. Another possibility could be that some of the intracellular antigens or proteolytic fragments of intracellular target might get externalised and displayed on the surface of cancer cells by unconventional secretion [152]. Further, cell surface ELISA was performed for the identification and localization of target antigens as well as the quantitative analysis of cell surface antigen expression. This technique enabled for the quantification of immunoreactive antibodies present in samples targeted specifically against tumor associated antigens expressed by immobilized/ adherent OVCAR3 cell on their cell surface [144].

It was also evident from our result that the complement system plays a vital role in regulation of tumor. The cytotoxic C activity in ascitic fluid was examined by exposing OVCAR cells to immunoglobulins purified from ascetic fluids. Normal human serum was used as a control source of C in the cell-killing assay. Maximal killing (25-30%) of OVCAR3 cells was obtained by treating them with a mixture of cMOV18 and cMOV19 was set as a positive control for this assay. Almost 75% of Cell surface ELISA positive samples collected from primary ovarian cancer patients was able to induce complement dependent killing of OVCAR cells (Fig 31). The antibody from noncancerous patients were not competent enough to cause any killing. This may be due to the fact that the absence of particular antibodies which might be required for complex formation to activate the complement pathway. Presence of C regulators might be another reason for constrained C-dependent lysis of these cells.

In this present study, we have verified the presence of tumor specific immunoglobulins in ascitic fluid collected from ovarian cancer patients directed against surface antigens and demonstrated that these molecules are capable to activate the complement system on binding to their cell surface antigen/ receptor followed by a cascade of events leading to C mediated killing of tumor cells. Hence, we would strongly suggest this as an effective immunological surveillance mechanism in regulation of tumor. In the case of ovarian cancer, the presence of tumor cells within the peritoneal cavity surrounded by a functional C system also makes this tumor type an attractive target for local monoclonal antibody therapy [50]. Isolation of cell surface tumor associated antigens and identifying them by mass-spectrophotometry will be another prospective aspect of this study.

Chapter 4

12. Conclusion

The strategy proposed within this work provides a systematic profiling of ovarian cancer ascites by coupling phage display to high-throughput screening technologies. This new valuable tool could be applied to obtain selection of tumor associated antigens with potential diagnostic value or biological relevance in any auto-antibody-antigen related pathologies such as cancer, autoimmune and various infective diseases. Beyond the advantage in identifying new antigens/autoantigens that can provide insights into the pathogenesis of the diseases studied, diagnosis and prognosis as well can be improved. Our approach could provide information about the pathological subtypes, recognize the state in the early stages of its development, specific antibody signatures produced by each patients which could be correlated with the survival. These great deal of information may anticipate the therapeutic intervention, thus avoiding or delaying the pathological manifestations.

In addition, our approach allows to focus the attention on the desired target (i.e. the specific organ or tissue), and screening its whole specific proteome, by isolating mRNA (representing all expressed genes) and cloning in an appropriate system. The possibility to select proteins (i.e. for their binding capability), provided by the phage display system, allows the enrichment for target proteins, decreasing the number of proteins to be assayed, enables the identification of the interactors/ molecular signature of disease from a high degree of complexity and present in low abundance with high sensitivity. Thus, overcoming the major limitations usually encountered in these systems when used separately. At the same time, the link with the genotype permits the rapid identification of the reactive polypeptides. In this regard, this global approach is proposed as a general tool the dissection of complex molecular interaction systems.

Chapter 5

13. Materials and Methods

13.1 Section 1

Abbreviations:

Ab, antibody
AP, Alkaline Phosphatase
BCIP, 5-bromo-4-chloro-3-indolyl-beta-D-galactopyranoside
B-PER, bacterial protein extraction reagent
BSA, Bovine Serum Albumine
DMSO, Dimethylsulfoxide
dNTPs, deoxynucleotides
DTT, dithiothreitol
GSH, glutathione
HRP, HorseRadish Peroxidase
IPTG, Isopropyl β -D-1-thiogalactopyranoside
NBT, NitroBlue Tetrazolium
NC, nitrocellulose
O/N, over night
PBS, phosphate buffered saline
PEG, polietilenglicole
RT, Room Temperature
TMB, Tetrametilbenzidine
ZYM5052, autoinducing medium

13.2 Section 2

Solutions and buffers

▪ PBS

8 g NaCl, 0.2 g KCl, 1.44 g Na₂HPO₄, 0.24 g KH₂PO₄ in 1000 mL H₂O, final pH 7.4.

▪ TAE buffer for DNA electrophoresis on agarose gels

0.04 M Tris-acetate, 0.001 M EDTA.

▪ 2xTY liquid broth for bacteria

16 g Bacto-tryptone, 10 g Bacto-yeast, 5 g NaCl, final pH 7.0. If required, ampicillin 100 μ g/mL, chloramphenicol 34 μ g/mL, streptomycin 75 μ g/mL

▪ ZYM5052 liquid broth for bacteria

Freshly prepared by adding each sterile stock solution in the following order: 80% ZY (10% Tryptone, 5% Yeast extract); 50x M (1.25M Na₂HPO₄, 1.25M KH₂PO₄, 2.5M NH₄Cl, 0.25M Na₂SO₄); 2mM MgSO₄; 100ox Metal Mix (50 mM FeCl₃, 20mM CaCl₂, 10mM MnCl₂, 10mM ZnSO₄, 2mM CoCl₂, 2mM CuCl₂, 2mM NiCl₂, 2mM Na₂MoO₄, 2mM Na₂SeO₃, 2mM H₃BO₃); 50x 5052 solution (25% glycerol, 2.5% glucose, 10% α-lactose monohydrate); 100 µg/mL of ampicillin, sterile water to volume.

▪ **2xTY Agar plates**

16 g Bacto-tryptone, 10 g Bacto-yeast, 5 g NaCl, 15 g Bacto-agar, final pH 7.0. If required, ampicillin 100 µg/mL, chloramphenicol 34 µg /mL, streptomycin 75 µg /mL.

▪ **CCMB80 for preparation of competent *E.coli* cells**

11,8 g CaCl₂ (dihydrate), 4,0 g MnCl₂ (tetrahydrate), 2,0 g MgCl₂ (hexahydrate), 10mM K-acetate (pH7), 10% Glycerol, H₂O to 1L. Adjust pH to 6.4 . Filtration with 0.2 µm filter.

Glycerol Buffer for preparation of electrocompetent *E.coli* cells

10% glycerol in milliQ water. Autoclave before use.

▪ **PBST**

PBS added with 0.1% Tween 20

▪ **MPBS**

PBS added with 2% non-fat milk powder.

Bacterial strains

The bacterial strains used in this study were:

- *Escherichia coli* DH5αF' (Gibco BRL), F'/endA1 hsd17 (rK- mK+) supE44 thi-1 recA1 gyrA (Nalr) relA1 _ (lacZYA-argF) U169 deoR (F80dlacD-(lacZ)M15)

- *Escherichia coli* BL21-CodonPlus(DE3)-RIPL strain B F- ompT hsdS(rB- mB-) dcm+ Tetr gal λ(DE3) endA Hte [argU proL/Camr] [argU ileY leuW Strep/Specr]

Oligonucleotides for general screenings

All primers were purchased from Biomers.

Oligo ID	Sequence (5'-3')
VHPT2 antisense	TGGTGATGGTGAGTACTATCCAGGCCAGCAGTGGGTTTG
VLPT2 sense	TACCTATTGCCTACGGCAGCCGCTGGATTGTTATTACTC
pGEX sense	GGGCTGGCAAGCCACGTTTGGTG
pGEX anti	CCGGGAGCTGCATGTGTGTCAGAGGTTTTCCACC

Table 14: Oligonucleotide sequences

13.3 Section 3

Standard protocols used

PCR (Polymerase chain reaction)

Thermus aquaticus DNA polymerase (Finnzymes) was used.

Reaction mixture:

▪ Template DNA	0.01-1 ng (plasmidic DNA)
▪ Sense primer	0.5 μ M
▪ Antisense primer	0.5 μ M
▪ Finnzymes Buffer 10x	2.0 μ L
▪ dNTPs (Promega)	0.25 mM
▪ MgCl ₂	1.5 mM
▪ Taq polymerase	0.025 units/ μ L
▪ H ₂ O	to 20 μ L

The following cycles were performed:

- Denaturation step, 5' at 94°C.
- 31 cycles of: denaturation, 45'' at 94°C; annealing, 45'' at 60°C; elongation, 1' every 1000bp at 72°C.
- Final elongation step: 10' at 72°C

Inverse PCR

Reaction was performed on plasmidic preparations as follows of the libraries subcloned in pGEX vector:

▪ DNA (10 ng)	1 μ L
▪ Primer sense (0,5 uM)	1 μ L
▪ Primer anti (0,5 uM)	1 μ L
▪ Buffer HF (5x)	4 μ L
▪ dNTPs (0,4 mM)	0.4 μ L
▪ Fusion Pfu polymerase (Finnzymes)	0.2 μ L
▪ H ₂ O	to 20 μ L

PCR amplification was performed as follows:

Initial denaturation

- 30'' at 98°C

31 cycles as follows:

- 10'' at 98°C
- 10'' at 70°C
- 1'15'' at 72°C (15''/kb)

Finale extension: 5' at 72°C

Amplicons were gel-purified and 10 ng of the purified product were ligated O/N at 16°C. After transformation in *E. coli* competent cells, cultures were plated onto ampicillin containing agar plates. After O/N growth at 28°C, colonies were screened by PCR with pGEX specific primers.

DNA electrophoresis on agarose gels

Agarose (Sigma) gels with a concentration of 1.5 % in TAE buffer were used to separate PCR products; 0.8 % agarose gels were used to separate plasmidic DNA preparations, before and after digestions. 1 µL of ethidium bromide (2mg/mL, Sigma) was added to 50 ml of agarose gel.

100 base-pairs plus and 1KB molecular weight markers were purchased from Fermentas.

DNA purification

The NucleoTraPCR kit (Macherey-Nagel) was used for purification of DNA from agarose gel and reaction mixtures, following the manufacturer instructions.

Plasmidic DNA extraction

The Perfectprep Plasmid kit (Eppendorf) was used for plasmidic DNA mini-preparations (1 to 5 ml of O/N bacterial culture), following the manufacturer instructions.

DNA digestion with restriction endonucleases

All restriction endonucleases (BssHII, NheI) were purchased from New England Biolabs.

Reaction mixture:

- DNA
- NEB Buffer 10x
- BSA 100x
- Restriction endonuclease, 1 unit / µg of DNA
- H₂O to 50 µL

Incubation for 1 hour at the temperature required by the specific endonuclease.

Ligation

Plasmidic vector DNA and insert DNA were mixed at a 1:3/1:5 ratio (number of molecules). T4 ligase was purchased from New England Biolabs.

Reaction mixture:

- DNA (about 100 ng)
- T4 ligase Buffer (NEB) 10x
- T4 ligase (NEB), 1 Unit/reaction
- H₂O to 10 µL

Incubation O/N at 16°C.

Preparation of competent *E. coli*

50 mL of *E. coli* culture, DH5α or BL21(DE3)RIPL strains, were grown at 37°C in 2xTY liquid broth to OD₆₀₀ 0.5. Bacteria were chilled in ice for 10' to stop growth, centrifuged at 4°C for 10' at 3000 rpm and the supernatant was discarded. The bacterial pellet resuspended in 8 mL of CCMB80 solution and put in ice for 20'. After centrifuging for

10' at 4°C, supernatant was discarded, bacterial pellet resuspended in 2 mL of CCMB80 and dispensed in 80 µL aliquotes. Competent cells were immediately used or stocked at -80°C up to four weeks.

Bacterial transformation

5 µL of ligation reaction mixture or 10-50 ng of plasmidic preparation were transferred into a tube containing 80 µL of competent cells. The mixture was incubated in ice for 20'. Heat shock was applied at 42°C for 1 minute and 15''; bacteria were then chilled in ice for 2 minutes, resuspended in 1 ml of liquid broth and allowed to grow in absence of selective antibiotic for 1 hour. Bacteria were then plated on antibiotic-containing agar plates and grown O/N at 30°C.

Preparation of electro-competent *E.coli* cells

The following protocol was used for preparation of *E.coli* DH5α F' electrocompetent cells.

- Grow *E.coli* DH5α strain in 200 ml of 2xTY liquid broth to OD₆₀₀ 0.8.
- Split the culture in 4 50ml-tubes and put on ice for 20'.
- Centrifuge at 5,000 rpm, at 4°C for 8'.
- Discard the supernatant and gently resuspend the pellet with glycerol buffer.
- Add glycerol buffer to 50 ml and incubate 10' on ice.
- Centrifuge at 5,000 rpm, at 4°C for 10'.
- Discard supernatant, resuspend pellet with glycerol buffer and collect in two 50-ml tubes.
- Add glycerol buffer to 50 ml and incubate 10' on ice.
- Centrifuge at 5,000 rpm, at 4°C for 10'.
- Discard supernatant, resuspend pellet with glycerol buffer and collect in one 50-ml tube.
- Add glycerol buffer to 50 ml and incubate 10' on ice.
- Centrifuge 5000rpm per 10' a 4°C.
- Discard completely the supernatant and resuspend the pellet with 125 µl of glycerol buffer for every 100 ml of bacterial culture.
- Use immediately or stock at -80°C for up to four weeks.

To test the efficiency of the so prepared cells an electroporation of 10 pg of purified commercial pUC119 vector was performed. The efficiency was generally about 10¹⁰ transformed clones / µg DNA.

DNA Sequencing

PCR products were purified with Eppendorf Perfectprep Gel Cleanup kit following manufacturer instructions.

Reaction mixture for sequencing were composed as follows:

- 50-100 ng of purified PCR product
- 1 µL primer (3,2 µM)
- 2 µL Terminator Mix (Applied Biosystems, BigDye Terminator v1.1 Cycle Sequencing Kit)
- 2 µL buffer 5x
- H₂O to 10 µL

and the sequencing program was:

- 1' at 96°
- 25 cycles: 15'' at 96°; 5'' at 50°; 4' at 60°

Reactions were purified with CENTRI SEP Spin Columns, following manufacturer instructions. 5 μ L of purified sequences were loaded on sequencing plates with 10 μ L of formamide, denatured for 2' at 96° and analyzed with 3100 Genetic Analyzer sequencer (ABI PRISM-HITACHI).

13.4 Section 4: Methods

13.4.1 Patient samples and cell line

13.4.1A Sample preparation

Ascites were collected from 153 patients representing various disease conditions which include ascites from patients diagnosed with ovarian cancer (69), other cancers (34) and non-cancerous control ascitic fluid (50) from female patients with no known history of cancer. Numbers in brackets indicate the number of patients for each group. Ascitic fluid samples were obtained from i) the Department of Clinical and Experimental Medicine, University of Eastern Piedmont, ii) Department of Life Science, University of Trieste, iii) Istituto Nazionale Tumori, Milan and iv) University of Turin. All ascite samples were centrifuged at 11000 rpm at 4°C for 5minutes and supernatants were stored at -80°C until processing. Immunoglobulins from all ascitic fluid were affinity purified using Protein A Agarose (Roche). 50 μ l of crude ascitic fluid was mixed with starting buffer containing 100mM TRIS-HCl pH 8, 1% IGEPAL CA630, 1mM EDTA, 1mM PMSF, 1:100 dilution of protease inhibitor, 40 μ l Protein A agarose in a final volume of 1ml. Incubated overnight at 4°C on a rotating platform. Washed and eluted to an equal volume of sample used with 100mM glycine pH 2.5, later added 20% 1M TRIS -HCl pH 8 for stability.

13.4.1B Cell lines

The human ovarian adenocarcinoma cell line (NIH: OVCAR-3, ATCC® HTB-161™) was grown in RPMI 1640 media containing 10% foetal calf serum, 2 mM glutamine, and 1% penicillin/streptomycin. Cells were maintained at 37°C in a humidified atmosphere containing CO₂.

13.4.2 Characterization of ascitic fluid based on autoantibody response

13.4.2A Western Blot of OVCAR-3 Cell Extract

Western blot was performed to confirm the presence of tumor specific antigens present in OVCAR-3 cell extract. OVCAR-3 cell extract was prepared under denaturing condition using 8M Urea. After 1hr blocking step with 4% MPBST, 1:50 dilution of antibodies isolated from ascites fluid from 20 patients were used as the source of primary antibodies. These samples were diluted in 2% MPBST and incubated at RT for 45 min. Membranes were incubated 1.5 hrs RT and followed by 1 hr incubation with secondary antibody, alkaline phosphatase conjugated anti-human IgG. The membrane was developed using chromogenic substrate (NBT/BCIP, Roche).

13.4.2B Ovarian Cancer Whole Cell ELISA

OVCAR-3 cells were seeded in 96-well culture plates at a density of 1×10^4 cells/well and incubated 24 hrs at 37 °C in presence of CO₂. Plates were subsequently washed 3 times with wash /blocking buffer (1M MgCl₂, 1M CaCl₂, BSA

(FC 2%) in PBS), fixed and permeabilized with methanol. After incubation on ice for 5 min, methanol was discarded and washed twice with wash /blocking buffer. Plates were incubated for 1.5 hr on ice at 4°C with 100 µl pre-blocked primary antibody (Purified and normalised Ascitic IgG)/well which were diluted 1:100 in wash /blocking buffer. The plate was subsequently washed 3 times with blocking buffer and incubated for 1 hr on ice at 4°C with 1:2000 dilution of peroxidase-conjugated secondary antibody in blocking buffer (Polyclonal Rabbit Anti-Human Immunoglobulins/HRP; Dako). Performed 3 washes and dried. 70µl of TMB (3,3',5,5'-Tetramethylbenzidine liquid substrate, Sigma) was added to each well and dark incubate on ice until proper intensity was observed. This TMB was transferred into a new ELISA plate already containing 35µl 1N H₂SO₄ to stop the enzymatic reaction. The absorbance at 450 nm was measured with a microplate reader. The cutoff value was calculated as cumulative mean + 2 (standard deviation) of the absorbance from non cancerous control wells.

13.4.2C Ovarian Cancer Cell Lysate ELISA

Cell extraction procedure: Confluent OVCAR-3 cells grown in a 100mm tissue culture plate were washed gently with ice cold PBS. Cells were scraped out into pre-chilled tube by adding 0.5 ml of complete non- denaturing extraction buffer containing 100 mM Tris, pH 7.4 ; 150 mM NaCl; 1 mM EGTGA; 1 mM EDTA; 1% IGEPAL; Protease inhibitor cocktail (Sigma p8340) and 1 mM PMSF. Cells were briefly sonicated after incubation on ice for 15-30 min. The soluble cell extract were transferred into new tube following centrifugation at 13,000 x rpm for 10 min at 4°C and the concentration was determined by BCA assay.

Cell Lysate ELISA: 96 well microtiter plate O/N coated with 3.2 µg/well of OVCAR-3 cell extract was blocked with 2% BSA in PBST (0.05%) for 1hr at 30°C. The plate was incubated for 1.5 hrs at 30°C with 100 µl primary antibody (1: 50 diluted purified ascitic IgG preblocked for atleast 30 min). The unbound antibodies were removed by washing with PBST (0.05%) and PBS 1x. Incubated for 1hr at 30°C with 1:5000 diluted anti-human IgG/horseradish peroxidase conjugate in each well and subsequently washed. 70 µL of 3,3',5,5'-Tetramethylbenzidine substrate solution was added and incubated in dark until a proper intensity of colour was observed. The reaction was stopped by adding 35 µL/well of 1 N H₂SO₄. Plates were read spectrophotometrically at 450 nm.

13.4.2D Immunofluorescence Assay

5 x 10⁴ OVCAR cells were plated onto poly-L-lysine-coated glass coverslips in a 10cm culture plate without any overlap. The culture was incubated at 37°C in presence of CO₂ until they attains 80% confluence. This culture plate was washed once and the cover slips were transferred individually to new wells of 24 well culture plate.

OVCAR Cells Surface Staining: The confluent cells on the cover slips were washed once with plain RPMI and 1: 10 diluted primary antibody in blocking buffer (5% BSA in serum free RPMI medium) was added. Incubated on ice at 4°C for 2 hrs. After primary incubation, the unbound antibodies were removed by washing 3 times with blocking buffer. The cells transferred to new well and were subsequently incubated for another 1 hr on ice at 4°C with secondary antibody (anti hIgG- cy5) diluted 1:200 in blocking buffer. Performed 2 washes, transferred them to new wells in which the cells were fixed with 200µl of 4% PFA + 4% Sucrose on ice for 15 min, and permeabilised the cells for 2-3min 0.2% triton in PBS. The fixed and permeabilized cells were incubated with 1:2000 dilution of propidium iodide

(PI: nuclear stain) in PBS. Cells were washed thrice with PBS 1x and once with dH₂O, mounted to a glass slide with a small drop of mountant and the cells on cover slip facing the mountant and sealed with nail polish. The cells were directly analyzed with a Leica TCS-SP confocal laser scanning microscope using sequential scan tool. Laser power and photomultiplier settings were kept identical for all the samples to be able to compare the results.

Fixed and permeabilized OVCAR Cells for intracellular staining: The confluent cells on the cover slips were washed twice with prewarmed phosphate-buffered saline (PBS). The cells were fixed with 200µl of 4% PFA + 4% Sucrose on ice for 15 min, and permeabilized the cells for 2-3min 0.2% triton in PBS. The fixed and permeabilized cells were washed once with RPMI and 1: 10 diluted primary antibody in blocking buffer (5% BSA in serum free RPMI medium) was added. After 2hr incubation at 37°C, the unbound antibodies were removed by washing 3 times with blocking buffer. The cells transferred to new well and were subsequently incubated for another 1 hr 37°C with secondary antibody (anti hIgG- cy5) diluted 1:200 in blocking buffer. Performed 2 washes, transferred them to new wells in which the cells were incubated with 1:2000 dilution of propidium iodide (PI: nuclear stain) in PBS. Cells were washed thrice with PBS and once with dH₂O, mounted to a glass slide with a small drop of mountant and the cells on cover slip facing the mountant and sealed with nail polish. The cells were directly analyzed with a Leica TCS-SP confocal laser scanning microscope using sequential scan tool. Laser power and photomultiplier settings were kept identical for all the samples to be able to compare the results.

13.4.3 Selection of cDNA Phage Display library

13.4.3A Phage production

An aliquot of the bacterial stock of the library was thawed from the -80°C freezer and diluted in 10 mL of 2xTY liquid broth added with chloramphenicol/ampicillin in order to have a starting OD₆₀₀ around 0.05. Bacteria were grown in a 100 mL flask shaking at 220 rpm and at 37° C, to OD₆₀₀ 0.5. Bacteria were infected with a wild-type helper phage (M13K.07) at a MOI (multiplicity of infection) of 20, at 37°C for 45 min, without shaking. After infection, bacteria were centrifuged at 1500 x g for 10 min at 30° C, the supernatant was discarded and the pellet resuspended in 40 mL of 2xTY broth added with chloramphenicol/ampicillin and kanamycin (helper phage resistance). Bacteria were then grown O/N, at 30° C and shaking at 220 rpm, to allow production of the recombinant phages in the culture supernatant. The following day bacteria were centrifuged at 7,000 rpm for 20 min at 4° C. The phages-containing supernatant was collected and precipitation was performed by adding 10 mL (1/5 of total volume) of PEG-NaCl solution (20% PEG-8000 (Fluka) in 2.5 M NaCl, filtered with a 0.22 µm filter before use) and incubating on ice for 45 min. The solution was then centrifuged at 7,000 rpm for 20 min at 4° C, to collect the phages; the supernatant was carefully and entirely discarded and the white pellet was resuspended in 1 mL of PBS. The solution was centrifuged for 5 min at 10,000 rpm, to pellet the remaining bacteria in solution; the phage-containing supernatant was then transferred into a fresh tube and kept in ice until needed.

13.4.3B Phage Display Library Selection

Phage selections were performed as described in Di Niro et al, 2009 [147]. Bacterial stock of library (Human ORF libraries from pancreatic islets (HPI), colon cancer (HCC) and lung fibroblasts (HF)) was grown and infected with wild type helper phage (M13k.07) for replication and recombinant phages were collected. Phage selection and enrichment using G-protein functionalized magnetic beads (Dynabeads) coated with ascite IgG.

Ascite antibodies were coupled to M450 Magnetic beads (Dynabeads) as follows: dynabeads were resuspended and 10 μ l of beads were transferred to a microcentrifuge tube; two washes were performed with 0.5 ml of acetate buffer, pH 5. 5 μ l of purified ascite antibody, diluted in 100 μ l of PBS were added to the beads, and incubated for 45' in rotation at RT. Beads were washed 3 times with acetate buffer pH 5 to remove unbound antibodies and other proteins.

Subtraction step: First a pre-clearing step for the removal of the non-reacting phages by incubated with negative bead preparation, ie coated with IgG healthy serum to avoid any sort of background. This was performed by adding 200 μ l of PEG-precipitated phages (10^{11} phages) to the beads functionalized with sera from healthy donors, and incubated for 30' in rotation. Magnetic field was then applied, so that the bound phages were washed away, while the unbound phage population was collected and incubated with the beads functionalized with ascite antibodies from ovarian cancer patients, and incubated for 90' in rotation.

The selection procedure was performed as follows: Subtraction step was followed by 2 rounds of selection to enrich bound peptide sequence by separate incubation with seven different IgG purified primary ovarian cancerous ascites. 0.2 mL of phage preparation, containing 10^{11} phages, were added with an equal volume of 4% MPBS and incubated for 1 hour at RT. The phages were then incubated with the beads coupled to antibodies from sera from healthy donors, for 30 min in rotation at RT. The supernatant was collected by applying a magnetic field to remove the beads and the bound phages. The phages were then incubated with the beads coated with antibodies from the ascitic fluids collected from ovarian cancer patients, for 90 min in rotation at RT. Washes were performed by adding 1 ml of PBST or PBS to the beads, and then by applying a magnetic field to remove the solution with unbound phages. The stringency of the washing steps increased with the selection rounds; 10 times with PBST and 10 times with PBS for the first round of selection, 15 and 15 for the second, 15 and 15 with additional 10 min with rotation in PBST in the between for the third. After the washing steps, bound phages were eluted by mixing the beads with 1 mL of *E.coli* DH5 α , at OD₆₀₀ 0.5, at 37° C, for 45 min, with occasional shaking. Bacteria were plated on 15 cm 2xTY agar plates added with chloramphenicol and grown O/N at 30° C. Bacteria are harvested and either grown immediately to undergo the following round of selection or stored in small aliquots at -80° C.

13.4.3C Subcloning of cDNA fragments in pGEX bacterial expression vector

The modified pGEX vector (GE Healthcare) was used.

Plasmid preparation of the selected library was obtained from an aliquot of bacteria after third cycle of selection and digested using restriction sites flanking the cDNA gene fragments (BssHII – NheI). The digested fragments in the 100-700 bp range were purified and ligated to the vector cut with the same enzymes. The ligation reaction (vector : insert molar ratio of 1:5) was purified and transformed into DH5 α ' *E.coli* strain.

The resulting mini-library size was around 10^5 clones.

13.4.4 High-throughput recombinant protein production of the selected clones in autoinducing medium

After immunoscreening, the selected cDNA fragments were subcloned into an expression vector, a modified pGEX Vector and amplified in the host bacteria *BL21* (DE3) RIPL cells for enhanced protein production. 95 single clones from each of the 7 selections were randomly picked from agar plates and inoculated into 96 deep well plates in order to produce GST fusion protein. Protein production was carried out by auto inducing medium ZYM₅₀₅₂ [148] in 96 wells format and grown overnight at 28°C. Purification of recombinant proteins was done using GSH magnetic beads. The production and purification of this fusion protein were analysed by SDS-PAGE and western blotting with few random samples. Full length fusion protein were identified by incubating nitrocellulose membrane with 1:5000 dilution of α FLAG primary antibody and screening with alkaline phosphatase-conjugated anti-human IgG secondary antibody.

13.4.5 Immunoscreening of the selected antigen by protein microarray

The immunoreactivity of the phage display selected antigens were determined by microarray analysis. With the aid of BioOdyssey Calligrapher (Biorad) all the purified GST-fusion proteins were spotted onto a nitrocellulose (NC) slide. The purified proteins along with the controls (dilution rows of purified human IgG (Sigma), ranging from 500 ng/mL to 100 μ g/mL) were printed in duplicate in two identical fields of the same slide maintaining all parameters (such as contact time, distance between spots, wash cycle) and conditions including 15°C temperature and 50% humidity. The slides were incubated for 1hr at room temperature (RT) with blocking buffer (3% non fat dry milk in PBS 0.1% Tween20 (3%MPBST)). Once the sides were saturated, each of the 2 identical fields was incubated with 1:50 dilution for primary antibody (acitic fluid from cancer patients, non-cancerous patients, also anti-GST and Anti-FLAG monoclonal antibody against the fusion Tag) in 2% MPBST for 1.5 hrs. The slide assayed with Anti-GST and Anti-FLAG ensures that the proteins a properly spotted on to the slide. Performed 2 washes with PBST for 15 min and once with PBS. Added 1:200 diluted secondary antibody, Cy5 conjugated anti-human IgG - Cy5 conjugated (anti-mouse IgG for the slide incubated with anti-GST and Anti-FLAG) in 2% MPBST and incubated at RT for 1 hr. Cy5 is highly sensitive even with very low amount of autoantibody and stable fluorophore which gets excited at 650 nm wavelength. Washed twice with PBST and once with PBS, 5min for each washing step and dried. All fluorescent signals were detected with a ScanArray Gx[®], PerkinElmer scanner and analyzed with ScanArray Expression Software, PerkinElmer. The fluorescence intensity of each feature was determined, based on the mean of pixels' intensity within the protein feature minus the mean intensity of pixels in the surrounding area. Optimized scanning conditions were used for each substrate in order to obtain maximal non-saturated signals. The sample giving highest florescent signals were selected for next level.

13.4.6 Identification novel putative tumour-associated antigens (TAA) by sequencing

The most immunoreactive clones identified by microarray analysis were further processed to decode their sequence. As the first step, these screened clones were PCR amplified using pGEX sense (GGGCTGGCAAGCCACGTTTGGTG) and anti-sense primers (GGTGAAAACCTCTGACACATGCAGCTCCGG). The PCR amplified products were purified

using nucleoside extract kit II (Macherey-Nagel) and the DNA fragment of varying size (150-800bp) were sequenced. Under optimised condition, a fluorescence based cycle sequencing reaction was performed with the purified PCR amplified fragments/template along with its sequence specific primer (pGEX sense or anti sense) and ABI BigDye Terminator v1.1. The extension products were purified using Centri-Sep Columns (Princeton separations) based on gel filtration. The reaction mixture was added directly on top of the hydrated Sephadex fine DNA grade (GE healthcare) gel bed and spun down at 3600RPM. This was done to remove all the free and labelled dNTP's and unwanted buffer salts. The sequencing was carried out using ABI 3100 sequencer.

13.4.7 Large Scale Production of Novel Putative Antigens

13.4.7A Expression and purification of selected antigen

Microarray screened and characterized immunoreactive clones were traced back to the 96 well stock plate stored at -80°C. The exact clones were picked from plate, were grown in 1mL of 2xTY medium at 28 ° C in a shaking platform for 16 hours in the presence of 2 % glucose , thus to minimize the expression from the lac promoter . The following day, they were moved to a larger volume and grown at 28 ° C until reaching an optical density of OD₆₀₀ 0.5. Protein induction was performed for 3 hours at 25°C with 0.1 mM IPTG (Millipore) , which acts on the lac promoter and induces gene expression.

Bacterial cultures were centrifuged at 5000 rpm for 15 minutes and the pellet was resuspended in lysis buffer (50mM TRIS HCl pH 7.4, 150mM NaCl, 1% IGEPAL CA630, 1mM EDTA, 1:100 dilution of protease inhibitor cocktail P3840 sigma) (10 mL / gram of pellet) . Then added lysozyme (1 mg / gram of pellet) (Fluka) and DNase (20-50 g / mL) (Sigma) and the samples were incubated for 1 hour at 4°C with gentle shaking. At this point, sonication was performed in case the sample is not completely lysed, using the sonicator (Bandelin sonoplus HD2070) . Clarified lysates were centrifuged at 5000 rpm for 15 minutes. The supernatant was recovered and incubated with prewashed glutathione agarose (GSH) resin (Sigma). The suspension was incubated with gentle mixing on a rotating platform at 4°C for 45 min; supernatant was applied to a filter column; column was washed twice with PBST0,1% and once with PBS. Two elution steps were performed at 4°C for 15 min with 100µL of freshly prepared elution buffer (50mM GSH reduced-Sigma, 100mM NaCl, PBS pH8). After incubation, the two fractions of eluted protein were collected, aliquoted and stored at -20°C .

The proteins produced were later analyzed for their quality. These purified proteins were denatured, loaded and performed polyacrylamide gel electrophoresis. The gels were stained with Coomassie blue or alternatively, the proteins were transferred onto a nitrocellulose membrane to analyzed by Western Blot.

13.4.7B Western blotting

Western blots were performed using purified GST fusion protein. After transferring step, membrane was blocked for 1 h at room temperature using 4% MPBST. Then incubated 90 min with 1:5000 dilution anti-FLAG/ anti-GST primary antibody in 2%MPBST. Subsequently were washed using PBST (0.1% v/v) and PBS 1X. Anti mouse IgG coupled to alkaline phosphatase (1:5000 dilution in 2%MPBST) was used as the secondary antibody. Membrane was developed by adding NBT/BCIP substrate.

13.4.8 Validation of Putative Antigenic Protein by Indirect ELISA

Presence of a specific antibody in ascitic fluids were tested by indirect ELISA. 96 well ELISA plate was pre coated (O/N at 4°C) with 1µg of purified full length GST fusion protein in 100 µL of PBS was saturated with blocking buffer (2% BSA in PBST(0.05%)) for 1 hr at 30°C. 1: 50 diluted primary antibodies in blocking buffer were incubated at RT for 45 min enabled with proper mixing and were subsequently transferred into their appropriate well and incubated at 30°C for 90 min. Primary antibody used were affinity purified IgG from 153 ascites from patients which includes ovarian cancer, other cancer and non-cancerous control. After incubation at 30°C, the unbound primary antibodies were removed by washing 3 times with PBST 0.05% and PBS 1x. Incubation at 30°C for 1hr with 1:5000 dilution of peroxidase-conjugated secondary antibody in 2% blocking buffer. 70 µL of 3,3',5,5'-Tetramethylbenzidine was added to all well after final wash (3 times) with PBST(0.05%) and PBS 1x. The plate was incubated in dark until they have attained proper intensity of colour. The reaction was stopped by adding 35 µL/well of 1 N H₂SO₄. Plates were read spectrophotometrically at 450 nm. For each antigen validation, the cut-off value was independently calculated as 'sum of (cumulative mean + twice the standard deviation) of the absorbance from non-cancerous control wells.

13.4.9 Analysis for the prognostic potential of the novel antigens and their clinical correlation

Based on the antigen ELISA result, Kaplan meier analysis calculates the proportion surviving to each point that a death occurs and was done to understand the clinical correlation of overall survival of the patients with the presence of specific antibodies. Later, a log-rank method was used to evaluate their significance. 52 patients with at least 18 months follow up details were used for the overall survival analysis.

13.4.10 Verification of Cell Surface Targets by Cell Surface ELISA on Live OVCAR-3 Cell Line

Added 100µl of 1x 10⁴ OVCAR cells into each well of the 96-well microplates and incubate in 5% CO₂ at 37° C in a cell culture incubator for 36hrs. The culture medium was removed from every well and washed once with 100µl RPMI medium containing 10 % FBS (pre warmed at 37° C). Primary antibody (Purified and normalized ascitic IgG) were diluted 1:100 in RPMI medium with 10% FBS and ensured proper mixing atleast 30 min at RT. 100 µl of this pre-blocked primary antibody along with 1:200 diluted anti folate receptor antibody (positive control for the assay) were transferred into their appropriate wells in triplicate and incubated 1h 30min at 37° C in presence of CO₂. The plates were washed thrice with pre warmed RPMI medium and incubated for 1hr at 37° C in presence of CO₂ with 1:2000 dilution of peroxidase-conjugated secondary antibody in RPMI medium (Polyclonal Rabbit Anti-Human Immunoglobulins/HRP; Dako). A triplicate negative control wells incubated with only secondary antibody was included thus to reduce the non specific signal from the final reading. 3 washes were performed with RPMI medium and once with PBS 1X. Pipette 70µl TMB/well (3,3',5,5'-Tetramethylbenzidine liquid substrate, Sigma) and dark incubate at RT until proper intensity was observed. This TMB was transferred into a new ELISA plate already containing 35µl 1N H₂SO₄ to stop the enzymatic reaction. The absorbance at 450 nm was measured with a microplate reader. The cutoff value was calculated as cumulative mean + 2 (standard deviation) of the absorbance from non-cancerous control wells.

13.4.11 Role of Cell Surface Antigen Interacting Antibodies in Tumor Regulation by Complement Dependent Cytotoxicity (CDC)

1×10^4 OVCAR cells were seeded into each wells of 96-well tissue culture plate (Euroclone) and incubated 36 hrs at 37 °C in presence of CO₂. Once the cells were grown to confluence, culture medium was carefully removed and washed with 380µl/well DPBS/Ca²⁺/Mg²⁺ containing 2% BSA (Wash/blocking buffer). To measure complement activation by antibody, the cells were incubated with 50 µl/well of wash/blocking buffer containing individual antibodies purified from ascites (20 µg/ml each) for 10 minutes at 37°C. Two controls were included in this assay i) we used the mixture of the two antibodies cMOV18 and cMOV19 (2 µg/ml each) as well as ii) cell incubated without antibody. NHS (Normal Human Serum: pool of human AB Rh+ sera) was then added without washing to a final volume of 100 µL (ie, 1:2 solution of NHS in DPBS/Ca²⁺/Mg²⁺/2% BSA (25 µl NHS + 25 µl Wash/blocking buffer), and incubation was continued for further 60 minutes at 37°C. The residual viable cells were counted using the 3-(4,5-dimethylthiazol-2-yl)-2,5-diphenyltetrazolium bromide (MTT) assay. 20 µl MTT solution (5mg/ml) in 200 µl fresh culture medium was added to each well and incubate 4 hours at 37°C. After careful removal of culture medium, MTT crystals were solubilized by adding 200µl DMSO and read at 570nm with a reference wavelength set to 650nm. The experiment was performed in quadruplicate.

14. References

1. Accessed online at <http://globocan.iarc.fr/> on 23-12-2013
2. Berek, J.S., C. Crum, and M. Friedlander, *Cancer of the ovary, fallopian tube, and peritoneum*. Int J Gynaecol Obstet, 2012. **119 Suppl 2**: p. S118-29
3. Accessed online at <http://seer.cancer.gov/statfacts/html/ovary.html> on 23-12-2013
4. Accessed online at <http://www.cancer.org/cancer/ovariancancer/> on 23-12-2013
5. Cannistra, S.A., *Cancer of the ovary*. N Engl J Med, 2004. **351**(24): p. 2519-29.
6. Gwinn, M.L., et al., *Pregnancy, breast feeding, and oral contraceptives and the risk of epithelial ovarian cancer*. J Clin Epidemiol, 1990. **43**(6): p. 559-68.
7. Ness, R.B. and C. Cottreau, *Possible role of ovarian epithelial inflammation in ovarian cancer*. J Natl Cancer Inst, 1999. **91**(17): p. 1459-67.
8. Cramer, D.W. and W.R. Welch, *Determinants of ovarian cancer risk. II. Inferences regarding pathogenesis*. J Natl Cancer Inst, 1983. **71**(4): p. 717-21.
9. Williams, T.I., et al., *Epithelial ovarian cancer: disease etiology, treatment, detection, and investigational gene, metabolite, and protein biomarkers*. J Proteome Res, 2007. **6**(8): p. 2936-62.
10. Green, A., et al., *Tubal sterilisation, hysterectomy and decreased risk of ovarian cancer. Survey of Women's Health Study Group*. Int J Cancer, 1997. **71**(6): p. 948-51.
11. Accessed online at <http://www.cancer.gov/cancertopics/factsheet/Risk> on 23-12-2013
12. Chung, D.C. and A.K. Rustgi, *The hereditary nonpolyposis colorectal cancer syndrome: genetics and clinical implications*. Ann Intern Med, 2003. **138**(7): p. 560-70.
13. Kohlmann, W. and S.B. Gruber, *Lynch Syndrome*, in *GeneReviews*, R.A. Pagon, et al., Editors. 1993: Seattle (WA).
14. Bast, R.C., Jr., B. Hennesy, and G.B. Mills, *The biology of ovarian cancer: new opportunities for translation*. Nat Rev Cancer, 2009. **9**(6): p. 415-28.
15. Harris, C.C. and M. Hollstein, *Clinical implications of the p53 tumor-suppressor gene*. N Engl J Med, 1993. **329**(18): p. 1318-27.
16. Havrilesky, L., et al., *Prognostic significance of p53 mutation and p53 overexpression in advanced epithelial ovarian cancer: a Gynecologic Oncology Group Study*. J Clin Oncol, 2003. **21**(20): p. 3814-25.
17. Accessed online at http://www.cancer.gov/cancertopics/pdq/genetics/breast-and-ovarian/HealthProfessional/page2#Section_148 on 23-12-2013
18. Giardiello, F.M., et al., *Very high risk of cancer in familial Peutz-Jeghers syndrome*. Gastroenterology, 2000. **119**(6): p. 1447-53.

19. Eltabbakh, G.H., P.R. Yadav, and A. Morgan, *Clinical picture of women with early stage ovarian cancer*. *Gynecol Oncol*, 1999. **75**(3): p. 476-9.
20. Accessed online at <http://www.cancer.gov/cancertopics/wyntk/ovary/page6> on 23-12-2013.
21. Clarke-Pearson, D.L., *Clinical practice. Screening for ovarian cancer*. *N Engl J Med*, 2009. **361**(2): p. 170-7.
22. Accessed online at <http://www.ovariancancer.org> on 23-12-2013.
23. Cvetkovic, D., *Early events in ovarian oncogenesis*. *Reprod Biol Endocrinol*, 2003. **1**: p. 68.
24. Bast, R.C., Jr., *Status of tumor markers in ovarian cancer screening*. *J Clin Oncol*, 2003. **21**(10 Suppl): p. 200s-205s.
25. Accessed online at <http://www.uptodate.com/contents/ovarian-cancer-diagnosis-and-staging-beyond-the-basics#H3> on 23-12-2013.
26. Hennessy, B.T., R.L. Coleman, and M. Markman, *Ovarian cancer*. *Lancet*, 2009. **374**(9698): p. 1371-82.
27. Kim, A., et al., *Therapeutic strategies in epithelial ovarian cancer*. *J Exp Clin Cancer Res*, 2012. **31**: p. 14.
28. Moss, C. and S.B. Kaye, *Ovarian cancer: progress and continuing controversies in management*. *Eur J Cancer*, 2002. **38**(13): p. 1701-7.
29. Burger, R.A., et al., *Incorporation of bevacizumab in the primary treatment of ovarian cancer*. *N Engl J Med*, 2011. **365**(26): p. 2473-83.
30. Raspollini, M.R., et al., *Correlation of epidermal growth factor receptor expression with tumor microdensity vessels and with vascular endothelial growth factor expression in ovarian carcinoma*. *Int J Surg Pathol*, 2005. **13**(2): p. 135-42.
31. Suh, K.S., et al., *Ovarian cancer biomarkers for molecular biosensors and translational medicine*. *Expert Rev Mol Diagn*, 2010. **10**(8): p. 1069-83.
32. Badgwell, D. and R.C. Bast, Jr., *Early detection of ovarian cancer*. *Dis Markers*, 2007. **23**(5-6): p. 397-410.
33. Das, P.M. and R.C. Bast, Jr., *Early detection of ovarian cancer*. *Biomark Med*, 2008. **2**(3): p. 291-303.
34. Tinelli, A., et al., *Ovarian cancer biomarkers: a focus on genomic and proteomic findings*. *Curr Genomics*, 2007. **8**(5): p. 335-42.
35. Le Page, C., et al., *Predictive and prognostic protein biomarkers in epithelial ovarian cancer: recommendation for future studies*. *Cancers (Basel)*, 2010. **2**(2): p. 913-54.
36. Veneroni.R., et al., *Patented Biomarkers for the Early Detection of Ovarian Cancer*. *Recent Patents on Biomarkers*, 2011. **1**(1): p.1-9.
37. Sangisetty, S.L. and T.J. Miner, *Malignant ascites: A review of prognostic factors, pathophysiology and therapeutic measures*. *World J Gastrointest Surg*, 2012. **4**(4): p. 87-95.

38. Kipps, E., D.S. Tan, and S.B. Kaye, *Meeting the challenge of ascites in ovarian cancer: new avenues for therapy and research*. Nat Rev Cancer, 2013. **13**(4): p. 273-82.
39. Adam, R.A. and Y.G. Adam, *Malignant ascites: past, present, and future*. J Am Coll Surg, 2004. **198**(6): p. 999-1011.
40. Sheid, B., *Angiogenic effects of macrophages isolated from ascitic fluid aspirated from women with advanced ovarian cancer*. Cancer Lett, 1992. **62**(2): p. 153-8.
41. Kuk, C., et al., *Mining the ovarian cancer ascites proteome for potential ovarian cancer biomarkers*. Mol Cell Proteomics, 2009. **8**(4): p. 661-9.
42. Verheul, H.M., et al., *Targeting vascular endothelial growth factor blockade: ascites and pleural effusion formation*. Oncologist, 2000. **5 Suppl 1**: p. 45-50.
43. Milliken, D., et al., *Analysis of chemokines and chemokine receptor expression in ovarian cancer ascites*. Clin Cancer Res, 2002. **8**(4): p. 1108-14.
44. Walport, M.J., *Complement. First of two parts*. N Engl J Med, 2001. **344**(14): p. 1058-66.
45. Macor, P. and F. Tedesco, *Complement as effector system in cancer immunotherapy*. Immunol Lett, 2007. **111**(1): p. 6-13.
46. Niculescu, F., et al., *Persistent complement activation on tumor cells in breast cancer*. Am J Pathol, 1992. **140**(5): p. 1039-43.
47. Lucas, S.D., et al., *Tumor-specific deposition of immunoglobulin G and complement in papillary thyroid carcinoma*. Hum Pathol, 1996. **27**(12): p. 1329-35.
48. Bjorge, L., et al., *Ascitic complement system in ovarian cancer*. Br J Cancer, 2005. **92**(5): p. 895-905.
49. Leone Roberti Maggiore, U., et al., *Monoclonal antibodies therapies for ovarian cancer*. Expert Opin Biol Ther, 2013. **13**(5): p. 739-64.
50. Markman, M., *Intraperitoneal therapy of ovarian cancer*. Semin Oncol, 1998. **25**(3): p. 356-60.
51. Macor, P., et al., *Complement activated by chimeric anti-folate receptor antibodies is an efficient effector system to control ovarian carcinoma*. Cancer Res, 2006. **66**(7): p. 3876-83.
52. Baneyx, F., *Recombinant protein expression in Escherichia coli*. Curr Opin Biotechnol, 1999. **10**(5): p. 411-21.
53. Makela, A.R. and C. Oker-Blom, *Baculovirus display: a multifunctional technology for gene delivery and eukaryotic library development*. Adv Virus Res, 2006. **68**: p. 91-112.
54. Park, J.B. and M. Levine, *Cloning, sequencing, and characterization of alternatively spliced glutaredoxin 1 cDNA and its genomic gene: chromosomal localization, mrna stability, and origin of pseudogenes*. J Biol Chem, 2005. **280**(11): p. 10427-34.
55. Barrientos, T., et al., *Two novel members of the ABLIM protein family, ABLIM-2 and -3, associate with STARS and directly bind F-actin*. J Biol Chem, 2007. **282**(11): p. 8393-403.

56. Park, J.H., et al., *Molecular cloning, expression, and structural prediction of deoxyhypusine hydroxylase: a HEAT-repeat-containing metalloenzyme*. Proc Natl Acad Sci U S A, 2006. **103**(1): p. 51-6.
57. Zhang, C. and S.H. Kim, *Overview of structural genomics: from structure to function*. Curr Opin Chem Biol, 2003. **7**(1): p. 28-32.
58. Henics, T., et al., *Small-fragment genomic libraries for the display of putative epitopes from clinically significant pathogens*. Biotechniques, 2003. **35**(1): p. 196-202, 204, 206 passim.
59. Prodromou, C., R. Savva, and P.C. Driscoll, *DNA fragmentation-based combinatorial approaches to soluble protein expression Part I. Generating DNA fragment libraries*. Drug Discov Today, 2007. **12**(21-22): p. 931-8.
60. Di Niro, R., et al., *Rapid interactome profiling by massive sequencing*. Nucleic Acids Res, 2010. **38**(9): p. e110.
61. Etz, H., et al., *Identification of in vivo expressed vaccine candidate antigens from Staphylococcus aureus*. Proc Natl Acad Sci U S A, 2002. **99**(10): p. 6573-8.
62. Gerth, M.L., W.M. Patrick, and S. Lutz, *A second-generation system for unbiased reading frame selection*. Protein Eng Des Sel, 2004. **17**(7): p. 595-602.
63. Li, M., *Applications of display technology in protein analysis*. Nat Biotechnol, 2000. **18**(12): p. 1251-6.
64. Mintz, P.J., et al., *Fingerprinting the circulating repertoire of antibodies from cancer patients*. Nat Biotechnol, 2003. **21**(1): p. 57-63.
65. Robinson, C., et al., *Serologic responses in patients with malignant mesothelioma: evidence for both public and private specificities*. Am J Respir Cell Mol Biol, 2000. **22**(5): p. 550-6.
66. Philip, R., et al., *Shared immunoproteome for ovarian cancer diagnostics and immunotherapy: potential theranostic approach to cancer*. J Proteome Res, 2007. **6**(7): p. 2509-17.
67. Kalnina, Z., et al., *Evaluation of T7 and lambda phage display systems for survey of autoantibody profiles in cancer patients*. J Immunol Methods, 2008. **334**(1-2): p. 37-50.
68. Cekaite, L., et al., *Analysis of the humoral immune response to immunoselected phage-displayed peptides by a microarray-based method*. Proteomics, 2004. **4**(9): p. 2572-82.
69. Scanlan, M.J., et al., *Characterization of human colon cancer antigens recognized by autologous antibodies*. Int J Cancer, 1998. **76**(5): p. 652-8.
70. Old, L.J. and Y.T. Chen, *New paths in human cancer serology*. J Exp Med, 1998. **187**(8): p. 1163-7.
71. Smith, G.P., *Filamentous fusion phage: novel expression vectors that display cloned antigens on the virion surface*. Science, 1985. **228**(4705): p. 1315-7.
72. Sidhu, S.S., *Engineering M13 for phage display*. Biomol Eng, 2001. **18**(2): p. 57-63.
73. Rodi, D.J. and L. Makowski, *Phage-display technology--finding a needle in a vast molecular haystack*. Curr Opin Biotechnol, 1999. **10**(1): p. 87-93.

74. Carmen, S. and L. Jermutus, *Concepts in antibody phage display*. Brief Funct Genomic Proteomic, 2002. **1**(2): p. 189-203.
75. Willats, W.G., *Phage display: practicalities and prospects*. Plant Mol Biol, 2002. **50**(6): p. 837-54.
76. Kehoe, J.W. and B.K. Kay, *Filamentous phage display in the new millennium*. Chem Rev, 2005. **105**(11): p. 4056-72.
77. Arap, M.A., Phage display technology: applications and innovations. Genet. Mol. Biol, 2005. 28(1):p. 1-9.
78. Scott, J.K. and G.P. Smith, *Searching for peptide ligands with an epitope library*. Science, 1990. **249**(4967): p. 386-90.
79. Hertveldt, K., T. Belien, and G. Volckaert, *General M13 phage display: M13 phage display in identification and characterization of protein-protein interactions*. Methods Mol Biol, 2009. **502**: p. 321-39.
80. Kiewitz, A. and H. Wolfes, *Mapping of protein-protein interactions between c-myc and its coactivator CBP by a new phage display technique*. FEBS Lett, 1997. **415**(3): p. 258-62.
81. Fuh, G., et al., *Analysis of PDZ domain-ligand interactions using carboxyl-terminal phage display*. J Biol Chem, 2000. **275**(28): p. 21486-91.
82. Hammer, J., B. Takacs, and F. Sinigaglia, *Identification of a motif for HLA-DR1 binding peptides using M13 display libraries*. J Exp Med, 1992. **176**(4): p. 1007-13.
83. Caberoy, N.B., et al., *Efficient identification of phosphatidylserine-binding proteins by ORF phage display*. Biochem Biophys Res Commun, 2009. **386**(1): p. 197-201.
84. Cheng, X., B.K. Kay, and R.L. Juliano, *Identification of a biologically significant DNA-binding peptide motif by use of a random phage display library*. Gene, 1996. **171**(1): p. 1-8.
85. Matsubara, T., et al., *Selection of ganglioside GM1-binding peptides by using a phage library*. FEBS Lett, 1999. **456**(2): p. 253-6.
86. Wang, S., et al., *Peptides with selective affinity for carbon nanotubes*. Nat Mater, 2003. **2**(3): p. 196-200.
87. Rodi, D.J., et al., *Screening of a library of phage-displayed peptides identifies human bcl-2 as a taxol-binding protein*. J Mol Biol, 1999. **285**(1): p. 197-203.
88. Hekim, C., et al., *Novel peptide inhibitors of human kallikrein 2*. J Biol Chem, 2006. **281**(18): p. 12555-60.
89. Wirsching, F., et al., *Directed evolution towards protease-resistant hirudin variants*. Mol Genet Metab, 2003. **80**(4): p. 451-62.
90. Doorbar, J. and G. Winter, *Isolation of a peptide antagonist to the thrombin receptor using phage display*. J Mol Biol, 1994. **244**(4): p. 361-9.
91. Giordano, R.J., et al., *Biopanning and rapid analysis of selective interactive ligands*. Nat Med, 2001. **7**(11): p. 1249-53.

92. Liang, S., et al., *Screening and identification of vascular-endothelial-cell-specific binding peptide in gastric cancer*. J Mol Med (Berl), 2006. **84**(9): p. 764-73.
93. Pasqualini, R. and E. Ruoslahti, *Organ targeting in vivo using phage display peptide libraries*. Nature, 1996. **380**(6572): p. 364-6.
94. Essler, M. and E. Ruoslahti, *Molecular specialization of breast vasculature: a breast-homing phage-displayed peptide binds to aminopeptidase P in breast vasculature*. Proc Natl Acad Sci U S A, 2002. **99**(4): p. 2252-7.
95. Arap, W., et al., *Steps toward mapping the human vasculature by phage display*. Nat Med, 2002. **8**(2): p. 121-7.
96. Pershad, K., et al., *Generating a panel of highly specific antibodies to 20 human SH2 domains by phage display*. Protein Eng Des Sel, 2010. **23**(4): p. 279-88.
97. Hoogenboom, H.R., *Selecting and screening recombinant antibody libraries*. Nat Biotechnol, 2005. **23**(9): p. 1105-16.
98. Moss, M.L., L. Sklair-Tavron, and R. Nudelman, *Drug insight: tumor necrosis factor-converting enzyme as a pharmaceutical target for rheumatoid arthritis*. Nat Clin Pract Rheumatol, 2008. **4**(6): p. 300-9.
99. Jones, S.E., *Metastatic breast cancer: the treatment challenge*. Clin Breast Cancer, 2008. **8**(3): p. 224-33.
100. Moroni, M., et al., *Gene copy number for epidermal growth factor receptor (EGFR) and clinical response to antiEGFR treatment in colorectal cancer: a cohort study*. Lancet Oncol, 2005. **6**(5): p. 279-86.
101. Dalle, S., et al., *Monoclonal antibodies in clinical oncology*. Anticancer Agents Med Chem, 2008. **8**(5): p. 523-32.
102. Krebber, C., et al., *Selectively-infective phage (SIP): a mechanistic dissection of a novel in vivo selection for protein-ligand interactions*. J Mol Biol, 1997. **268**(3): p. 607-18.
103. Lankes, H.A., et al., *In vivo gene delivery and expression by bacteriophage lambda vectors*. J Appl Microbiol, 2007. **102**(5): p. 1337-49.
104. Larocca, D., et al., *Gene transfer to mammalian cells using genetically targeted filamentous bacteriophage*. FASEB J, 1999. **13**(6): p. 727-34.
105. Larocca, D., et al., *Targeting bacteriophage to mammalian cell surface receptors for gene delivery*. Hum Gene Ther, 1998. **9**(16): p. 2393-9.
106. Barry, M.A., W.J. Dower, and S.A. Johnston, *Toward cell-targeting gene therapy vectors: selection of cell-binding peptides from random peptide-presenting phage libraries*. Nat Med, 1996. **2**(3): p. 299-305.
107. Arap, W., R. Pasqualini, and E. Ruoslahti, *Cancer treatment by targeted drug delivery to tumor vasculature in a mouse model*. Science, 1998. **279**(5349): p. 377-80.
108. Naora, H., et al., *A serologically identified tumor antigen encoded by a homeobox gene promotes growth of ovarian epithelial cells*. Proc Natl Acad Sci U S A, 2001. **98**(7): p. 4060-5.

109. Vidal, C.I., et al., *An HSP90-mimic peptide revealed by fingerprinting the pool of antibodies from ovarian cancer patients*. *Oncogene*, 2004. **23**(55): p. 8859-67.
110. Chatterjee, M., et al., *Diagnostic markers of ovarian cancer by high-throughput antigen cloning and detection on arrays*. *Cancer Res*, 2006. **66**(2): p. 1181-90.
111. Zhang, L., et al., *In vitro screening of ovarian tumor specific peptides from a phage display peptide library*. *Biotechnol Lett*, 2011. **33**(9): p. 1729-35.
112. Charoenfuprasert, S., et al., *Identification of salt-inducible kinase 3 as a novel tumor antigen associated with tumorigenesis of ovarian cancer*. *Oncogene*, 2011. **30**(33): p. 3570-84.
113. Zhang, J.Y., *Tumor-associated antigen arrays to enhance antibody detection for cancer diagnosis*. *Cancer Detect Prev*, 2004. **28**(2): p. 114-8.
114. MacBeath, G. and S.L. Schreiber, *Printing proteins as microarrays for high-throughput function determination*. *Science*, 2000. **289**(5485): p. 1760-3.
115. Zhu, H., et al., *Global analysis of protein activities using proteome chips*. *Science*, 2001. **293**(5537): p. 2101-5.
116. Harris, T.M., A. Massimi, and G. Childs, *Injecting new ideas into microarray printing*. *Nat Biotechnol*, 2000. **18**(4): p. 384-5.
117. Stadler, V., et al., *Combinatorial synthesis of peptide arrays with a laser printer*. *Angew Chem Int Ed Engl*, 2008. **47**(37): p. 7132-5.
118. Sumerel, J., et al., *Piezoelectric ink jet processing of materials for medical and biological applications*. *Biotechnol J*, 2006. **1**(9): p. 976-87.
119. Avseenko, N.V., et al., *Immunoassay with multicomponent protein microarrays fabricated by electrospray deposition*. *Anal Chem*, 2002. **74**(5): p. 927-33.
120. Gao, X., E. Gulari, and X. Zhou, *In situ synthesis of oligonucleotide microarrays*. *Biopolymers*, 2004. **73**(5): p. 579-96.
121. Petrou, P.S., et al., *A biomolecule friendly photolithographic process for fabrication of protein microarrays on polymeric films coated on silicon chips*. *Biosens Bioelectron*, 2007. **22**(9-10): p. 1994-2002.
122. Lee, K.B., et al., *Protein nanoarrays generated by dip-pen nanolithography*. *Science*, 2002. **295**(5560): p. 1702-5.
123. Zhu, H. and M. Snyder, *Protein chip technology*. *Curr Opin Chem Biol*, 2003. **7**(1): p. 55-63.
124. Angenendt, P., *Progress in protein and antibody microarray technology*. *Drug Discov Today*, 2005. **10**(7): p. 503-11.
125. Gnjatic, S., et al., *Seromic profiling of ovarian and pancreatic cancer*. *Proc Natl Acad Sci U S A*, 2010. **107**(11): p. 5088-93.

126. Gunawardana, C.G., N. Memari, and E.P. Diamandis, *Identifying novel autoantibody signatures in ovarian cancer using high-density protein microarrays*. Clin Biochem, 2009. **42**(4-5): p. 426-9.
127. Bischoff, R. and T.M. Luider, *Methodological advances in the discovery of protein and peptide disease markers*. J Chromatogr B Analyt Technol Biomed Life Sci, 2004. **803**(1): p. 27-40.
128. Usui-Aoki, K., et al., *A novel approach to protein expression profiling using antibody microarrays combined with surface plasmon resonance technology*. Proteomics, 2005. **5**(9): p. 2396-401.
129. Lee, Y., et al., *ProteoChip: a highly sensitive protein microarray prepared by a novel method of protein immobilization for application of protein-protein interaction studies*. Proteomics, 2003. **3**(12): p. 2289-304.
130. Lee, J.H., et al., *Immunoassay of prostate-specific antigen (PSA) using resonant frequency shift of piezoelectric nanomechanical microcantilever*. Biosens Bioelectron, 2005. **20**(10): p. 2157-62.
131. Matsuno, H., K. Niikura, and Y. Okahata, *Design and characterization of asparagine- and lysine-containing alanine-based helical peptides that bind selectively to A.T base pairs of oligonucleotides immobilized on a 27 mhz quartz crystal microbalance*. Biochemistry, 2001. **40**(12): p. 3615-22.
132. Mor, G., et al., *Serum protein markers for early detection of ovarian cancer*. Proc Natl Acad Sci U S A, 2005. **102**(21): p. 7677-82.
133. Schweitzer, B., et al., *Multiplexed protein profiling on microarrays by rolling-circle amplification*. Nat Biotechnol, 2002. **20**(4): p. 359-65.
134. Wang, X., et al., *Autoantibody signatures in prostate cancer*. N Engl J Med, 2005. **353**(12): p. 1224-35.
135. Zhang, J.Y., *Tumor-associated antigen arrays to enhance antibody detection for cancer diagnosis*. Cancer Detect Prev, 2004. **28**(2): p. 114-8.
136. Hudson, M.E., et al., *Identification of differentially expressed proteins in ovarian cancer using high-density protein microarrays*. Proc Natl Acad Sci U S A, 2007. **104**(44): p. 17494-9.
137. Taylor, D.D., C. Gercel-Taylor, and L.P. Parker, *Patient-derived tumor-reactive antibodies as diagnostic markers for ovarian cancer*. Gynecol Oncol, 2009. **115**(1): p. 112-20.
138. Skates, S.J., et al., *Preoperative sensitivity and specificity for early-stage ovarian cancer when combining cancer antigen CA-125II, CA 15-3, CA 72-4, and macrophage colony-stimulating factor using mixtures of multivariate normal distributions*. J Clin Oncol, 2004. **22**(20): p. 4059-66.
139. Accessed online at <http://www.ncbi.nlm.nih.gov/pubmedhealth/PMH0001891/> on 03-09-2011
140. Stockert, E., et al., *A survey of the humoral immune response of cancer patients to a panel of human tumour antigens*. J Exp Med, 1998. **187**(8): p. 1349-54.
141. D'Angelo, S., et al., *Profiling celiac disease antibody repertoire*. Clin Immunol, 2013. **148**(1): p. 99-109.
142. *Proteomics, transcriptomics: what's in a name?* Nature, 1999. **402**(6763): p. 715.

143. Rifai, N., M.A. Gillette, and S.A. Carr, *Protein biomarker discovery and validation: the long and uncertain path to clinical utility*. Nat Biotechnol, 2006. **24**(8): p. 971-83
144. Erdile, L.F., D. Smith, and D. Berd, *Whole cell ELISA for detection of tumor antigen expression in tumor samples*. J Immunol Methods, 2001. **258**(1-2): p. 47-53.
145. Coney, L.R., et al., *Chimeric murine-human antibodies directed against folate binding receptor are efficient mediators of ovarian carcinoma cell killing*. Cancer Res, 1994. **54**(9): p. 2448-55.
146. Miotti, S., et al., *Simultaneous activity of two different mechanisms of folate transport in ovarian carcinoma cell lines*. J Cell Biochem, 1997. **65**(4): p. 479-91.
147. Di Niro, R., et al., *Profiling the autoantibody repertoire by screening phage-displayed human cDNA libraries*. Methods Mol Biol, 2009. **570**: p. 353-69.
148. Studier, F.W., *Protein production by auto-induction in high density shaking cultures*. Protein Expr Purif, 2005. **41**(1): p. 207-34.
149. Lokhov, P.G. and E.E. Balashova, *Cellular cancer vaccines: an update on the development of vaccines generated from cell surface antigens*. J Cancer, 2010. **1**: p. 230-41.
150. Lokhov, P.G. Improving cellular cancer vaccines. Available from Nature Precedings, <http://precedings.nature.com/documents/4356/version/1/files/npre20104356-1.pdf> , 2010
151. Lourenco, E.V. and M.C. Roque-Barreira, *Immunoenzymatic quantitative analysis of antigens expressed on the cell surface (cell-ELISA)*. Methods Mol Biol, 2010. **588**: p. 301-9.
152. Nickel, W. and C. Rabouille, *Mechanisms of regulated unconventional protein secretion*. Nat Rev Mol Cell Biol, 2009. **10**(2): p. 148-55
153. Chan, C.P., K.H. Kok, and D.Y. Jin, *CREB3 subfamily transcription factors are not created equal: Recent insights from global analyses and animal models*. Cell Biosci, 2011. **1**(1): p. 6.
154. DenBoer, L.M., et al., *Luman is capable of binding and activating transcription from the unfolded protein response element*. Biochem Biophys Res Commun, 2005. **331**(1): p. 113-9.
155. Kim, H.C., et al., *HDAC3 selectively represses CREB3-mediated transcription and migration of metastatic breast cancer cells*. Cell Mol Life Sci, 2010. **67**(20): p. 3499-510
156. Jin, D.Y., et al., *Hepatitis C virus core protein-induced loss of LZIP function correlates with cellular transformation*. EMBO J, 2000. **19**(4): p. 729-40.
157. Eleveld-Trancikova, D., et al., *DC-STAMP interacts with ER-resident transcription factor LUMAN which becomes activated during DC maturation*. Mol Immunol, 2010. **47**(11-12): p. 1963-73.
158. Brouwer, R., et al., *Autoantibodies directed to novel components of the PM/Scl complex, the human exosome*. Arthritis Res, 2002. **4**(2): p. 134-8
159. Bluthner, M. and F.A. Bautz, *Cloning and characterization of the cDNA coding for a polymyositis-scleroderma overlap syndrome-related nucleolar 100-kD protein*. J Exp Med, 1992. **176**(4): p. 973-80.

160. Gelpi, C., et al., *Identification of protein components reactive with anti-PM/Scl autoantibodies*. Clin Exp Immunol, 1990. **81**(1): p. 59-64.
161. Ge, Q., et al., *Analysis of the specificity of anti-PM-Scl autoantibodies*. Arthritis Rheum, 1994. **37**(10): p. 1445-52.
162. Brouwer, R., G.J. Pruijn, and W.J. van Venrooij, *The human exosome: an autoantigenic complex of exoribonucleases in myositis and scleroderma*. Arthritis Res, 2001. **3**(2): p. 102-6
163. Staals, R.H. and G.J. Pruijn, *The human exosome and disease*. Adv Exp Med Biol, 2010. **702**: p. 132-42.
164. Carim-Todd, L., et al., *Cloning, mapping and expression analysis of C15orf4, a novel human gene with homology to the yeast mitochondrial ribosomal protein Ym130 gene*. DNA Seq, 2001. **12**(2): p. 91-6.
165. Huynh, K.D., et al., *BCoR, a novel corepressor involved in BCL-6 repression*. Genes Dev, 2000. **14**(14): p. 1810-23.
166. Polo, J.M., et al., *Specific peptide interference reveals BCL6 transcriptional and oncogenic mechanisms in B-cell lymphoma cells*. Nat Med, 2004. **10**(12): p. 1329-35.
167. Ng, D., et al., *Oculofaciocardiodental and Lenz microphthalmia syndromes result from distinct classes of mutations in BCOR*. Nat Genet, 2004. **36**(4): p. 411-6.
168. Grossmann, V., et al., *Whole-exome sequencing identifies somatic mutations of BCOR in acute myeloid leukemia with normal karyotype*. Blood, 2011. **118**(23): p. 6153-63.
169. Kim, J.H., et al., *HIP1R interacts with a member of Bcl-2 family, BCL2L10, and induces BAK-dependent cell death*. Cell Physiol Biochem, 2009. **23**(1-3): p. 43-52.
170. Wilbur, J.D., et al., *Actin binding by Hip1 (huntingtin-interacting protein 1) and Hip1R (Hip1-related protein) is regulated by clathrin light chain*. J Biol Chem, 2008. **283**(47): p. 32870-9.
171. Porpaczy, E., et al., *Gene expression signature of chronic lymphocytic leukaemia with Trisomy 12*. Eur J Clin Invest, 2009. **39**(7): p. 568-75.
172. Scanlan, M.J., et al., *Cancer-related serological recognition of human colon cancer: identification of potential diagnostic and immunotherapeutic targets*. Cancer Res, 2002. **62**(14): p. 4041-7.
173. Porkka, K., et al., *A fragment of the HMGN2 protein homes to the nuclei of tumour cells and tumour endothelial cells in vivo*. Proc Natl Acad Sci U S A, 2002. **99**(11): p. 7444-9.
174. Xiong, W.B., et al., *Creation and anti-cancer potency in HeLa cells of a novel chimeric toxin, HMGNCIDIN, composed of HMGN2 a-helical domain and PE38 KDEL domain III*. Chin Med J (Engl), 2008. **121**(1): p. 82-5.
175. Li, H., et al., *Deletion of the olfactomedin 4 gene is associated with progression of human prostate cancer*. Am J Pathol, 2013. **183**(4): p. 1329-38.
176. Marimuthu, A., et al., *Identification of head and neck squamous cell carcinoma biomarker candidates through proteomic analysis of cancer cell secretome*. Biochim Biophys Acta, 2013. **1834**(11): p. 2308-16.

177. Duan, C., et al., *Oestrogen receptor-mediated expression of Olfactomedin 4 regulates the progression of endometrial adenocarcinoma*. J Cell Mol Med, 2014.
178. Zacchi, P., et al., *Selecting open reading frames from DNA*. Genome Res, 2003. **13**(5): p. 980-90.
179. Berchuck, A., M.F. Kohler, and R.C. Bast, Jr., *Molecular genetic features of ovarian cancer*. Prog Clin Biol Res, 1996. **394**: p. 269-84.
180. Aunoble, B., et al., *Major oncogenes and tumor suppressor genes involved in epithelial ovarian cancer (review)*. Int J Oncol, 2000. **16**(3): p. 567-76.
181. Kolch, W., H. Mischak, and A.R. Pitt, *The molecular make-up of a tumour: proteomics in cancer research*. Clin Sci (Lond), 2005. **108**(5): p. 369-83.
182. An, H.J., et al., *Comparative proteomics of ovarian epithelial tumors*. J Proteome Res, 2006. **5**(5): p. 1082-90.
183. Li, X.Q., et al., *Proteomic identification of tumor-associated protein in ovarian serous cystadenocarcinoma*. Cancer Lett, 2009. **275**(1): p. 109-16.
184. Jackson, D., et al., *Proteomic profiling identifies afamin as a potential biomarker for ovarian cancer*. Clin Cancer Res, 2007. **13**(24): p. 7370-9.
185. Petricoin, E.F., et al., *Use of proteomic patterns in serum to identify ovarian cancer*. Lancet, 2002. **359**(9306): p. 572-7.
186. Zhang, Z., et al., *Three biomarkers identified from serum proteomic analysis for the detection of early stage ovarian cancer*. Cancer Res, 2004. **64**(16): p. 5882-90.
187. Diamandis, E.P., *Analysis of serum proteomic patterns for early cancer diagnosis: drawing attention to potential problems*. J Natl Cancer Inst, 2004. **96**(5): p. 353-6.
188. Capello, M., et al., *Autoantibodies to Ezrin are an early sign of pancreatic cancer in humans and in genetically engineered mouse models*. J Hematol Oncol, 2013. **6**: p. 67.
189. Chen, Y.T. Cancer vaccine: identification of human tumor antigens by SEREX. *Cancer J*. **2000**, 6, S208–S217
190. Chen, Y.T., A.O. Gure, and M.J. Scanlan, *Serological analysis of expression cDNA libraries (SEREX): an immunoscreening technique for identifying immunogenic tumor antigens*. Methods Mol Med, 2005. **103**: p. 207-16.
191. Stone, B., et al., *Serologic analysis of ovarian tumor antigens reveals a bias toward antigens encoded on 17q*. Int J Cancer, 2003. **104**(1): p. 73-84.
192. Luo, L.Y., et al., *Identification of heat shock protein 90 and other proteins as tumour antigens by serological screening of an ovarian carcinoma expression library*. Br J Cancer, 2002. **87**(3): p. 339-43.
193. Hong, C.W. and Q. Zeng, *Awaiting a new era of cancer immunotherapy*. Cancer Res, 2012. **72**(15): p. 3715-9.

194. Moore, R.G., et al., *The use of multiple novel tumour biomarkers for the detection of ovarian carcinoma in patients with a pelvic mass*. Gynecol Oncol, 2008. **108**(2): p. 402-8.
195. Visintin, I., et al., *Diagnostic markers for early detection of ovarian cancer*. Clin Cancer Res, 2008. **14**(4): p. 1065-72.
196. Easton, J.M., B. Goldberg, and H. Green, *Demonstration of surface antigens and pinocytosis in mammalian cells with ferritin-antibody conjugates*. J Cell Biol, 1962. **12**: p. 437-43.
197. Comisso, C., et al., *Macropinocytosis of protein is an amino acid supply route in Ras-transformed cells*. Nature, 2013. **497**(7451): p. 633-7.
198. Vodnik, M., et al., *Phage display: selecting straws instead of a needle from a haystack*. Molecules, 2011. **16**(1): p. 790-817.
199. Larralde, O.G., et al., *Identification of hepatitis A virus mimotopes by phage display, antigenicity and immunogenicity*. J Virol Methods, 2007. **140**(1-2): p. 49-58.

Figure references

1. Figure 1: Modified images accessed online at <http://www.lilianamereu.it/ita-patologie-dettaglio.php?id=19> and <http://www.aacc.org/publications/cln/2013/march/Pages/Ovarian-Cancer.aspx> on 23-12-2013
2. Figure 2: Accessed online at <http://globocan.iarc.fr/> on 23-12-2013
3. Figure 3 : Accessed online at <http://ovariancancer.jhmi.edu/typesca.cfm> on 23-12-2013 on 23-12-2013
4. Figure 4: . Kipps, E., D.S. Tan, and S.B. Kaye, *Meeting the challenge of ascites in ovarian cancer: new avenues for therapy and research*. Nat Rev Cancer, 2013. **13**(4): p. 273-82.
5. Figure 5: Modified images accessed online at <http://www.nano-reviews.net/index.php/nano/article/viewFile/17240/23317/66794> on 23-12-2013
6. Figure 6: Kehoe, J.W. and B.K. Kay, *Filamentous phage display in the new millennium*. Chem Rev, 2005. **105**(11): p. 4056-72.
7. Figure 7: Modified figure accessed from Sidhu, S.S. and S. Koide, *Phage display for engineering and analyzing protein interaction interfaces*. Curr Opin Struct Biol, 2007. **17**(4): p. 481-7.
8. Figure 8: Modified figure accessed from Zacchi, P., et al., *Selecting open reading frames from DNA*. Genome Res, 2003. **13**(5): p. 980-90.
9. Figure 9: Hultschig, C., et al., *Recent advances of protein microarrays*. Curr Opin Chem Biol, 2006. **10**(1): p. 4-10.
10. Figure 29: Modified graph accessed from Lokhov, P.G. Improving cellular cancer vaccines. Available from Nature Precedings, <http://precedings.nature.com/documents/4356/version/1/files/npre20104356-1.pdf> , 2010

Table references

1. Table 1: Williams, T.I., et al., *Epithelial ovarian cancer: disease etiology, treatment, detection, and investigational gene, metabolite, and protein biomarkers*. J Proteome Res, 2007. **6**(8): p. 2936-62.
2. Table 2: Suh, K.S., et al., *Ovarian cancer biomarkers for molecular biosensors and translational medicine*. Expert Rev Mol Diagn, 2010. **10**(8): p. 1069-83.

3. Table 3: References 24, 31-35

4. Table 4: Veneroni.R., et al.,*Patented Biomarkers for the Early Detection of Ovarian Cancer*. Recent Patents on Biomarkers, 2011. 1(1): p.1-9.

5. Table 5: References 108-112

6. Table 6: Angenendt, P., *Progress in protein and antibody microarray technology*. Drug Discov Today, 2005. **10**(7): p. 503-11.

7. Table 7: References 110, 125,126,132,135,137